Materials Advances

ROYAL SOCIETY OF CHEMISTRY

REVIEW

View Article Online
View Journal | View Issue

Cite this: *Mater. Adv.*, 2021, 2, 3474

The role of metal substitutions in the development of Li batteries, part I: cathodes

Alex Hebert and Eric McCalla *

Metal substitutions into known structures have served a pivotal role in developing two of the three main components in state-of-the-art Li-ion batteries: the cathode and electrolyte. In this first installment of this review, we will discuss the design principles established for cathodes, focusing on the benefits and limitations of substitutions in terms of the performance metrics of highest import for high-energy applications such as electric vehicles and grid storage. We emphasize the high number of metrics that must be simultaneously optimized and review the methods best suited to determine such metrics. In particular, partial metal substitutions have proven to be important in increasing energy density, but also in improving safety and cyclability. However, for many materials, cathode particle coatings have been found to be as effective as partial metal substitution in improving the lifetime of the battery since lifetime in state-of-the-art batteries is limited by reactions between the cathode particles and the liquid electrolyte, which can be addressed through surface coating. Though, the effects of substitutions and coatings can be additive to some degree. After a detailed overview of the main classes of cathodes used commercially and in development; we find a number of potentially interesting cathodes that operate at such high potentials that the use of liquid electrolytes becomes impractical that open the door to large leaps in Li-ion battery energy density. This motivates the development of solid electrolytes, the topic of part II of this review.

Received 29th January 2021,
Accepted 10th May 2021

DOI: 10.1039/d1ma00081k

rsc.li/materials-advances

1. Motivation

Metal substitution is a common technique used to tune and enhance the properties of many classes of solid-state materials. It has a long history in the form of metal alloys where one metal is mixed with another (*i.e.* some of the metal is substituted for another) to obtain more desirable physical and chemical properties than the initial metal alone.[1] A few examples are worth considering as an introduction to the various competing roles that substitutions can play in optimizing materials properties. Titanium alloys continue to be studied actively, with metal substitutions impacting physical properties such as Young's modulus, hardness, and thermal conductivity; all of which improve the suitability for a wide array of applications in aerospace and the automotive industry.[2] By contrast, on-going work in aluminum alloys focuses on improving corrosion resistance.[3] While the physical properties are typically bulk properties requiring quite high levels of substitution to have a significant impact, the corrosion resistance is a surface chemical property that can be greatly improved with low-level substitutions. In particular, targeted substitutions at vulnerable locations on the material's surface can play a dramatic role.[3] Herein, we will review the multiple roles that metal substitutions have played in improving Li-ion battery materials. Analogous to metallic alloys, the substitutions can either play a role in improving the bulk properties (such as energy density) or the surface dominated properties (such as electrochemical stability of the electrolytes). Multiple examples of which will be discussed throughout this article.

The above examples of substitutions to make alloys are typically in the % levels. There are also numerous cases in the literature where far lower substitutions into other materials can be very significant. The most important of which is, of course, doping into crystalline semiconductors. These substitutions are routinely used to tune a material's electronic properties, producing desirable band gaps for semiconducting materials,[4] leading to improvements in light-emitting diodes[5] and solar cells;[6,7] as well as improving catalytic yields in metal–organic frameworks.[8,9] In the case of battery materials, there are certain classes of electrode materials that are electronically insulating such that metal substitutions have been utilized to improve their electronic properties. It therefore becomes apparent that methods used in a wide variety of materials science and engineering prove to be of interest in improving battery materials. In this article, we will use the term doping exclusively for cases where the substitution is at a very low level and impacting the electronic properties.

Department of Chemistry, McGill University, Montreal, Canada.
E-mail: eric.mccalla@mcgill.ca

In this work, we focus on the role of metal substitution in the development of Li-ion battery materials. Specifically, in this first installment of this 2 part review, we evaluate the role metal substitutions have played in the development of Li-ion cathode materials. Li-ion batteries (LIBs) are fundamental to our modern lives. They power our smartphones, tablets, laptops, and, increasingly, our vehicles. Their prevalence is due to their high energy density compared to other battery chemistries, allowing them to store a large amount of energy in portable applications. While Li-ion battery technology has improved significantly over the past several decades, there is still room, and need, for improvement. Electric vehicles (EVs) still lag behind internal combustion engine (ICE) vehicles in terms of range.[10] In order for EVs to reach the range of ICE vehicles and for Li-ion batteries to find new uses, such as in other modes of transport, we must continue to improve Li-ion battery energy density, power, and lifetime. Much of the focus on battery improvement lies on the cathode material. It is the limiting factor of LIB capacity, accommodating fewer Li^+ ions per unit weight than the anode, thus defining the maximum capacity of the battery. Presently, layered transition metal oxide cathodes have the largest market share of cathode materials. The most popular of which are $LiNi_xMn_yCo_zO_2$ (NMC) and $LiCoO_2$ (LCO).[11] These materials have high energy densities in excess of 600 W h kg^{-1},[12] as well as a respectable lifetimes, but contain Co which is expensive and leaves an undesirable environmental impact on extraction and disposal.[13,14] LCO was the first of the layered cathode materials to be commercialized,[15] but by substituting Ni and Mn for Co, its performance was improved while reducing the cobalt content, leading to the superior NMC.[16,17] In a similar vein, $LiNi_xCo_yAl_2O_2$ (NCA) was developed through metal substitution into layered transition metal oxide materials and also holds an appreciable market share.[11] These two examples of massively successful commercialization of layered oxides with metal substitutions has served as motivation for a great number of further studies looking at the impact of substitutions into many classes of cathodes for Li batteries. This idea of metal substitution to improve cathode structural and electrochemical properties has continued with small amounts of metals being substituted into these layered transition metal oxides to continue to improve their overall performance.

Outside of layered transition metal oxides, metal substitution has been applied to other cathode materials such as olivine phosphate cathode materials have an appreciable spot in the market, namely $LiFePO_4$, which has a lower capacity than the layered transition metal oxides, but is safer and has a longer lifetime. Substitution of iron for other metals has led to the development of ''high voltage'' olivine cathodes such as $LiCoPO_4$ and $LiNiPO_4$, which operate near 5 V *vs.* the 4 V of NMC and NCA, which could bring about a leap in LIB energy density. In addition to olivine cathode materials, spinel and disorder rock salts show promise in the high voltage space. Currently, these high voltage cathodes are restricted by electrolyte development, as traditional carbonate electrolytes break down when operating at these high potentials. Though, through partial metal substitution, these high-voltage cathodes are becoming more compatible with electrolyte and through the continued improvement of both the cathode and electrolyte, high voltage, high energy Li-ion batteries may be realized.

Part I of this review will provide an overview of cathode improvements resulting from metal substitutions (both complete and partial), as well as provide an overview of the methods that should be used for evaluating these materials in a manner that provides accurate screening of battery performance. Specifically, partial metal substitutions have been used extensively to enhance the following properties in Li-ion cathodes:

(1) Energy density (bulk property, % level substitutions required to have an impact)

(2) Material stability (surface property, preferential substitutions at the surface of particles can be impactful; also bulk property, cation migration and phase transformations can be suppressed)

(3) Rate performance (both bulk and surface property, often dominated by particle morphology).

Given the fundamental differences between these 3 properties, it is not surprising that successful substitution techniques differ for each key property, and the challenge is to optimize all 3 simultaneously. The methods used to reliably evaluate each of these properties also differ and will be reviewed in the next section, prior to a detailed discussion of the role of metal substitutions into improving each class of cathode in detail.

2. Cathode material metrics

There are a number of performance metrics that must be optimized simultaneously in designing advanced cathodes for Li-ion batteries. These include: (1) a high energy density, (2) a long cycle life, (3) a high energy conversion efficiency, (4) a good rate performance, (5) a high safety during battery operation, and (6) a low cost. These metrics are often shown in radar plots similar to that shown in Fig. 1. Thus, any study looking at improving one metric with the use of a substitution must also be mindful of any unintended detrimental impacts on the other metrics. This, in a nutshell, is what makes going beyond the state-of-the-art so difficult in Li-ion batteries. This section focusses on describing the methods used to extract the important metrics to assess battery performance, and in particular focusses on what conditions should and should not be used in order to ensure that conclusions hold up under real conditions in commercialized cells. Here, we assume a target application of electric vehicles as this is currently driving battery research and development worldwide. Electric vehicles being the objective has consequences for what cycling rates are appropriate, and it should be noted that for niche applications (*e.g.* power tools where faster rates are needed) different conditions (*e.g.* faster cycling) become appropriate. For the purpose of this review, we seek to understand how substitutions improve performance for conditions comparable to those of interest for electric vehicles, *i.e.* charging in 15–60 min,

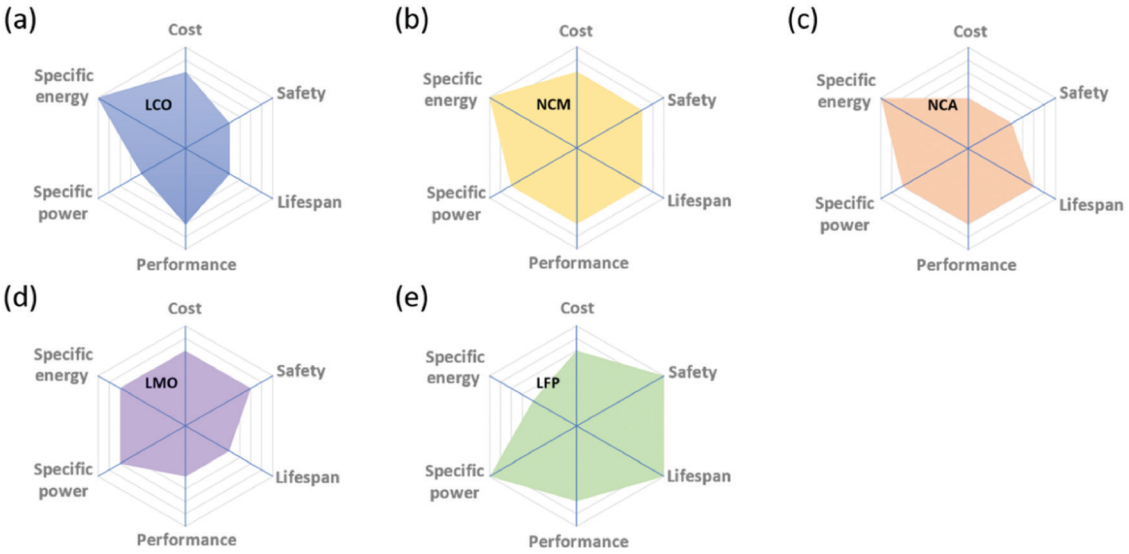

Fig. 1 Radar plots demonstrating the relative qualities of different classes of cathode materials: $LiCoO_2$ (LCO), $Li[Ni,Co,Mn]O_2$ (NMC), $Li[Ni,Co,Al]O_2$ (NCA), $LiMn_2O_4$ (LMO), and $LiFePO_4$ (LFP). Reproduced with permission from ref. 18. Copyright (2020 and 2019, respectively) Elsevier.

a slow discharge on the order of 10 h, and usage on the scale of 10 years.

2.1 Standard electrochemical testing

Electrochemical techniques are at the heart of cathode material evaluation. Typically, the electrochemical cycling is performed galvanostatically, *i.e.* using constant current. Though other methods are sometimes used such as constant current-constant voltage (CCCV), where the cell is first charged at a constant current until a threshold potential is reached, at which point that potential is maintained for a specified interval to simulate how batteries are charged in practice. For the sake of cathode evaluation, purely galvanostatic charging is the accepted technique in academia.

The rate at which cells are charged is often reported as a C-rate where a current of 1C is the current at which the cell will be charged to its expected capacity in one hour (and, *e.g.* C/5 would require 5 h). The expected capacity is determined by multiplying the specific capacity (mA h g^{-1}) by the mass of active material in the prepared electrode. This is trivial for well-characterized materials, as their specific capacities are known under a variety of conditions. However, for novel materials whose capacitates are not known, C-rate may still be used, using an estimate of the specific capacity to determine the C-rate. It is of the utmost importance that the capacity used for the determination of the C-rate be reported, as the observed capacity of the cell is highly dependent on experimental conditions and cannot be assumed from data shown elsewhere in the article. Often, the capacity of a first charge cycle will be used as the expected capacity of a cell and the C-rate determined from this value. Measuring charging current in this unit compensates for variation in cathode capacity, making method standardization easier, as well as easing interpretation for the reader. Alternatively, current densities may be reported instead of C-rate. The current in mA g^{-1} is typically used to denote the current per gram of active material and gives the same information as the C-rate. The two can be converted by dividing the current density by the specific capacity of the material. The current may also be reported in units of mA cm^{-2}. This, however, is the most difficult for the reader to digest and compare with other studies, as the cathode loading must be reported to allow the reader to calculate the C-rate. All electrochemical metrics will have a different value for different rates making it challenging to compare results from two different articles, more details follow on how this was handled in this review.

Although galvanostatic cycling is the typical protocol for battery performance determination, researchers also often use the more traditional technique of cyclic voltammetry. In cyclic voltammetry, an alternating linear sweep potential is applied to the cell and the current response is measured, indicating at which potential redox processes are occurring. It may be due to intercalation or side reactions. Different materials have signature CV curves, with peaks typically corresponding to TM redox or phase transitions (Fig. 2). CV experiments should be conducted over the same, or a slightly larger, voltage window as cycling tests. dQ/dV plots yield similar information to CV (CV can be converted to dQ/dV using the sweep rate) but are obtained from galvanostatic cycling. This has the inherent advantage of being able to obtain dQ/dV plots during traditional cycling experiments. Additionally, unlike CV, dQ/dV peaks do not deform due to changes in resistance of the cell. Instead, they shift laterally, making them easier to interpret (Fig. 2). It is important to note that while these methods can be used to evaluate cell degradation, they alone do not give direct insight into the mechanism behind cell degradation. With novel materials, it is best to use these methods in conjunction with other *in situ* and *ex situ* techniques to determine what CV and dQ/dV peaks correspond to physically.

In the next sections, we focus on how key battery performance metrics should be extracted from electrochemical

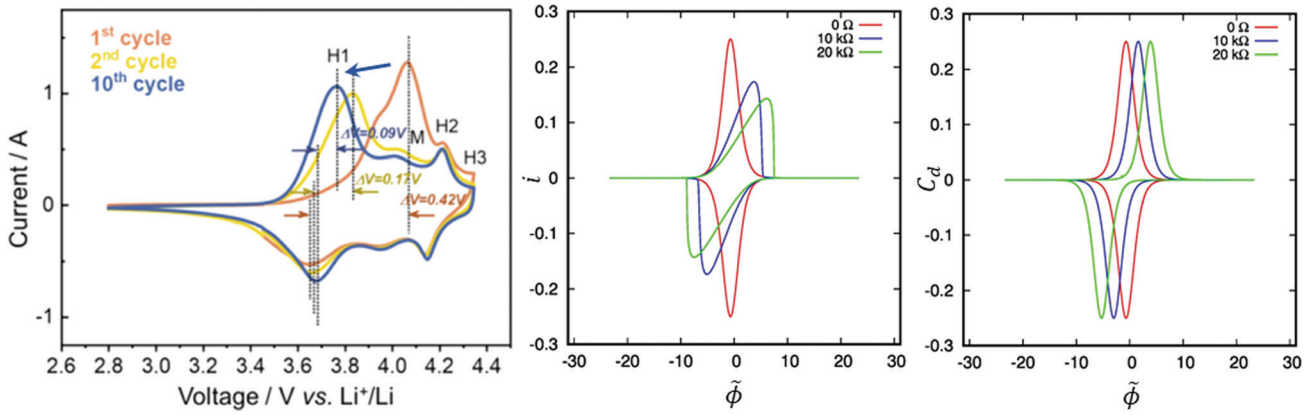

Fig. 2 CV during cycling of NMC 811 with H1 phase transition onset potential shift denoted with the blue error (left), influence of bulk resistance on CV (center) and dQ/dV (right). Reproduced with permission from ref. 19 and 20. Copyright (2020 and 2019) Elsevier.

testing and describe some of the pitfalls that can lead to results not holding up in batteries under typical conditions for commercialized products.

2.2 Extracting energy density

Specific capacity may be converted to another important battery metric, energy density, by multiplying the specific capacity of the material by the average voltage of the cell during discharge. The accepted method of representing the charge/discharge of a cell is using a charge/discharge curve, also called a voltage or potential curve as shown in Fig. 3. It is a plot of the potential against the capacity or the stoichiometry of the intercalant. The charge and discharge capacities may be interpreted from the length of the charge and discharge curves, respectively and the shape of the curves provide information about Li^+ intercalation in the material. These curves are sensitive to material composition,[21,22] charging rate,[23] temperature,[24] and the state of health of the material.[25] Charge/discharge plots are useful in identifying how the charge and discharge of the material changes under different charging conditions and over repeated charges (Fig. 3). An important point to note is that in the case of a two-electrode system, which is typical for most studies, the curve is affected by both the cathode and anode of the cell. It is common to use a Li metal anode to maintain excess Li and sufficient capacity to not limit the capacity over many cycles if Li is consumed. However, a solid electrolyte interphase composed of electrolyte decomposition products forms on the anode affecting the kinetics of charge transfer which makes voltage measurements unreliable at current densities above 1 mA cm^{-2}.[26] A three-electrode cell may be used to obtain the curve uniquely representative of the cathode, typically using a Li pseudo-reference electrode.[27] Three-electrode techniques are not the norm in galvanostatic experiments evaluating cathode materials and will not be further discussed in this review.

2.3 Extracting lifetime with long-term cycling

The lifetime of a cell can be evaluated through repeated charging and discharging of the cell and observing the capacity degradation and voltage decay. Specifically, the discharge capacity, or reversible capacity, is of interest as that is the origin of the accessible energy of the cell. Thus, the charge capacity is often omitted when presenting long-term cycling data (Fig. 3). A cycle life of a cell does not have a universal definition. Commonly, it is considered to be when the cell capacity declines to 80% of the original reversible capacity.[30] The phenomenon of the capacity decreasing over multiple cycles is termed "capacity fade". The lifetime of a cell may also be characterized as the point where capacity fade accelerates sharply before reaching 80%

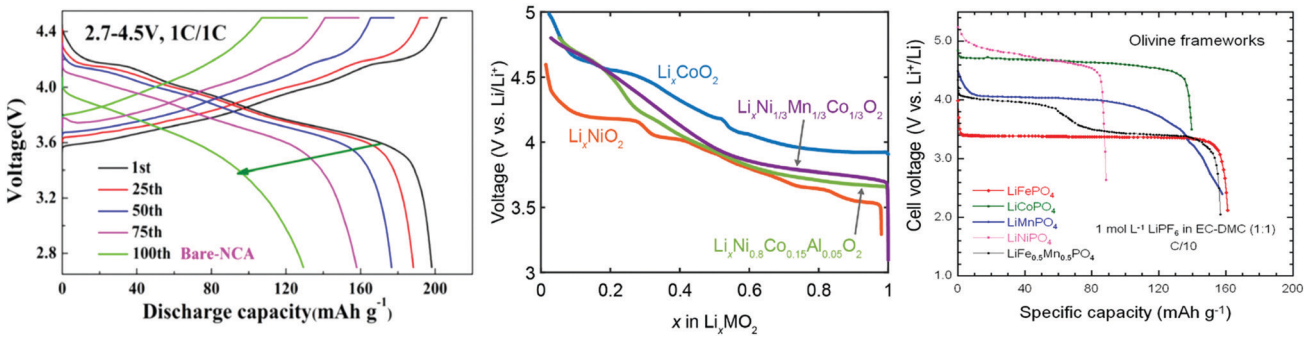

Fig. 3 Charge/discharge curves of $LiNi_{0.85}Co_{0.10}Al_{0.05}O_2$ (left). Discharge curves of various layered oxides with respect to Li composition instead of capacity (center) and for olivine cathode materials. (right) Figures reproduced with permission from ref. 21, 28 and 29. Copyright (2017) Wiley, (2019) American Chemical Society, (2017) Multidisciplinary Digital Publishing Institute.

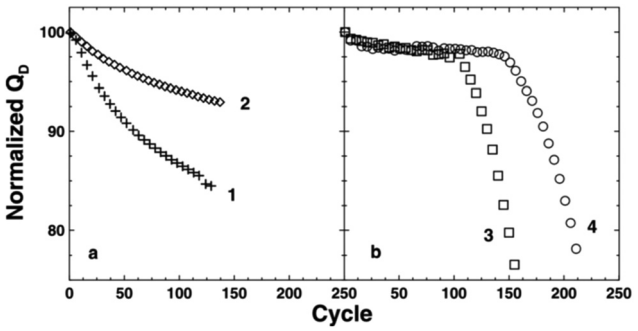

Fig. 4 Charge *vs.* cycle number plots showing gradual capacity lose (left) and rollover failure (right). Reproduced with permission from ref. 31. Copyright (2013) IOP Publishing.[31]

capacity, referred to as a "knee" in the capacity *vs.* cycle number plot, or "rollover failure" (Fig. 4). Dahn showed that rollover arises from poor Li diffusion kinetics arising from the formation of an impeding layer on the negative electrode, comprised of electrolyte degradation products.[31]

The rate used to evaluate cycle life varies and this can have dramatic impact on the results obtained. C/3, C/2, or 1C are popular rates, though higher rates may be used to demonstrate high-rate capabilities of cathode materials, and lower rates may also be used, especially to compare materials that show very poor longevity. It is very important to recognize that the lifetime performance of Li-ion batteries is not only a function of the number of cycles but also of time. Thus, a cell that maintains a high capacity over many cycles at 1C will typically lose much more capacity at C/10 due to the fact that there is more time for negative side reactions to occur, depending on the voltage to which it is charged.[32] This approach to inflate the lifetime metrics of a material is unfortunately commonplace in studies examining nanostructured materials where high rates are achievable. One must consider the total measurement time and then extrapolate to reasonable battery lifetimes in order to obtain useful metrics. That said, at higher rates, structural degradation may be so severe that capacity will degrade much faster at 2C and above compared to 1C, depending on the rate capability of the cathode material.

Regardless of the chosen rate for long-term cycling, the first one to three cycles are typically performed at a low rate of C/10 or C/20. This is to ensure proper formation of the solid electrolyte interphase (SEI), which serves to protect the electrodes from reactions with the electrolyte that negatively affect performance. The appropriate potential window in which the cell is cycled may vary depending on the cathode material being studied.

Given all the different experimental parameters affecting the lifetime metric for the same material, in the context of this article, we must compare the substituted and unsubstituted from the same article in order to get any usable information. A good example of this is shown in Fig. 5a, c, and d where it is clear that lifetime metrics depend strongly on the cycling rate;

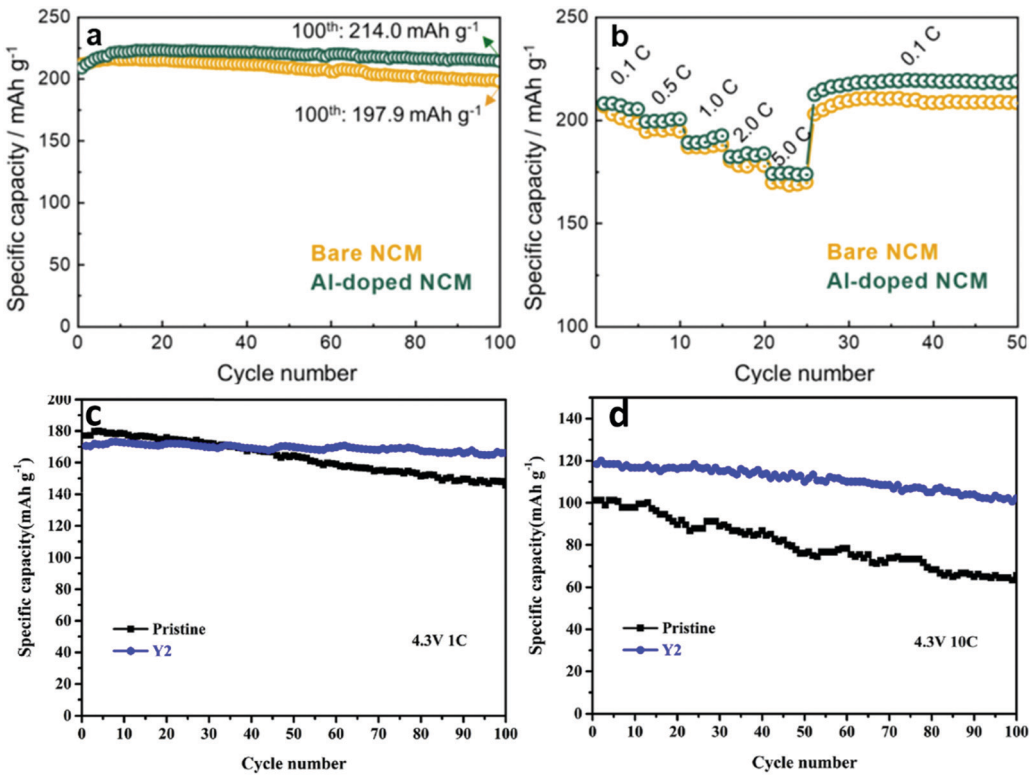

Fig. 5 (a) Long term cycling of NMC and Al-substituted NMC at a rate of 0.1C (a). (b) Rate performance and recovery of NMC and Al-substituted NMC.[19] (c) Long term cycling performance of NMC and Y-substituted NMC at 1C (c) and 10C (d). Figures reproduced with permission from ref. 19 and 33. Copyright (2020 and 2019) Elsevier.

and so we can only determine the impact of a substitution by comparing to the unsubstituted from the same article.

2.4 Extracting lifetime with coulombic efficiency

Another important metric during the charge/discharge of the cell that can, in many cases, be an indication of lifetime is the ratio of the discharge capacity and the previous charge capacity. This is referred to as the coulombic efficiency (CE) and represents the charge efficiency of the cell: how much of the lithium put into the anode during charge is given back during discharge. When a battery is charged, not all the lithium goes into intercalation into the electrodes, there are many side reactions that can occur, driven by the electric potential put across the cell, including the formation of the SEI. This lithium is often lost for subsequent cycling such that it leads to capacity fade and eventual cell death. Thus, CEs are typically less than 1 (1 would represent a battery that lasts forever). The CE typically begins smaller and increases approaching 1, as the initial formation of the SEI causes a large discrepancy, which decreases as the SEI matures.[34] Typical values of the CE are $>99\%$ after initial SEI formation and state-of-the-art Li-ion batteries show CEs $>99.9\%$ and these are the batteries that can last up to 10 years in commercial settings. Thus, it is completely uninformative to present the CE on a scale of 0–100%, but nonetheless this practice is common and leaves the reader unable to evaluate the CE properly. It is also important that if CE is to be taken as a useful metric of battery health, it must be measured with a sufficient accuracy ($\sim\pm0.01\%$) to have any predictive power. In such cases, CE values have correlated extremely well with long-term cycling[31,35–37] and have been used predictively to accelerate the design of advanced batteries. However, when CE values are reported that do not meet the above standards, there is no correlation to lifetime and so no CE values will be discussed in this review article unless they meet the standard of usefulness (0.01% precision).

2.5 Rate performance

The rate performance of a cell is tested similarly to lifetime, but with a varying charge rate. The cell is first cycled multiple times at a low rate (C/10 or C/20) to ensure good SEI formation and to serve as a capacity baseline. Then, the rate is increased incrementally with several cycles occurring at each rate (Fig. 4b). Depending on the material, the rate may be increased as high as 10C or 20C, *i.e.* a full charge in 6 or 3 minutes. After the highest rate, the cell is then cycled several times at the first rate and the capacity compared to the first cycles to determine if performance was affected by the high-rate exposures. The current target application of many battery researchers are electric vehicles and the key target for rates is to be able to charge in 15 minutes (4C charging). As such, rate tests provide an important metric for advanced batteries. For example, in Fig. 5b, we see 33% capacity loss when cycled at 5C compared to C/10. However, it should also be mentioned that in state-of-the-art batteries, rate performance is limited by the anode[38] and as such this is not so essential in the current review article dealing with cathodes. The exception is where substitutions have such a detrimental impact on rate performance such that the cathode in fact becomes limiting.

2.6 Voltage fade

As mentioned previously, voltage fade during long-term cycling also decreases the energy density of a battery. It is important to note that many battery management systems rely on voltage as an indicator of state-of-charge,[39] and this relation cannot be used if the voltage of the battery gradually decreases over time and this makes battery management far more challenging. Battery health monitoring and prediction is an active area of development and is steadily improving making voltage fade less of an issue with regard to battery state of health estimation.[40] Nonetheless, it remains an important metric to track given that cathode materials experience structural transformations as they age and, in some materials, the accumulated changes cause the average voltage during the discharge of the cell to decrease significantly. This causes a reduction in the available energy of the cell. While not a large problem with current market-leading battery chemistries, it is a large factor hindering next-generation materials from being realized. It can be evaluated simultaneously with capacity fade by taking the average voltage of each discharge cycle and monitoring the decay. The mechanisms behind both capacity and voltage fade are discussed in more detail within the material sections.

2.7 Safety

The most important aspect of safety for Li-ion batteries is preventing thermal runaway.[41] Thermal runaway occurs when the battery reaches a temperature where exothermic reactions occur at such rates that the resulting heating of the battery is sufficient to accelerate the rate of these exothermic reactions to such an extent that the electrolyte ignites causing the cell to rupture violently.[42] The cathode material plays a role in the self-heating of the battery as well as the onset of thermal runaway by reacting with the electrolyte. The most common techniques of evaluating the onset temperatures of exothermic reactions are differential scanning calorimetry (DSC) and accelerating rate calorimetry (ARC).[43–46] DSC consists of measuring the difference in energy it takes to heat a reference and the sample as a function of temperature.[47] Accelerating rate calorimeters confine the sample to an adiabatic environment where energy loss is minimal and measures the rate at which the temperature increases as a function of temperature to monitor self-heating.[48] ARC is a more precise technique than DSC to determine the onset temperature for exothermic degradation of battery components leading to thermal runaway.[48,49] Either technique must be performed on the fully charged cathode (this is the most reactive state of the cathode) in the presence of electrolyte in order to correlate to thermal runaway in a full battery. Fig. 6 shows an example of ARC and DSC on various cathode materials.

3. Advanced characterization to determine mechanisms

The previous section outlined the techniques used to screen for important battery metrics. These are essential in evaluating the

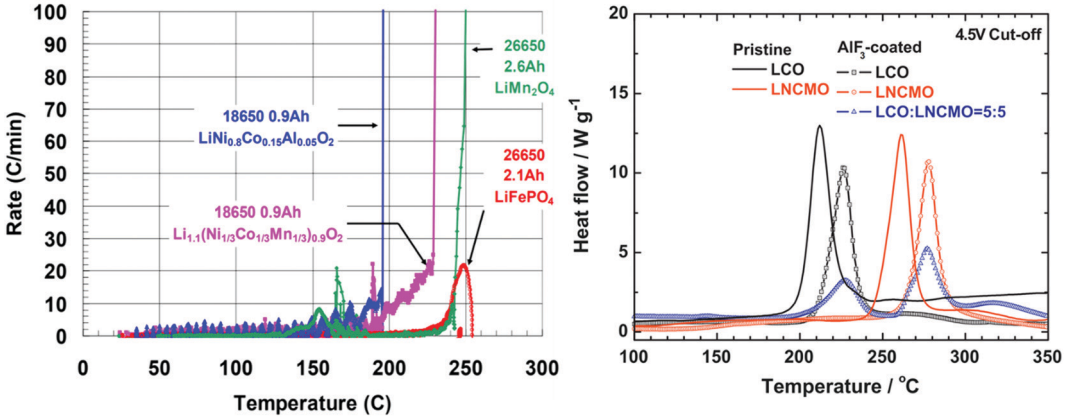

Fig. 6 ARC of various batteries using different cathode materials in EC:PC:DMC electrolyte and graphite anodes (left) and DSC of various cathode materials (right). Figures reproduced with the permission of ref. 50 and 51. Copyright (2012) IOP Publishing and (2011) Elsevier.

usefulness of substitutions into the cathodes. However, a great variety of techniques are also used extensively in order to further understand the mechanisms involved in either improving or deteriorating battery performance with substitutions. A few of the key techniques that will be discussed throughout this review are described in this section.

3.1 Electrochemical impedance spectroscopy

Aging of a cell is typically accompanied by impedance growth due to a thickening SEI and material degradation, specifically at the surface.[52] An increase in cell impedance can negatively impact the performance of the cell, lowering efficiency and reducing rate capability, and may be indicative of reduced safety due to increased risk of thermal runaway.[53] The method of choice to evaluate cell impedance is electrochemical impedance spectroscopy (EIS). EIS consists of perturbing the battery with a low amplitude alternating current pulse and monitoring the voltage response. This is repeated over a wide range of frequencies (Hz–MHz) and the impedance at each perturbation is determined.[54] The data are typically represented using a Nyqvist plot wherein the impedance is plotted parametrically in the plane consisting of the imaginary impedance on the *y*-axis and the real impedance on the *x*-axis. For Li-ion batteries, the plot typically takes the shape of successive semicircles. The utility of EIS relies on modelling the obtained response with a simple circuit. With a circuit model, a resistor and capacitor in parallel respond with a semicircle on the Nyqvist plot and placing a resistor in series with these parallel components results in a shift in the semi circle's position on the real axis. A typical response (Fig. 7), can be fitted with multiple of these parallel resistors and capacitors in series. The values of the fitted circuit can be assigned to different components of the battery. This is where care needs to be taken, as the model is not prescriptive: it does not assign meaning to the obtained values, that is up to the researcher. The accepted interpretation of the model is that there is a "bulk" impedance between electrodes where the electrolyte and separator are, R_0 in Fig. 7, as well as a interfacial impedances such as between cathode material and electrolyte which is caused by the surface

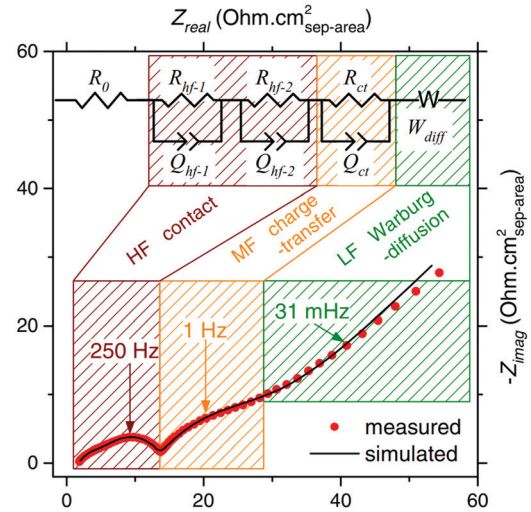

Fig. 7 Example Nyqvist plot of a LIB with interpretation. Contact resistance (red), charge-transfer resistance (yellow), Warburg diffusion (green). Figure reproduced with the permission of ref. 55. Copyright (2016) IOP Publishing.

structure of the cathode and the SEI. This is typically the area of interest when EIS is used, as it is desirable for a cell to keep a consistent impedance as it ages and a large increase in impedance represents a poor state of health for the battery.

3.2 Scanning electron microscopy

The performance of a cathode material is closely tied to its structure. Therefore, it is critical to understand and evaluate changes to the structure during and after cycling to identify changes that occur that affect the performance of the cell. These changes can occur on multiple length scales, from the size of cathode particles (typically tens of microns) to the displacement of individual atoms within the crystal lattice. There are many microscopy, diffractometry, and absorbance techniques to characterize the structure of cathode materials across these scales; the most popular of which will be discussed here, starting with scanning electron microscopy (SEM).

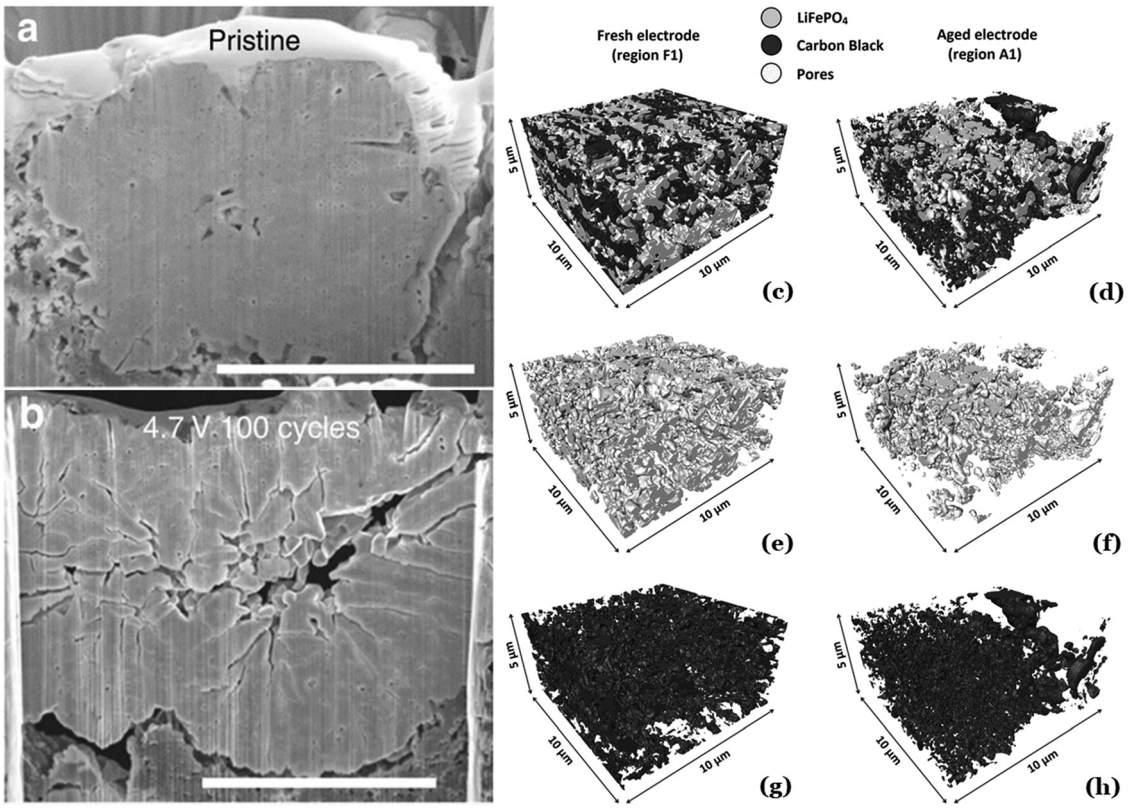

Fig. 8 Example of cracks formed in NMC cathode material after cycling. 3D reconstruction of fresh and aged LFP electrode. Figures reproduced with permission from ref. 61 and 68. Copyright (2016) Elsevier and (2017) Nature.

SEM is useful for characterizing both as-synthesized cathodes and evaluating particle degradation after cycling. Particle morphology directly affects the performance of cathode materials. The size and shape of particles can significantly impact both energy density and rate performance. SEM can be used to qualitatively evaluate particle morphology and validate proper synthesis. It is possible to use SEM images to quantitatively determine particle size with the aid of image analysis software, but it is standard to use laser particle size distribution instruments to obtain particle size distributions instead. SEM is particularly well-suited to comparing pristine and cycled material to qualitatively compare the degree of particle degradation through cracking (Fig. 8a and b).[56–59] This is of particular use in understanding the long-term cycling performance, particularly when surface coatings or core–shell structures are used in an attempt to prevent particle fracture. Using focused ion beam SEM tomography, 3D reconstructions of the cathode can be made before and after cycling to obtain a more complete image of the structural evolution of the material (Fig. 8c–h).[60–63] SEM is also commonly paired with energy-dispersive spectroscopy (EDS) to map the distribution of consistent metals across the particle. This can be used to verify the uniform distribution of a coating or can validate the synthesis of uniformly substituted materials or core–shell and gradient materials by imaging the cross-section of the particle obtained *via* focused ion beam.[64–67]

3.3 X-ray and neutron diffraction

To determine the bulk crystal structure of a cathode material, X-ray diffraction spectroscopy (XRD) is the most popular method. XRD spectra can be refined using Rietveld refinement to obtain structural parameters, crystallite size, as well as the amount of impurity phases.[69–75] XRD spectra are also used to evaluate certain structural defects such as Li/transition metal mixing. XRD can also be used *in situ* to investigate changes in cathode structure during cycling to identify when structural transformations occur as illustrated in Fig. 9.[76–81] This can be accomplished using cell materials with an X-ray transparent window. This allows the determination of structural changes during battery operation and is essential in identifying the mechanisms taking place during cathode use. Substitutions have been shown to suppress certain transformations during cycling[82–84] (*e.g.* Mg substitution into NMC 811 in Fig. 9).[85]

Like XRD, neutron diffraction can be used to investigate the structure of cathode materials. It operates on a similar principle to XRD, only using neutrons instead of X-rays. The main advantage of neutron diffraction is that it is more sensitive to lighter elements (Li and O is of particular interest in the present context) and can distinguish between elements with similar atomic numbers.[86] It has been used to study the distribution of transition metals in transition metal oxides. For example, in $LiNi_{1/3}Mn_{1/3}Co_{1/3}O_2$, neutron diffraction was used to determine that there is non-random ordering of Ni,

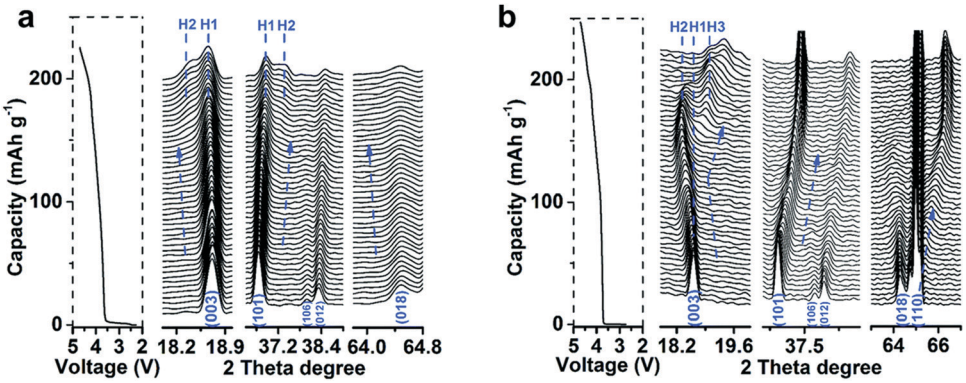

Fig. 9 *In situ* XRD of Mg-substituted (a) and pristine (b) NMC 811 showing suppression of transition to H3 shown *via* the (003) peak shift and splitting as well as the reduced shifting of the 101 peak. Figure reproduced with the permission of ref. 85. Copyright (2019) Royal Society of Chemistry.

Mn, and Co within transition metal layers.[87] It has also been used to determine the degree of Li/Ni mixing through Rietveld refinement (Fig. 10).[88] Recently, *in situ* neutron powder diffraction has also been performed on materials in the pouch cell format: Liu investigated irreversible structural changes in $Li[Li_{0.2}Ni_{0.18}Mn_{0.53}Co_{0.1}]$[89] and Goonetilleke used it to compare the structural stability of various NMC cathode compositions, finding NMC 442 to be more stable than NMC 111 and NMC 811, with the smallest change in the c lattice parameter when charged.[90]

3.4 Transmission electron microscopy

To investigate local crystalline structures, transmission electron microscopy (TEM) may be used. It is particularly useful for evaluating structural changes at the surface of cathode particles as well as changes occurring on the atomic scale. For instance, one can observe the transition from layered to spinel to disordered rock salt occurring at the surface of NCA and Ni-rich NMC particles as they are cycled (Fig. 11).[91–94] The technique has also been used to evaluate SEI growth.[95] TEM in conjunction with energy-dispersive X-ray spectroscopy (EDX) or electron energy loss spectroscopy (EELS) is also used to evaluate changes in metal compositions of cathode materials at the surface.[96,97] TEM is standard in determining the thickness and structure of surface coatings[98–102] and can be used to observe stacking faults in the material or other crystal defects.[103–106]

An example of TEM being used to explore nanoscale changes in the cathodes is the formation of O–O dimers in Li-rich Ir oxides.[107] Although this technique can be used to observe the atomic scale, it should be noted that the materials are very sensitive to beam damage and that great care must be taken during TEM, including using low energies and aberration correction.[108]

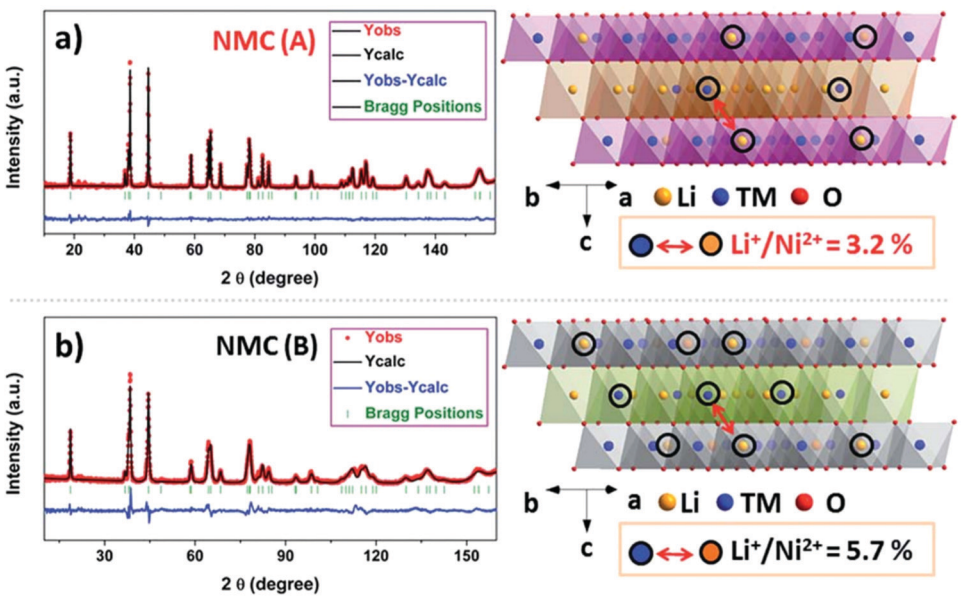

Fig. 10 Neutron diffraction refinement of NMC to determine extent of Li/Ni mixing. Reproduced with the permission of ref. 88. Copyright (2017) Royal Society of Chemistry.

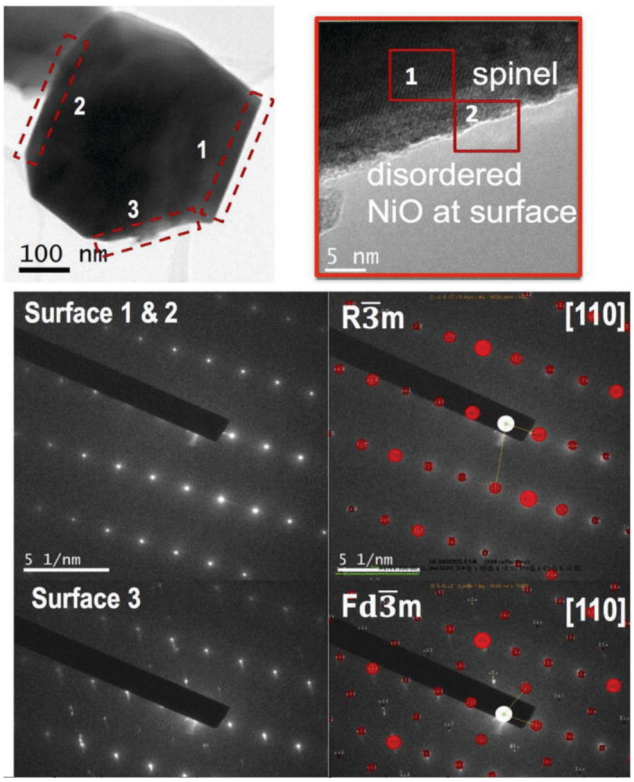

Fig. 11 TEM images demonstrating decomposition of NCA particle surface. Reproduced with permission from ref. 91. Copyright (2016) AIP Publishing.[91]

3.5 Spectroscopies

While the above techniques are important for understanding physical structure and structural changes during the cycling of cathode materials, they tell little of the changes in oxidation state of metals during charge/discharge. X-ray absorbance techniques can be used to identify the electrochemical activity of constituent metals in the electrode. In particular, X-ray absorption near-edge structure (XANES) can be used *in situ* to determine the average oxidation state of metals in the cathode material during charge and discharge, elucidating which metals are oxidized at different states of charge and how it may change over multiple cycles.[109–111] This can be achieved by fitting the edge of the spectrum. For example, the oxidation state of Ni has been investigated during the cycling of Li_4NiTeO_6 cathode materials as demonstrated in Fig. 12.[112]

While XANES can be used to study the bulk oxidation state of metals in a material, X-ray photoelectron spectroscopy (XPS) may be used to investigate the oxidation state of metals at the surface of the cathode material.[113–115] For example, in the same study by Ting,[112] XPS was used to determine the oxidation state of Ni at the surface of the model cathode material, thus allowing for a comparison of the behaviour of bulk and surface metals, a powerful combination of techniques to probe changes in the surface of cathode materials. XPS may also be used to investigate the chemistry of the SEI[116–118] and explore the reactivity and mechanism of action of various surface coatings.[119–121]

4. Impact of substitutions into $LiMO_2$ compositions

Having reviewed the key methodologies used in studies looking at the impact of substitutions into Li cathodes, the rest of this review will examine in detail the impact of substitutions into particular classes of cathodes. We begin with this section looking at layered oxides.

4.1 Unsubstituted $LiMO_2$

The predominant class of Li-ion cathodes for high energy batteries is layered transition metal oxides. The history of these cathodes goes back to 1980 with the discovery of $LiCoO_2$ (LCO) as a cathode material by Goodenough[122] leading to the creation of the first modern lithium-ion battery by Yoshino in the 1980s,[11] consisting of a $LiCoO_2$ (LCO) cathode and carbonaceous anode.[123] This cell was commercialized by Sony and was the first in a plethora of LIB chemistries to come in the past four decades. To this day, the most-used cathode materials are isostructural with LCO.

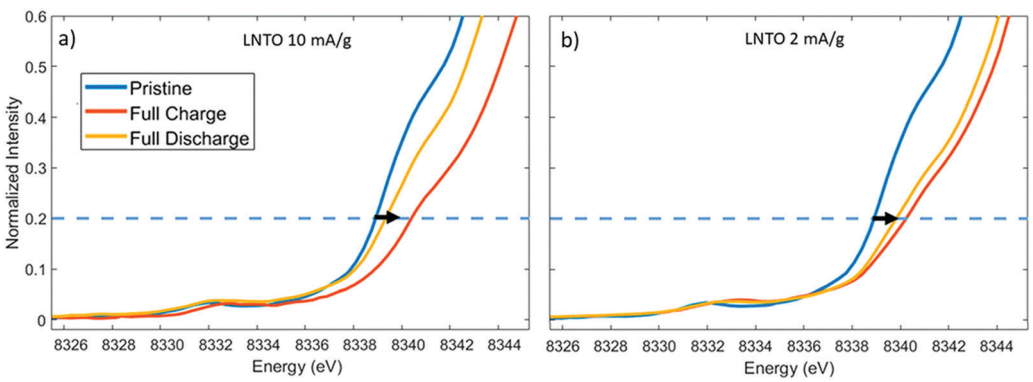

Fig. 12 Relevant portion of the Ni K-edge for determining oxidation state from XANES spectra of Li_4NiTeO_6.[112] The edge position can be used, along with references, to calculate the average oxidation state of Ni. Figure reproduced with permission from ref. 112. Copyright (2020) American Chemical Society.

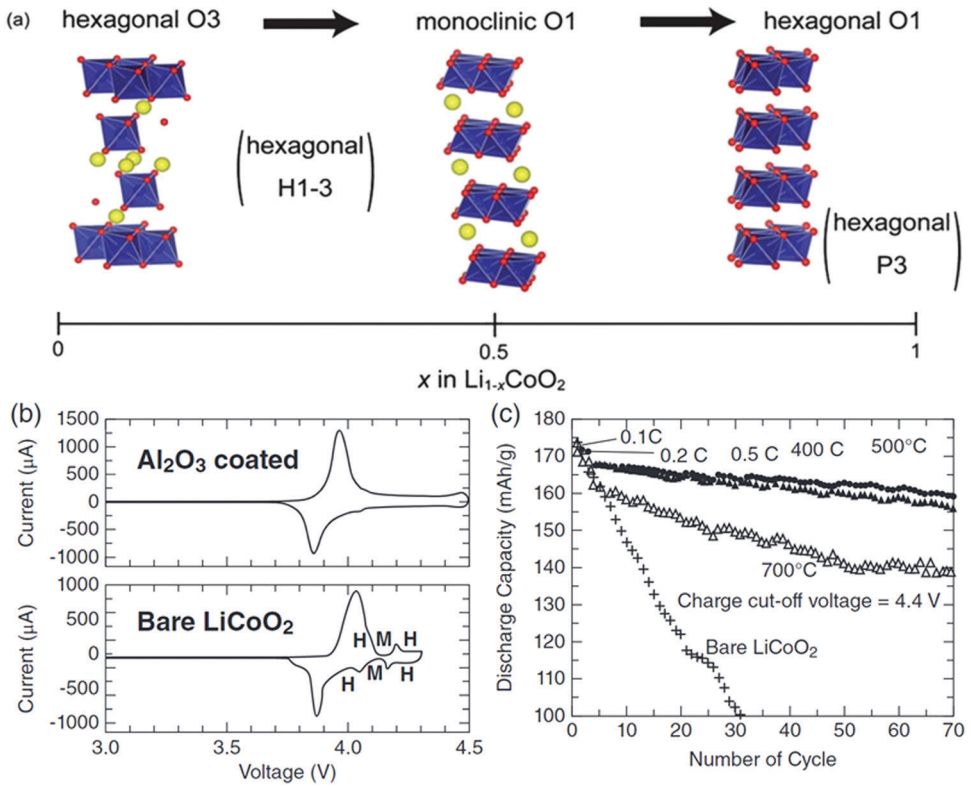

Fig. 13 O3 and monoclinic and hexagonal O1 structures of LCO (a). Cyclic voltammograms (b) of bare and coated LCO. The phase transformations yielding the O1 structure (labelled H → M → H) are suppressed by the coating, yielding better long-term cycling (c). Figures reproduced with permission from ref. 126 and 127. Copyright (2012) Royal Society of Chemistry and copyright (2017) Wiley.[126,127]

LCO consists of planes of Li atoms sandwiched between extensive slabs of CoO_2, forming a rocksalt structure that can be described in the $R\bar{3}m$ space group. The structure is shown in Fig. 13 and is called the O3 structure in the battery literature as Li takes octahedral cites and 3 CoO_2 slabs must be stacked in the vertical direction before repetition. The cobalt atoms occupy octahedral sites within CoO_2 slabs and Li are found in octahedral sites between the slabs. This material reversibly intercalates Li through these 2D sheets. The removal of lithium during charge is, in principle, compensated by Co^{3+} converting to Co^{4+} during charge. The theoretical capacity of LCO assuming complete removal of lithium is 273 mA h g^{-1}.[124] However, in practice the capacity is substantially less ($\sim$140 mA h g^{-1}), as only half of the Li can be accessed before the structure converts from the O3 stacking of the pristine material to the O1 stacking of CoO_2 (see Fig. 13a and 15c).[125] The shearing required to transform from the O3 to the O1 structure results in very poor long-term cycling as shown in Fig. 13c. This rapid fade has been mitigated dramatically by either substitution (to be discussed below) or by coatings such as Al_2O_3 (Fig. 13b and c). The battery literature contains many such cases where either coatings or substitutions may improve certain battery metrics, in such cases it is important to look at all metrics to see which solution is optimal.

There are a number of other materials that can be made with this same structure by completely replacing Co with another transition metal. Two materials, in particular, were widely studied to replace LCO: $LiNiO_2$ (LNO) and $LiMnO_2$, both with theoretical capacities very close to LCO.[128] LNO can be synthesized quite readily, though it is difficult to synthesize with perfect stoichiometry, as some Ni^{3+} is reduced to Ni^{2+} and mixes into the lithium layer due to similar atomic radii of Ni^{2+} and Li^{+}, resulting in reduced capacity and structural stability.[129–132] The material shows good cycling on the first cycle (Fig. 15d). However, it suffers from structural instability during electrochemical cycling, notably due to the M → H2 transition (Fig. 15f). Nickel can migrate to vacant Li^{+} sites during charging and this migration occurs to such an extent that the material converts to a disordered rocksalt structure and this results in the blocking of Li^{+} intercalation pathways. This leads to an increased impedance as well as active material loss and a dramatically shortened cycle life. Overall, this leads to a cathode material with a high initial capacity, but very poor cycle life as shown in Fig. 15e. Numerous substitutions into LNO have been attempted to prevent these transformations as discussed in the next section.

Another metal that has been extensively studied as a replacement for Co is Mn. The use of Mn is particularly attractive due to the fact that it is less costly than Ni or Co and is more environmentally benign. $LiMnO_2$ has, in fact, been prepared in an orthorhombic layered structure (Fig. 14). Although it has a high theoretical capacity of 285 mA h g^{-1}, it is easily converted

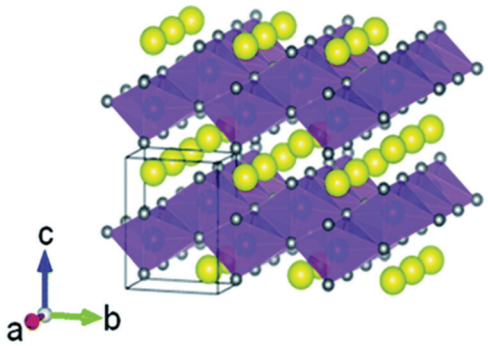

Fig. 14 Layered structure of $LiMnO_2$. Figure reproduced with permission from ref. 133. Copyright (2018) Royal Society of Chemistry.

to a spinel-like $LiMn_2O_4$ phase upon Li^+ deintercalation and has proven difficult to synthesize, often containing Li_2MnO_3 and $LiMn_2O_4$ phases which increase the rate of capacity fading. Although the conversion to $LiMn_2O_4$ actually increases the capacity of the material (Fig. 15h), the average voltage is so low that it is not competitive. Additionally, $LiMnO_2$ is susceptible to Mn dissolution in the electrolyte, degrading the structure at the surface and shortening the cycle life. Even with these deficiencies, it has reached practical capacities of $\sim$160 mA h g^{-1} and has seen some commercial use in primary batteries (non-rechargeable), though its lower energy density and poor lifetime compared to other layered oxides limit its application. Fig. 15g–i show the electrochemistry of LMO. The differential capacity plot in Fig. 15i illustrates the structural transformation from the first few cycles onward with the evolution of the peaks at 3.7–4.2 V.

4.2 NMC: Ni, Mn co-substitution into $LiCoO_2$

With the above limitations of LCO, LNO, and LMO, it is not surprising that significant efforts have been invested in looking for solid solutions with 2 or more of Ni, Mn and Co in the LCO structure. In the early 1990s, Delmas[141] suggested a solid solution of $LiNi_{1-y}Co_yO_2$ which allowed up to 0.6 Li to be reversibly deintercalated, increased from the 0.5 of LCO, and with optimization could reach 0.75 reversibly.[142] The material

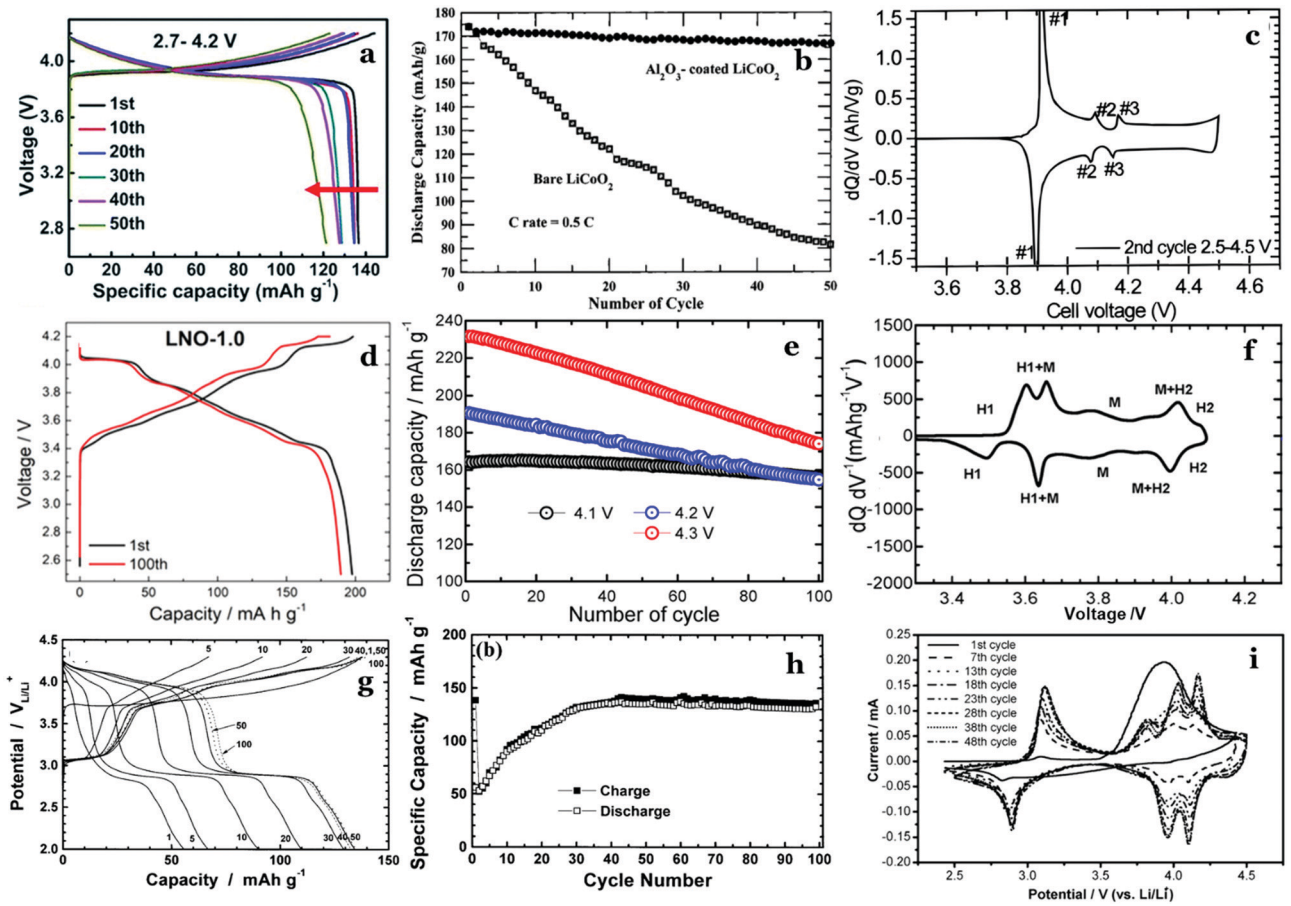

Fig. 15 (a) Charge/discharge curves for LCO cycling at a rate of 0.2C.[134] (b) First 50 cycles of bare and coated LCO cycled at 0.5C.[135] (c) dQ/dV plot of LCO second cycle illustrating structural transitions.[136] (d) First and 100th cycle (at C/3) of LNO prepared *via* optimized synthesis in pressurized atmosphere.[137] (e) Long term cycling of LNO at various upper cutoff potentials all at a rate of 0.5C.[138] (f) dQ/dV of LNO first cycle, denoting hexagonal (H) and monoclinic (M) phases and transtions.[138] (g) Charge/discharge curves of *o*-$LiMnO_2$ cycled at C/3.[139] (h) Long term cycling of *o*-$LiMnO_2$ at a rate of C/3.[139] (i) dQ/dV of *o*-$LiMnO_2$ over multiple cycles.[140] Figures reproduced with permission from ref. 134–140. Copyright (2019) Royal Society of Chemistry, copyright (2000) American Chemical Society, copyright (2000) IOP Publishing, copyright (2020) American Chemical Society, copyright (2017) American Chemical Society, copyright (2002) Elsevier, copyright (2007) Elsevier.[134–140]

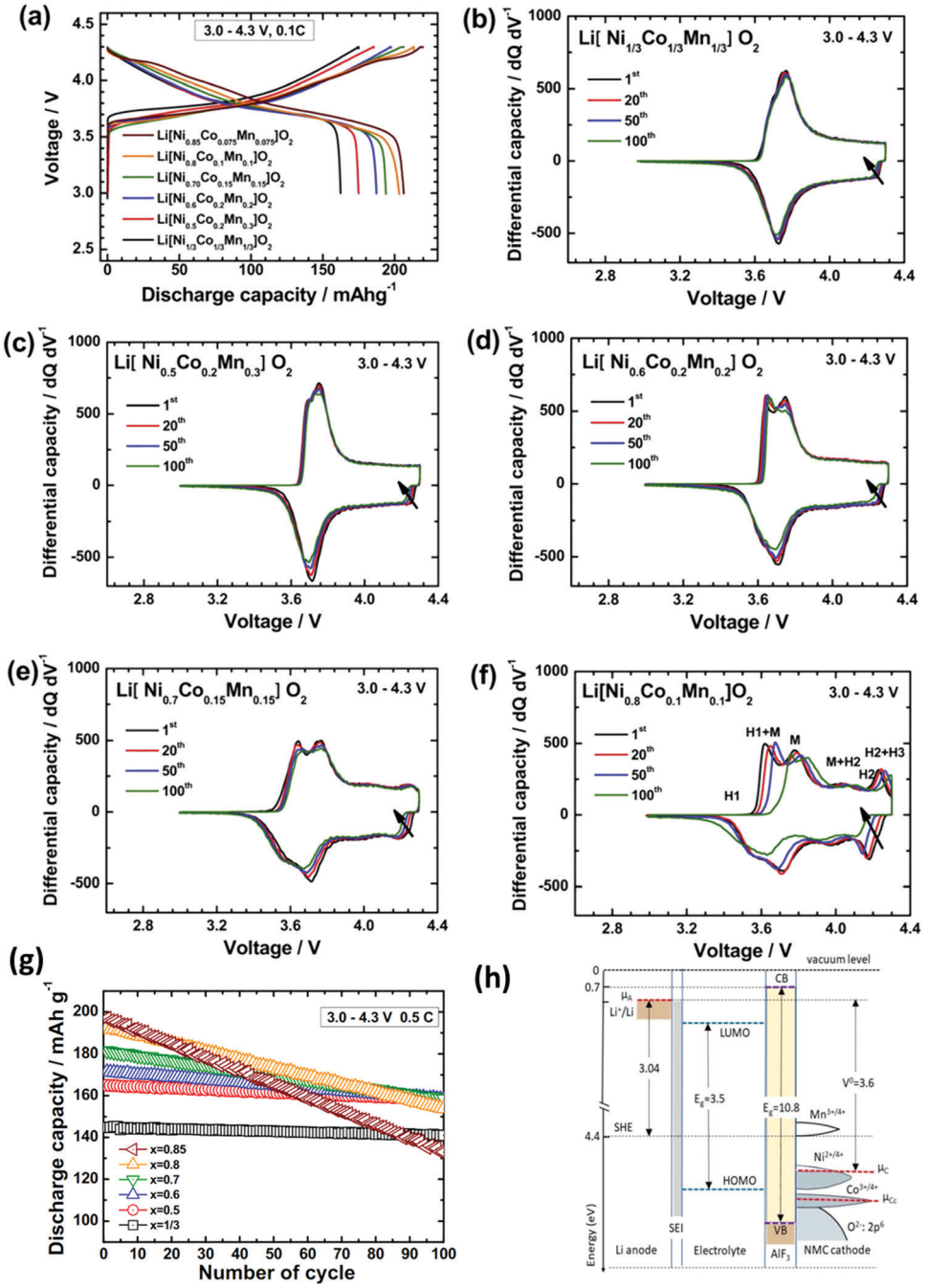

Fig. 16 (a) Charge/discharge curves for a variety of NMC compositions. (b)–(f) Differential capacity plots of various NMC compositions with increasing Ni content. (g) Long-term cycling of carious NMC compositions.[144] (h) Energy level diagram of NMC (with AlF_3 coating) relative to Li/Li^+.[145] Figures reproduced with permission from ref. 144 and 145. Copyright (2013) Elsevier and copyright (2019) AIMS Press.[144,145]

had the same structure as LCO, but with some Co replaced by Ni. It was found that the phase transitions of LNO were suppressed at 20% atom cobalt at potentials less than 4.08, only showing a single phase transition white LNO undergoes two (H1 → M → H2).[143] However, the $LNi_{0.8}Co_{0.2}O_2$ had worse cycling performance. The Dahn and Ohzuku groups simultaneously explored solid solutions of the form $Li[Ni_xMn_xCo_{1-2x}]O_2$ wherein the square brackets indicate the transition metal layer. In this material, Co takes the 3+ state while Ni and Mn take the 2+ and 4+ states, respectively.[16,17] These showed very good electrochemistry, comparable to LCO without phase transitions at high voltage as shown in Fig. 16(b–f). Fig. 16 shows the electrochemical properties of a wide range of NMC compositions.

Although this early work on NMC compositions gave rise to commercialized materials, given that nickel can take either the 2+ or 3+ oxidation states during synthesis, the chemistry of the NMCs is far richer than a single composition line. If one allows for Li non-stoichiometry (more to come on this in the Li-rich

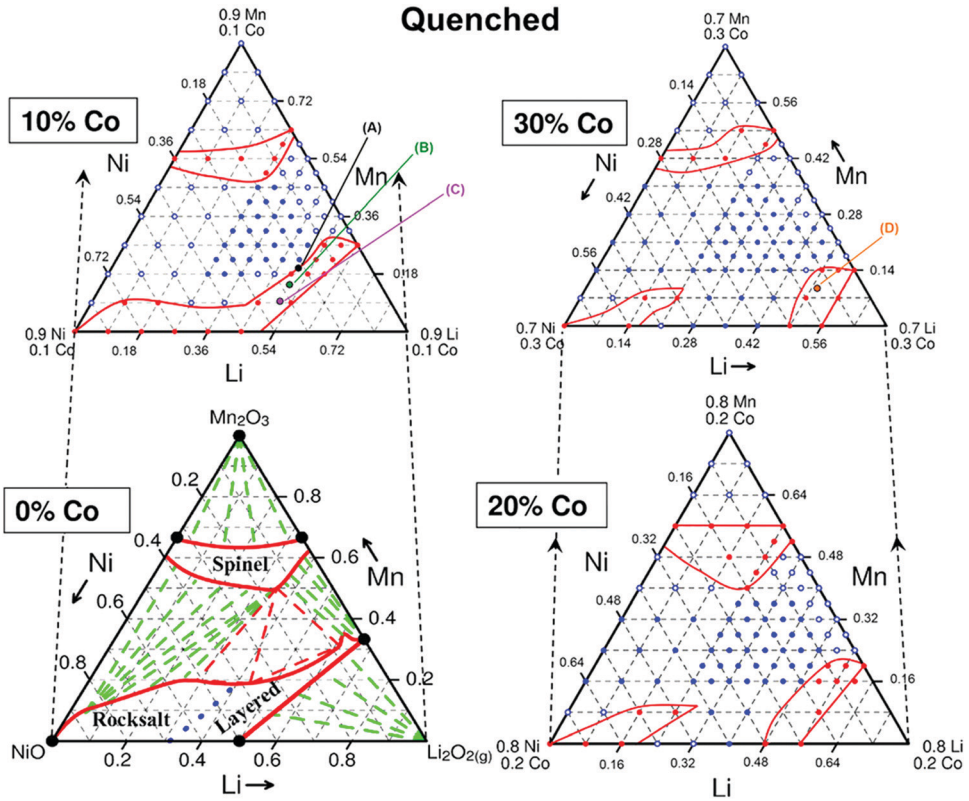

Fig. 17 Slices through the Li–Co–Mn–Ni–O pseudo-quaternary pyramid. The purple region in each slice represents the layered oxides of interest as Li-ion cathodes. Reproduced with permission from ref. 147. Copyright (2015) American Chemical Society.

oxide section below) then the solid solution region is a 3-D volume within the Li–Co–Mn–Ni–O pseudo-quaternary pyramid as illustrated in Fig. 17. In the combinatorial work that gave rise to the phase diagrams, it was found that the materials transform during cooling from high temperature such that the quenched samples may sometimes take different phases that the more slowly cooled samples.[146–148] Recently, in addition to structural characterization, there have been reports of combinatorial electrochemical characterization in the layered metal oxide cathode space paving the way to rapid complete cathode screening, allowing orders of magnitude more data to be obtained in the same amount of time as traditional methods.[149] Thus, a great deal of work has gone into examining NMC compositions of the form $Li[Ni_xMn_yCo_{1-x-y}]O_2$, which are often referred to by their TM compositions, for example NMC 532 refers to $Li[Ni_{0.5}Mn_{0.3}Co_{0.2}]O_2$, some of which are summarized in Table 1. Over a wide composition of x and y (particularly with low y to avoid high Mn compositions), NMC maintains the layered structure of LCO with the Co layers becoming transition metal layers with a distribution of all three TMs. Co is present in the 3+ oxidation state, while Ni is in the 2+ or 3+ oxidation state, depending on the relative amount of Mn, which is predominantly found in the 4+ oxidation state. If the ratio of Ni to Mn is 1 : 1, Ni is in the 2+ state. If Ni is in excess, the excess Ni is in the 3+ state.[150] There is, however, evidence to suggest that this is not always the case, as NMC 442 has been shown to have 20% of the Mn content in the 3+ oxidation state and 20% of the Ni in the 3+ oxidation state to compensate.[151] During cycling, the dominant redox-active metal is Ni, undergoing redox between Ni^{2+}/Ni^{4+}, while it has been suggested that Co^{3+}/Co^{4+} redox can be accessed once two thirds of Li are depleted in NMC111.[152,153] However, an irreversible change from O3 to O1 stacking occurs before 0.75 Li can be extracted.[154] In practice NMC has a capacity of around 150–190 mA h g^{-1} when cycled to 4.3 V,[155] depending on the composition, with a longer cycle life than both LNO and LMO attributed to an increased structural stability. NMC is also a safer cathode material than LCO, with a higher onset temperature for thermal runaway (Fig. 18).

Table 1 Summary of NMC compositions and typical capacities when charged to 4.3 V

Composition	Abbreviation	$Q_{Theoretical}$ (mA h g^{-1})	Q_{Actual} (mA h g^{-1})	Ref.
$LiNi_{1/3}Mn_{1/3}Co_{1/3}O_2$	NMC 111	278	145–175	166–168
$LiNi_{0.4}Mn_{0.4}Co_{0.2}O_2$	NMC 442	279	150–175	166 and 168–171
$LiNi_{0.5}Mn_{0.3}Co_{0.2}O_2$	NMC 532	278	150–170	172–174
$LiNi_{0.6}Mn_{0.2}Co_{0.2}O_2$	NMC 622	277	145–180	175–177
$LiNi_{0.8}Mn_{0.1}Co_{0.1}O_2$	NMC 811	276	170–200	164 and 178–180

While NMC is one of the most performant cathodes to date, like state-of-the-art-LCO, the cathode particles can crack due to the change in volume from intercalation/deintercalation and phase transformations, resulting in a larger surface area to

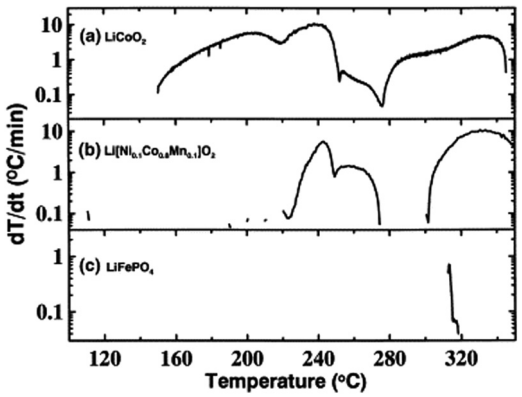

Fig. 18 ARC of LCO, NMC 118, and LFP showing the later onset of thermal runaway in both NMC and LFP compared to LCO. Figure reproduced with permission from ref. 159. Copyright (2004) Elsevier.

react with electrolyte and poorer overall performance.[68,156–158] Thus, the stability could be improved through substitutions and coating, which will be discussed in the next section.

Another issue addressed by the wide composition window of NMCs is related to an on-going effort to minimize the cobalt content. Cobalt is the most expensive element in the material and its sourcing is ethically questionable due to unsafe mining practices, contaminating local communities, and in some cases utilizing child labour.[160–162] As a result, contemporary cathodes have been moving toward Ni-rich compositions. The most studied in order of increasing Ni content are $LiNi_{0.4}Mn_{0.4}Co_{0.2}O_2$ (NMC 442), then $LiNi_{0.5}Mn_{0.3}Co_{0.2}O_2$ (NMC 532), $LiNi_{0.6}Mn_{0.2}Co_{0.2}O_2$ (NMC 622), and $LiNi_{0.8}Mn_{0.1}Co_{0.1}O_2$ (NMC 811). Specific discharge capacity tends to increase with increasing Ni content, but comes at the cost of decreased structural stability and cycle life.[144] Particularly problematic forms of structural instability are cation mixing and surface reconstruction due to metal loss through reactions with the electrolyte. In cation mixing, Ni migrates to Li sites, blocking Li diffusion. This phenomenon can be identified using a few indicators in XRD spectra: the c/a ratio, the intensity ratio of the 003 and 104 peaks.[163,164] Additionally, Ni-rich cathodes suffer from poor thermal stability due to the reactivity Ni^{4+} with the electrolyte, decreasing cycle life, poor rate performance, and decreased safety. A review of these issues can be found here.[165] Several methods have been explored to resolve the issue of structural instability and surface reactivity, most notably: coatings, metal substitutions, and core–shell structures (considered to be non-uniform substitutions within the context of this review article). Coating consists of applying a layer of a different material to the surface of cathode particles to prevent surface reactions, structural degradation, and cracking. Metal substitutions involve making a change to the TM composition through the entire material. Core–shell structures are a hybrid of these two approaches: the core of the particle is composed of one layered oxide, while the shell of the particle (usually significantly thicker than a traditional coating), is composed of a different, more structurally resilient, cathode material. The two materials must be close enough in structure to maintain the particle's integrity during battery operation. Herein, we focus primarily on metal substitutions but will also briefly explore other methods for the sake of comparison in order to evaluate whether the substitutions are warranted or if, for example, a simple coating yields a better battery material.

4.3 NCA: Co, Al co-substitution into $LiNiO_2$

The other mixed metal layered oxide of note is $LiNi_{1-x-y}Co_xAl_yO_2$ (NCA). The rationale of this material is similar to that of high Ni NMCs: Ni acts as the main redox-active component, while Co serves to enhance structural order and Al increases structural stability, though Co can contribute electrochemically at high potentials. The most common composition of NCA is $LiNi_{0.8}Co_{0.15}Al_{0.05}O_2$.[155] NCA materials have a high theoretical capacity of 279 mA h g^{-1} and in practice achieves 180–200 mA h g^{-1}.[181] It also has improved rate capability over NMC, giving it a higher specific power making it more suitable for the booming electric vehicle industry. As with NMC, LCO, and LNO, NCA also has a layered rock salt structure with alternating transition metal oxide and lithium layers with a mix of metals in each TM layer. NCA also suffers from similar issues to Ni-rich NMC materials. Li/Ni mixing is still an issue, causing structural degradation and impeding Li^+ intercalation paths. $LiNi_{0.8}Co_{0.15}Al_{0.05}O_2$ has been shown to have the best electrochemical performance out of a range of compositions,[182] balancing a high capacity with decent cycling life. There is also evidence that Aluminate impurities can form at concentrations above 5%.[182,183] Additionally, NCA has an improved thermal stability when compared to aluminum-free $LiNi_{0.8}Co_{0.2}O_2$, improving safety and high-temperature performance. Like other Ni-based cathode materials, Ni^{4+} is highly unstable at high temperature, reacting with HF in electrolyte and causing material degradation, namely at the surface.[184] Ultimately, NCA suffers from worse cyclability compared to non-nickel-rich NMC cathodes. Like NMC, coatings and substitutions have been studied to improve the structural stability and electrochemical performance, these will be discussed in the next section.

4.4 Substitutions into NMC and NCA

One appeal of studying the impact of substitutions on the layered oxides is that metal substituents can be easily incorporated into existing synthesis methods thus ensuring easy scale-up. The most commercially-relevant synthesis route for layered TM oxides is a solution-based co-precipitation synthesis.[185,186] This method takes place in two stages. First, a precursor material is prepared by dissolving the desired metals in the form of sulfates, nitrates or acetates into a pH-controlled solution at the desired stoichiometric ratios. Ammonium is then added to the solution to act as a chelating agent, and NaOH is added to cause co-precipitation. With careful control of the reaction conditions (temperature, pH, stir rate, flow rates of reactants), the morphology can be tuned to give large spherical particles as shown Fig. 19.[187] The second phase is to add a lithium source such as LiOH is then added to the dried and rinsed precursor ($M(OH)_2$ where M is the mixture of TMs) and heated to high temperature 800–1050 °C are commonly

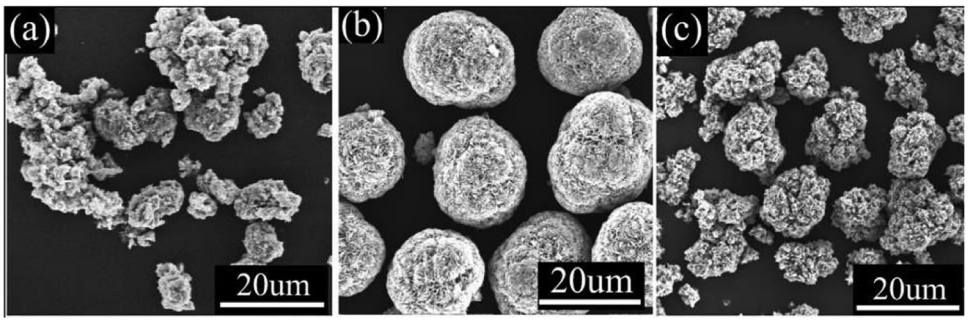

Fig. 19 Optimized synthesis of layered oxide cathode material. Figure reproduced with permission from ref. 187. Copyright (2015) Elsevier.

used to obtain a lithiated layered cathode material. Successful syntheses have been reported by either adding the metal substituent at the precursor or at the lithiation phase. Although these are in principle equivalent, one would expect a more uniform substitution when done at the precursor stage while substitutions at the lithiation stage might yield a structure closer to a core–shell (*i.e.* more of the substituent would be found at the surface of particle unless aggressive sintering conditions are used). Alternatively, the material can be produced through a purely solid-state reaction wherein metal oxides or hydroxides (including Li) are mixed in the desired stoichiometric ratio using a mortar and pestle or milling before being heated to the desired temperature to yield the final product.[188,189] However, this tends to give a less homogeneous product and requires much longer sintering times in order to reach the equilibrium layered phase.[190] Given that the industrial norm is to use co-precipitation, this is the synthesis route of choice for studies of substitutions into NMC or NCA. After synthesis, it is important to determine the composition of the material. While in the case of doping into semiconductors, the substitution levels are so low that the level of substitution can only be confirmed by the impact on the properties, this is not the case in the vast majority of substitution studies into battery materials. Specifically, the %-level substitutions can be readily verified using inductively coupled plasma coupled with optical emission spectroscopy, atomic emission spectroscopy, or mass spectroscopy (ICP-OES, ICP-AES, or ICP-MS).[191–193] Though ICP techniques do not distinguish between coatings, bulk substitutions, and additional material phases, it is useful for verifying the presence of the substituted metal and, more importantly, the Li content of the synthesized material.[194] To verify whether the metal substitution was successful in penetrating the material, electron microscopy and X-ray techniques such as SEM-EDX and XRD may be used to determine where the substituent ended up within the material (see Section 3 for more detail).[195]

Many metals have been substituted into layered oxide materials to increase their performance and longevity, including Al, Ti, Mg, Zr, Nb, Y, La (Fig. 20). The effects of the substitutions are manifold and a single substituent may result in multiple effects making it difficult to fully evaluate its impact. Substitutions have been shown to prevent cation mixing, suppress phase transitions, and prevent reaction with electrolyte. For layered metal oxide cathode materials, the two most well-studied substitutions are Al and Ti. Both have been shown to increase lifetime, but at the cost of capacity, as both substituents are electrochemically inactive. These will be explored in more significant detail due to the volume of experimental and theoretical work.

Fig. 20 shows a summary of the impact of substituent metals and select surface coatings on discharge capacity and percent capacity loss per cycle on various NMC compositions. Fig. 21 shows the same information, but for NCA cathodes. In all cases, one finds a wide variety of performance for unsubstituted NMC/NCA, which makes comparison between studies impossible. Thus, for Fig. 20 and 21, we report the performance for the unsubstituted material for that study in blue and the optimum substituted performance in red. For long-term cycling, the minimum number of cycles was 50 and maximum 250. It is clear that many substituents and coatings decrease capacity fade while having only a small impact on capacity, and sometimes a beneficial one. It is also clear that there is significant variation in pristine cathode materials making direct comparisons between different articles difficult, though looking at the relative picture of the performance of pristine materials *vs.* their substituted counterparts useful conclusions can be made. It is also worth noting that in many cases, a series of substituent concentrations were presented in the papers from which these data were extracted; only the best performing composition is reported here.

The variance in material performance is exemplified by the inconsistent behaviour of Al-substituted NMC. In most reports of Al-substituted NMC, the initial capacity is decreased,[222,223] though there are some experiments that show the contrary using a similar composition and synthesis method. An increased capacity has also been reported in NMC 111 by Hashem *et al.*[224] who suggest that the increased capacity is due to reduced anti-site defects and the reduced cyclability is due to strain placed on the lattice through Al substitution. It is also possible that the discrepancy may be the result of synthesis conditions, as the material by Hashem *et al.* was synthesized by the sol–gel method while the others cited in this work used the co-precipitation technique. In Ni-rich NMC, Al^{3+} has been shown to increase the retained capacity by nearly 20% while only reducing the initial capacity by less than 1.2%.[198] This is attributed to a relief in lattice strain caused by Co^{3+} as it is substituted by Al^{3+} introducing stronger

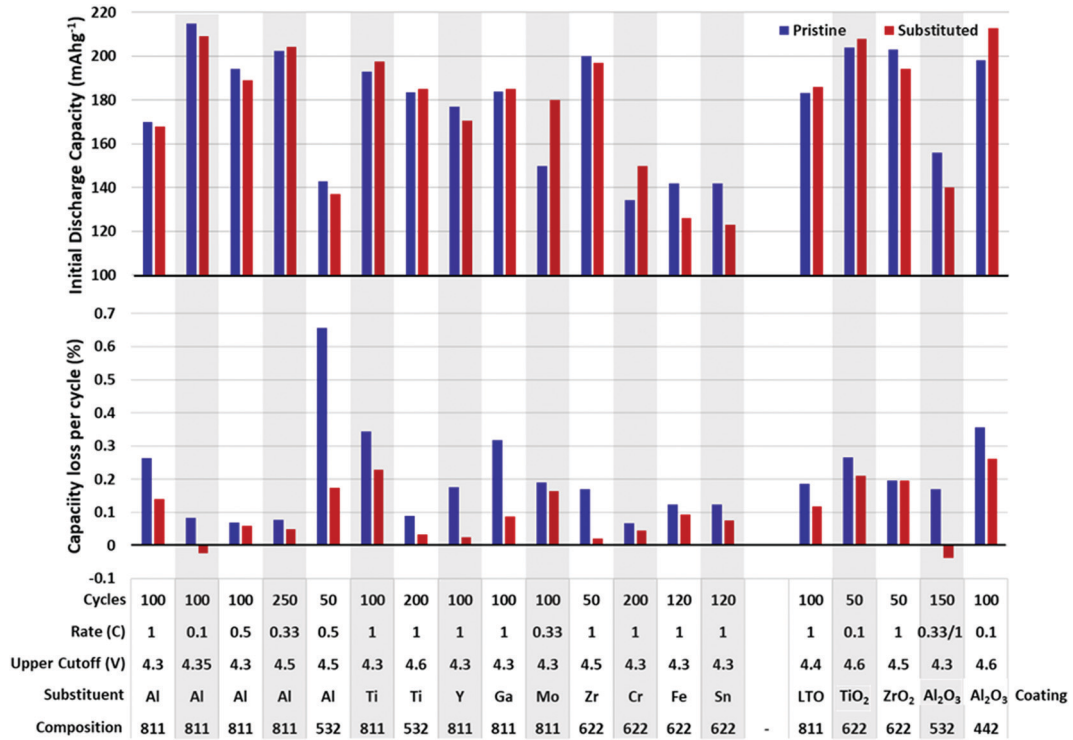

Fig. 20 Initial reversible capacity (top) and capacity lost per cycle (bottom) of pristine and substituted or coated NMC materials. Data extracted from ref. 19, 33, 178, 188 and 196–208. Below each plot is listed the cycling rate, upper cutoff voltage, substituent/coating, composition of unsubstituted. The gap in the *x*-axis separates substitutions from coatings.

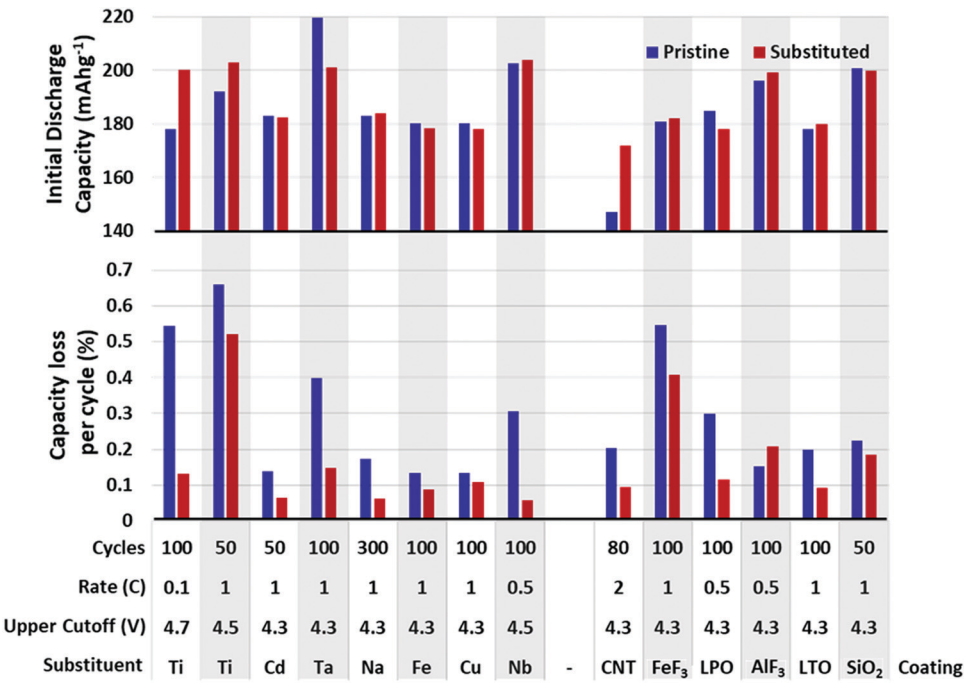

Fig. 21 Initial reversible capacity (top) and capacity lost per cycle (bottom) of pristine and substituted or coated NCA materials. Data extracted from ref. 209–221.

Al–O bound that reduces the amount of cracking and electrolyte penetration. This is supported by calculations on the NMC 532 composition, which point to the strong Al–O iono-covalent bonding stabilize the cathode structure.[225] The decreased

capacity fade observed by Zhao[198] was also attributed to the formation of Al–O compounds on the surface of the NMC particles, acting as a weak coating that can scavenge HF and prevent structurally compromising reactions between the cathode and electrolyte.[197] The protective effects at the surface can be improved through gradient substitution, where the more susceptible surface of the material has a higher Al content to protect from material degradation, while the less vulnerable centre maintains its pristine, or near-pristine composition, gaining the improved capacity of the unsubstituted material without compromising cycle life.[226] Al^{3+} substitution also increases thermal stability and safety of Ni-rich NMC materials, offsetting the onset of exothermic reactions and making their onset more gradual.[197,226] Aluminum substitution has also been shown to decrease Li/Ni mixing in NMC 662 when substituted for Mn and in 811 which likely contributes to the increased stability seen in these compositions when substituted.[226,227]

Titanium also proves to be an effective substitution for layered metal oxides. Like Al, it has been shown to increase capacity retention significantly, while actually increasing reversible capacity.[188,199,228] Though, there have been capacity decreases reported in NMC 811.[229] When Ti^{4+} is substitutes Co^{3+} the charge is compensated *via* Mn^{4+} reduction to Mn^{3+}. While Mn^{3+} is Jahn–Teller active, the structural stability gained through Ti substitution appears to outweigh any negative effects of Mn^{3+}.[228] The increase in cycle life in Ti-substituted NMC is broadly attributed to stronger Ti-O bonds improving the structural integrity of the material and preventing particle cracking and is supported by DFT calculations.[229,230] In Ni-rich NMC, Ti^{4+} substituent increases the reversibility of the H2-H3 phase transition and reduces lower polarization during cycling, which would also improve electrochemical performance.[231] Ti has also been shown to be an effective substitution in NCA. In contrast with NMC, Ti^{4+} has been shown to reside in octahedral Li^+ sites. This expands the interlayer distance, allowing for easier Li^+ movement as well as reducing the severity of Li/Ni mixing.[210,232] Liu *et al.* have found the concentration of 1% atom to be optimal. Ti may also act as ''pillar'' ions, supporting the structure through repeated lithiation/delithiation and preventing collapse.[233]

Zirconium has also been explored as a substituent in both NMC and NCA.[202] Similar to Ti, Zr has a larger radius than Ni, Mn, and Co in their regular oxidation state in NMC, causing a volume expansion of the lattice and interlayer spacing. Zr has also been found occupying Li^+ sites, increasing the lattice spacing on the *c* axis and serving similarly to Ti in NCA as a ''pillar'' ion, stabilizing the structure during lithiation/delithiation and discouraging Li/Ni mixing. Zr has been found to perform similarly in terms of cycling performance and capacity loss as Ti substitution.[234] Zr and Zr, F co-substitution was also shown to increase capacity retention by over 15% over 200 cycles in NCA.[235]

The poor performance of Fe substitution in both NMC and NCA is attributed to a hindrance of Li diffusion. Though it has also been shown that the incorporation of Fe^{3+} increases the thermal stability of NMC 622.[204] Fe was also shown to decrease Li/Ni disorder in NCA along with Cu substitution.[214] The electrochemical performance of some other substituents are shown in Fig. 20 and 21.

While many metals have been used as substituents in layered transition metal oxides, there is still much to explore. Multi-metal substitutions are studied sparingly and open an enormous space of possible combinations to be optimized. Several metals have not been used as substituents in the literature, specifically many of the lanthanides and heavy d-block elements, and the concentration and method of substitution has not been optimized for many materials. There is also the issue of ensuring that scale-up is feasible for the substituted layered oxide materials, as many studies use solid-state syntheses that are not employed at the industrial scale. Thus, there is work to be done adapting metal-substituted cathode synthesis with scalability in mind.

4.5 Substitutions *vs.* coatings

Coatings for layered metal oxide materials come in a wide variety. There are metal oxides,[172,236,237] polyanionic lithium compounds,[238,239] fluorides,[240,241] and more that have been used with some success. Coatings serve to stabilize the surface of the cathode particle without inhibiting Li^+ diffusion. There are several methods of applying coatings to cathode materials such as co-precipitation, sol–gel, and various deposition techniques. Wet chemical techniques are desirable, as they are economical compared to other methods while being easier to integrate into industrial cathode syntheses. In co-precipitation synthesis, the metal oxide precursor is synthesized as described previously. Then the synthesized cathode and soluble form of the material to be coated (*e.g.* the acetate, nitrate, or sulphate of the metal to be coated as a metal oxide) are stirred in a reactor, dried, and annealed at 300–500 °C.[242–244] This method also works with metal phosphate and fluoride coatings by adding the metal phosphate for phosphate coatings, or the metal nitrate and ammonium fluoride for fluoride coatings, in solution with the prepared pristine cathode material before drying and annealing.[245,246] Note the reduced temperature in the annealing process compared to the calcination temperature of 800–1050 °C used for the layered oxide synthesis. If the temperature used for sintering the coating is too elevated, substitutions into the layered oxide may occur. In such cases, non-uniform coatings will occur, potentially leaving some surface area of the cathode material exposed, thereby reducing the effectiveness of the coating.[247] Sol–gel techniques suffer a similar deficiency. Alternatively, deposition techniques such as atomic layer deposition and sputtering can be used to achieve a more uniform coating. However, due to their cost, it is unlikely these methods will be used in full-scale cathode production.

Alumina is perhaps the most studied coating, as discussed previously, it was used to stabilize LCO and has been used to stabilize NMC.[208,248–253] It has been shown to prevent TM reduction at the surface, oxygen loss, and even prevents phase transformations.[208,254,255] It has also been shown to scavenge

HF, forming protective Al–F compounds, resulting in a healthier SEI layer.[256] Titanium coatings have been shown to be similarly effective.[206,257–259] See Guan for a more rigorous review of cathode coatings.[18]

Alternatively, performance can be improved using a core–shell structure, or a core–gradient–shell structure.[260–267] The idea behind a core–shell particle is to have high energy density cathode material in the core, surrounded by a more stable, yet still active, cathode material to protect the core from degradation (Fig. 22a–c). Fig. 22d demonstrates how effective this approach can be in prolonging cycle life, while only minimally reducing the specific capacity of the overall cathode. This technique can also improve the safety of Li-ion batteries by improving the thermal stability of the cathode overall. For example, a core–shell gradient was able to suppress the cathode self-heating onset temperature by over 40 °C.[268] Being an active cathode material itself, the shell is ionically conductive toward Li^+ and does not significantly dampen rate performance.[266,267] One shortcoming of core–shell particle design is the susceptibility to internal separation of the core and shell.[260] Upon repeated expansion/contraction of the materials, strain is placed on the interface, eventually causing a separation of the two materials. This separation allows electrolyte to access the more-susceptible core and react with its surface, causing material degradation and metal dissolution. This problem has been partially addressed by using gradient compositions to smooth the transition between core and shell. This has reduced the propensity for internal separation of core and shell to occur, but cracking of the particle remains an issue. Fig. 23 shows the effectiveness of several core–shell compositions.

5. Li-Rich layered oxide cathodes

5.1 Ordered Li-rich oxides

At the same time as NMC solid solutions were being discovered and studied for commercialization, another class of layered oxide cathodes was discovered. In 2001, the Dahn group looked at $Li[Ni_xLi_{1/3-2x/3}Mn_{2/3-x/3}]O_2$ which take the same layered structure as LCO, NMC and NCA, but with some excess lithium present on the transition metal layer[277–279] Fig. 24 shows the electrochemistry for these materials. Up to 4.4 V, the cycling looks very much like any other layered material. However, above 4.5 V, the material transforms during first charge and the result is a far larger reversible capacity well beyond that expected based on Ni redox alone (*e.g.* for x = 1/4, Ni

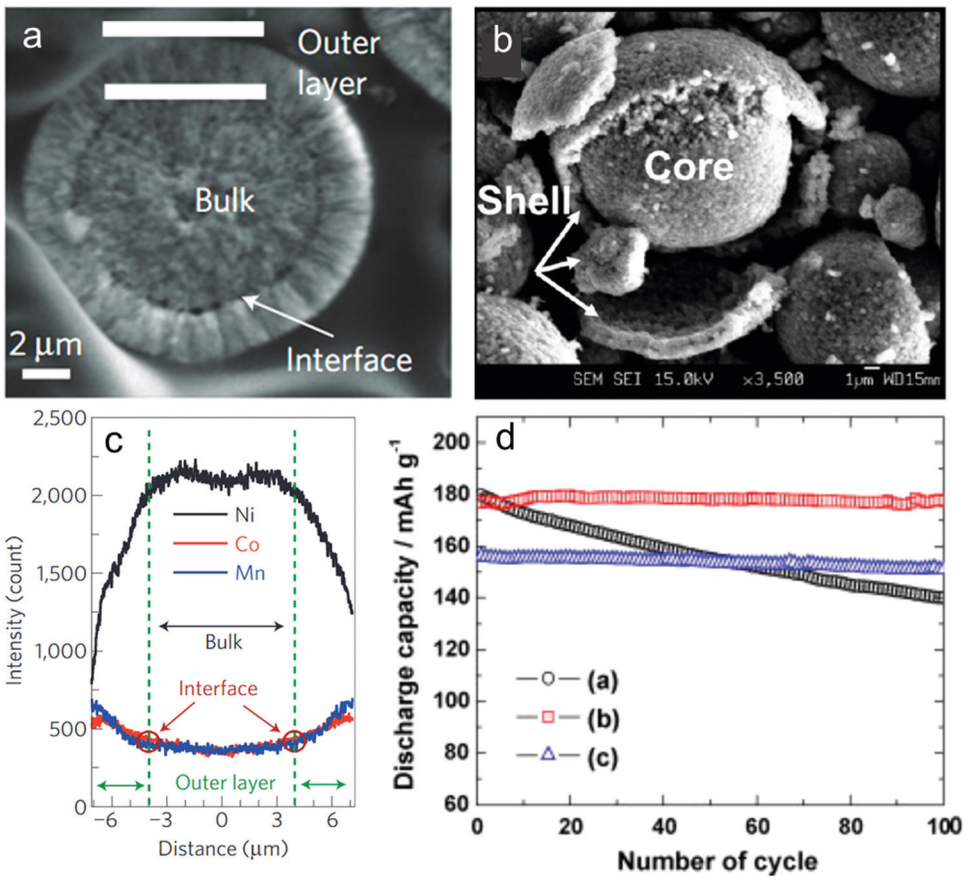

Fig. 22 (a) Pristine core–shell particle. (b) Particle with core–shell separation. (c) Metal concentration distribution in core–shell particle. (d) Long-term cycling of (a) NMC 111 core material, (b) $LiNi_{0.5}Mn_{0.5}O_2$ shell material, (c) $Li[(NiCo_{1/3}Mn_{1/3})_{0.8}(Ni_{1/2}Mn_{1/2})_{0.2}]O_2$ core–shell material. Figures reproduced with permission from ref. 260, 269 and 270. Copyright (2014) American Chemical Society, copyright (2009) Nature, copyright (2010) Elsevier.

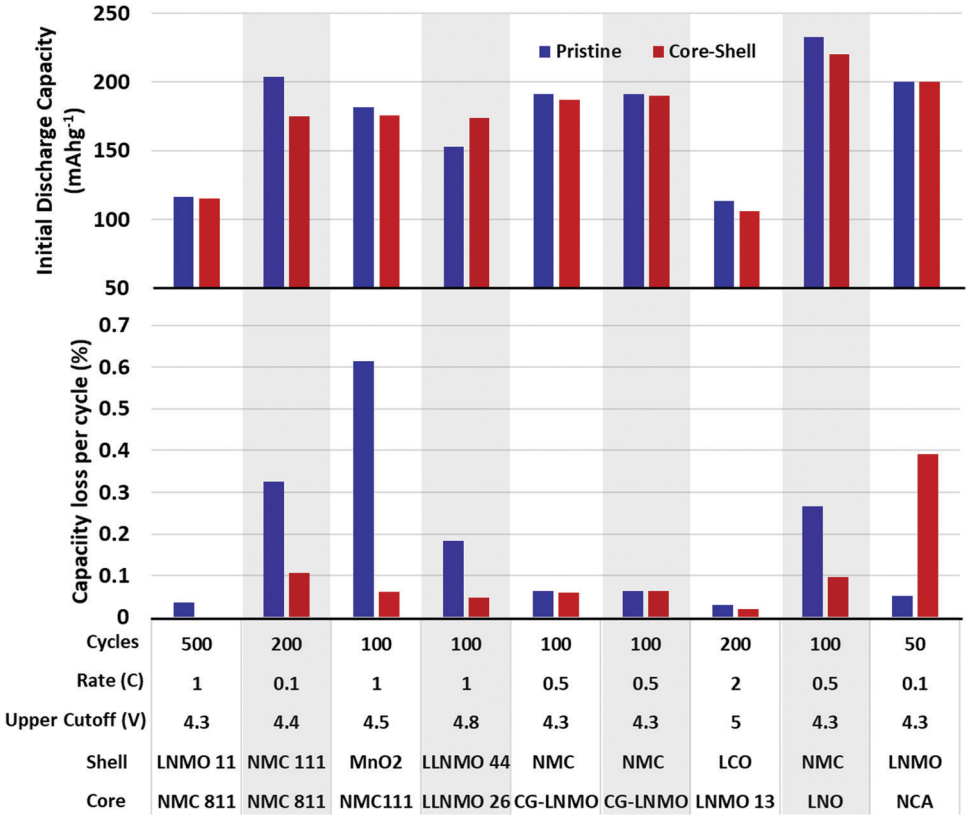

Fig. 23 Initial reversible capacity (top) and capacity lost per cycle (bottom) of core–shell materials. Data extracted from ref. 261, 262 and 271–276.

redox accounts for the first 120 mA h g^{-1} then the remaining 180 mA h g^{-1} on charge is unaccounted for).

This peculiar class of material has now been studied extensively both in terms of designing a better commercial cathode but also from the fundamental point of view to understand the mechanisms involved. We will review both here. This new class of cathode materials are the Li-rich cathode materials, where more than one Li atom is present per atom of transition metal in the layered structure such that the stoichiometry is of the form $Li[Li_xM_{1-x}]O_2$. The materials of highest interest for commercialization have Ni, Mn, and Co as the M atoms such that they are referred to as Li-rich NMC. As shown previously in Fig. 17, there is a wide range of compositions in the layered region in the Li–Ni–Mn–Co–O system, and a high portion of these are Li-rich. A few key compositions have been studied extensively including: $Li_{1.2}Mn_{0.6}Ni_{0.2}O_2$ (x = 0.2 in the $Li[Ni_xLi_{1/3-2x/3}Mn_{2/3-x/3}]O_2$ notation),[280–283] and $Li_{1.2}Mn_{0.54}Co_{0.13}Ni_{0.13}O_2$.[284–288] Each of these materials show the same key features: (1) a large reversible capacity beyond that expected from metal redox, (2) an irreversible transformation on first charge, and (3) a gradual decrease in average voltage with extended cycling (voltage fade). The Li-rich oxides therefore show a significant increase in capacity over all commercialized cathodes, reaching greater than 250 mA h g^{-1}.[289] However, this class of material is plagued by voltage fade, poor rate capability, and a gradual transformation towards a spinel-like material particularly in the Li-rich materials that have a high Mn content.[25,95,290,291] Nonetheless, Fig. 24 makes it clear that composition has a great impact on the cycling performance and so continued study in varied compositions, including substitutions into Li-rich NMCs, are certainly warranted.

5.2 Mechanisms during battery operation of Li-rich oxides

The complex electrochemistry taking place in the Li-rich oxides has taken over 15 years to understand, with some clarity still lacking. It is impossible to discuss the role of substitutions into these materials without first discussing the mechanisms involved during battery use. As mentioned above, the simple model of TM redox compensating all Li removal that worked so well for 30 years in layered oxides fails entirely when it comes to Li-rich oxides. Ten years after their discoveries, two groups simultaneously identified that much of the reversible redox that is generated after the first charge comes from reversible oxidation of oxygen.[55,285–287,292–295] There is still debate on whether or not the oxidation of oxygen results in O–O dimers in the Li-rich NMC,[296] but there is no longer any debate as to whether or not reversible oxidation of oxygen occurs. This accounts for a great deal of the extra capacity seen, and a great hunt has been underway to find materials that engage oxygen redox while minimizing oxygen gas loss. Oxygen loss in Li-rich oxides certainly occurs,[280,297] but only from the surface of particles[286] and this results some activation of Mn (*i.e.* it can be reduced from 4+ to 3+ during the next discharge) but it also

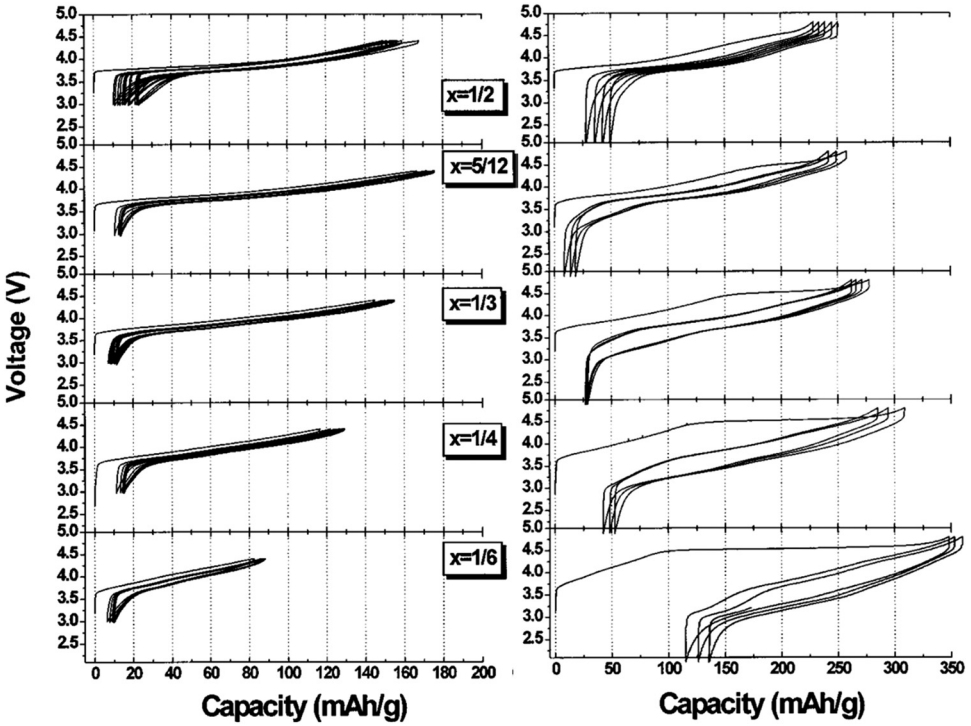

Fig. 24 Voltage curves for $Li[Ni_xLi_{1/3-2x/3}Mn_{2/3-x/3}]O_2$ up to 4.4 V (left) and up to 4.8 V (right). Whereas all samples look similar to traditional layered oxides like LCO up to 4.3 V, they all undergo an irreversible change upon cycling above 4.5 V and this leads to a large reversible capacity as high as 230 mA h g^{-1}. Figure reproduced with permission from ref. 279. Copyright (2002), IOP Publishing.[279]

gives rise to some irreversible capacity if there is insufficient Mn to compensate.

However, none of these mechanisms explain voltage fade. Studies on model systems (Li–Ru–Ti–O) showed that during the first charge, there is a massive migration of TMs from the TM layers to the vacant Li layers.[292,298] This occurs reversibly, with a return to the highly ordered layered structure at the end of discharge. Mobile atoms like Ti do this readily, but gradually with continued cycling, the Ti was found to be trapped in tetrahedral sites near the Li layer. This trapping of Ti simultaneously gives voltage fade and starts the transformation towards the spinel-like material since in Li-rich NMCs. Thus, it appears that the voltage fade comes from an imperfect TM migration during cycling.[299] The working principle has been that, in the Li-rich NMC materials, the severe voltage fade is attributed to the formation of spinel-like domains where Mn gets trapped in tetrahedral sites. Additionally, surface stability remains an issue due to Mn dissolution through electrolyte loss, causing structural disorder at the surface, increasing impedance, lowering capacity and contributing to voltage fade. Thus, improving the structural stability and interfacial stability of these materials is of the utmost importance. Several coatings and substitutions have been applied to achieve these goals and will be reviewed in the next section.

5.3 Substitutions into Li-rich oxides

There has been a significant effort investigating the effects of substitutions in lithium-rich materials (Fig. 25). As mentioned earlier, these Li-rich materials suffer from significant capacity and voltage fade, thus improving structural stability is the goal of substitutions in this case. Stemming from work done on layered oxides, Al and Ti have been substituted extensively into Li-rich materials to varying effect. In $Li_{1.5}Mn_{0.675}Ni_{0.1675}Co_{0.1675}O_2$, Al^{3+} occupies Li^+ sites, improving the kinetics of lithiation/delithiation and reducing impedance, thus increasing rate performance.[300] In $Li[Li_{0.23}Ni_{0.15}Mn_{0.52}Al_{0.10}]O_2$ it was found that the presence of Al improved long-term cycling performance, and rate performance.[301] It has been hypothesized that Al helps prevent Mn migration causing the conversion to spinel-like phases. In $Li_{1.2}Ni_{0.16}Mn_{0.56-x}Al_xCo_{0.08}$, Al^{3+} was substituted for Mn^{4+} at compositions ranging from x = 0–0.08 and mainly occupied TM layer sites while causing the formation of some Ni^{3+} to compensate for the aliovalent substitution. This reduced initial capacity, likely due to suppression of material activation, while greatly increasing capacity retention and reducing voltage fade by over 50% in the case of x = 0.08.[302]

Ti has been shown to function similarly to Al. Ti^{4+} has also been shown to occupy Li^+ sites and increase repulsion with Mn^{4+}, suppressing Mn migration while reducing oxygen loss due to stronger Ti–O bonds.[303] Feng *et al.* showed through theoretical work that Ti in the Li later reduced the band gap in Li_2MnO_3, increasing the electrical conductivity of the material and confirmed that the activation energy of Mn migration increased compared to the pristine material.[304]

Chromium has also been substituted into Li-rich oxides with some success. When Cr was substituted into TM sites, it suppressed

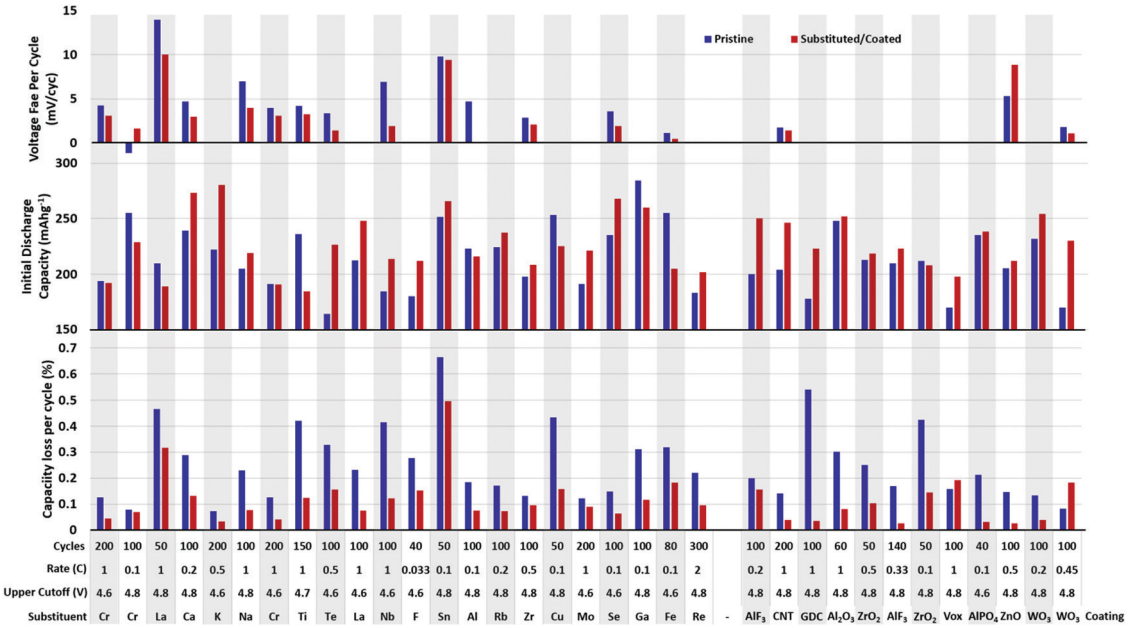

Fig. 25 Voltage loss per cycle (top), initial reversible capacity (middle), and capacity lost per cycle (bottom) of pristine and substituted or coated NCA materials. Data extracted from ref. 100, 303, 305 and 308–337.

voltage fade, but also lowered the energy density. The authors hypothesized that the stronger Cr–O bonds may hinder anionic redox. Stronger TM–O bonds may also prevent full activation of the Li-rich material, lowering capacity.[305]

Magnesium substitution can behave similarly to Ti substitution, replacing Li and acting as a pillar, while also opening Li-ion channels, improving structural stability and rate capability.[306] Mg^{2+} substitution has also been shown to lower capacity if it replaces Mn. This capacity loss is attributed to the inactivity of Mg and potentially also due to stronger Mg–O interactions preventing anionic redox or hindering activation of Li_2MnO_3.[307] Similarly to the stoichiometric layered metal oxides, there is still much to explore in the multi-metal substitution space with Li-rich materials. The greatest need is in preventing the voltage fade, where numerous studies have shown this can be done *via* metal substitutions in model systems (using expensive metals such as ruthenium and iridium),[293] the key now is to obtain the same performance using materials that are cost-effective. Some work has been done in this regard, using selenium[308] and iron[309] substituents, but there is far more optimization required to see the potential benefit of metal substitution on reducing voltage decay.

5.4 Disordered rocksalt Li-rich oxides

In the Li–Ni–Mn–Co–O system (Fig. 17), there are the ordered layered materials that have been of high interest, but at lower Li content we see the rocksalt region. The rocksalt structure (or disordered rocksalt) is identical to that of the layered oxide, except every metal layer is a random distribution of Li and TMs. At low Li contents ($x < 1.2$ in $Li_xM_{2-x}O_2$), the Li lies in 3-D networks but there is insufficient Li to ensure percolation and as such these prove to be very poor cathode materials due to limited Li diffusion. In 2014, the Ceder group showed that at higher Li content one can obtain a disordered rocksalt phase with percolation of Li, such that the cathode can be charged by 3-D diffusion through the disordered Li channels wherein Li may diffuse through paths without any nearest-neighbour TMs.[338] This was obtained on Li–Mo–Cr–O materials that in fact crystallized in the layered structure but converted to the disordered rocksalt (DRX) structure during the first charge.

Since that time, there has been a search for Li-rich materials that can be made directly in the DRX structure and this has proven to be a very rich chemistry allowing for vast substitutions (both cationic and anionic with F being partially substituted for O). As such, these materials are of high interest in the current review article. It should be noted that one DRX material, $LiNi_{0.5}V_{0.5}O_2$, shows a high capacity of 264 mA h g^{-1} despite not having excess Li,[339] thus the percolation condition may not prove essential in these materials. Regardless of composition, the synthesis method of choice for DRX materials is mechanochemistry wherein ball milling is used to make the desired materials. Room-temperature ball milling prevents the layered materials from forming and also keeps the particles small, which proves necessary in order to extract the lithium. An example of a DRX formed during synthesis is Li–Mn–V–O and the electrochemistry of this material is shown in Fig. 26. The cycling curve no longer shows an irreversible transformation during the first charge, in fact the irreversible capacity is negligible.[340] The discharge capacity is also extremely high, approaching 300 mA h g^{-1}, slightly greater than that achieved in the best Li-rich layered oxides. Despite these very promising features, there are a number of detrimental features in the electrochemical performance that are making industrial application of these materials difficult. In particular, the transport

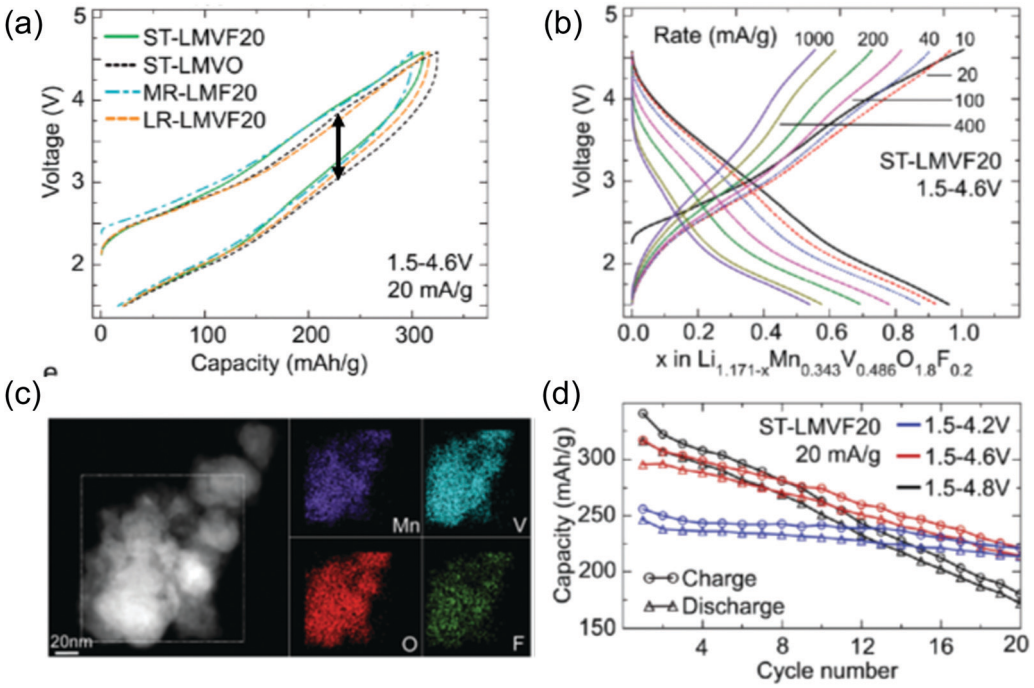

Fig. 26 Battery performance of DRX Li–Mn–V–O–F: (a) first cycle voltage curves for Li1.143Mn0.286V0.572O2 (ST-LMVO) as well as some materials with partial substitution of oxygen with fluorine, (b) the rate performance, (c) SEM with EDX map showing the small particles, and (d) extended cycling showing the rapid capacity fade. Adapted with permission from ref. 340. Copyright (2018) Royal Society of Chemistry.

properties are poor and as such the materials must be made with nanoscale size particles (Fig. 26c) in order to shorten the diffusion lengths, and they must be coated with carbon to increase the electronic conductivity. Both these approaches have proved very successful in cathodes operating well within the stability window of the electrolytes (*e.g.* $LiFePO_4$ to be discussed in the next section), but the DRX materials are typically cycled to 4.6 V or higher. The high surface area of the small particles with carbon present to catalyze reactions yields a high rate of electrolyte degradation. This in part leads to the poor long-term cycling seen in Fig. 26d. Another concern with the DRX materials is the large hysteresis seen during cycling (difference between charge and discharge voltages, shown as a black double-ended arrow in Fig. 26a). This is often on the order of 1 V; since the average voltage is on the order of 3.1 V[341] this hysteresis results in an inefficiency of about 33% in the battery simply based on voltage. Commercial Li-ion batteries are about 90% efficient and the cathode typically has a hysteresis around 1% or less (*e.g.* 1% in Fig. 24 up to 4.4 V). The high efficiency is one of the strong selling points of Li-ion batteries over other energy storage/conversion systems such as hydrogen fuel cells. A large hysteresis implies a much larger strain on the electric grid in order to obtain the same battery performance. It should be noted that the Li-rich oxides also have a larger hysteresis but this is considerably mitigated compared to DRX (0.25–0.4 V is seen in Fig. 24 up to 4.8 V). Also, similarly to Li-rich layered oxides, the DRX materials show voltage fade as shown in Fig. 27 where it is about 20 mV per cycle. This fade is larger than most of the Li-rich oxides discussed previously. Great care must now be taken to track these key metrics as more studies are performed on the DRX class of cathodes.

Despite these challenges, the DRX materials are promising given their very high capacities and they also are of high interest given that they can accommodate a wide variety of substituents.[341] Recently, DRX materials were demonstrated with both 5TMs and 11TMs, implying a very rich chemistry of possible substitutions.[341] This class of materials is still quite early in its development, and it is now essential to track the key metrics limiting its use (hysteresis, voltage fade, and capacity fade) as substitutions are made. In the case of the 6 cation substitution, the impact on these metrics was mitigated, but there was a marked improvement in the rate performance suggestive that the transport properties were improved.[341] Despite this, the hysteresis remains high (0.9–1.3 V during cycling and 0.4 V during relaxation measurements, GITT). The GITT measurements show that a significant portion of the hysteresis is intrinsic to the material and cannot be eliminated by cycling more slowly. We speculate that this is due to the disordered 3D percolation paths, which one would expect to have a higher intrinsic resistance to Li transport than do the ordered 2D sheets in traditional layered oxides.

It is too early to discuss systematic studies looking at the impact of substitutions into DRX materials as there are no clear compositions that are being optimized. But there are a number of studies looking at the performance of various DRX materials and they are summarized in Table 2. A more complete review[342] has been published recently and clearly demonstrates that to date the emphasis has been solely on maximizing the discharge capacity and improving the lithium conductivity, with few

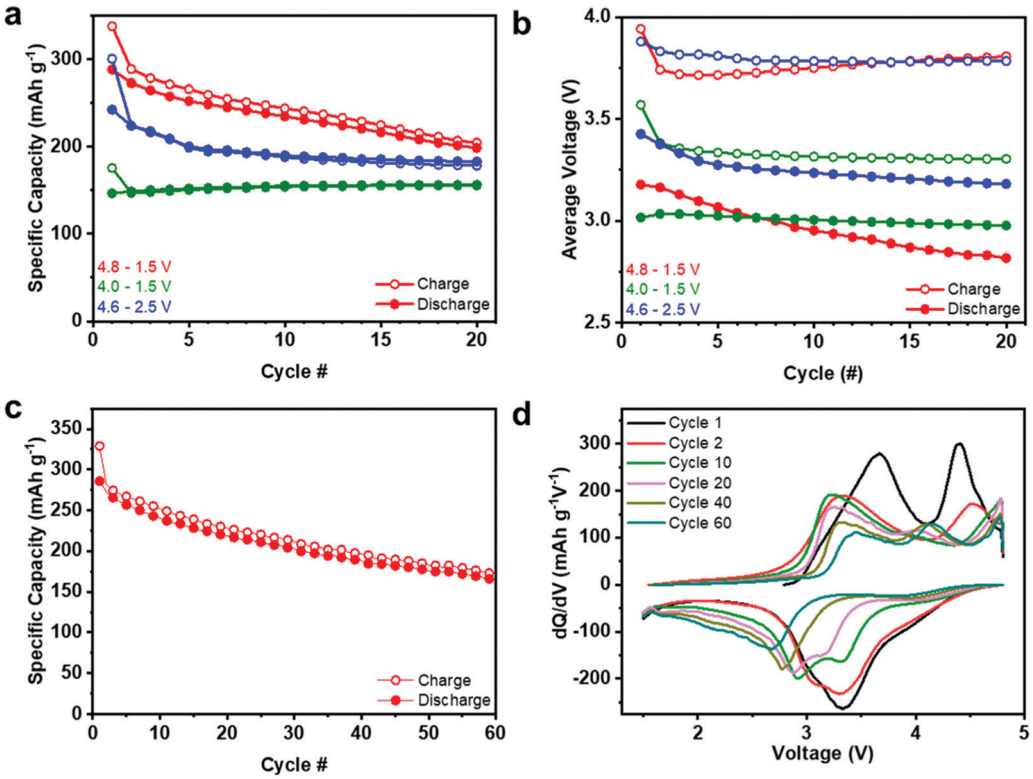

Fig. 27 Long-term cycling showing specific capacity (a), average voltage (b), specific capacity over extended cycling (c), and dQ/dV for a Li–Mn–Nb–O–F disordered rocksalt material. The voltage fade in (b) is approximately 20 mV per cycle over the full voltage window. Figure reproduced with permission from ref. 346. Copyright (2020) American Chemical Society.

Table 2 Electrochemical properties of disordered rocksalt materials: the first discharge capacity (Q_1), the first cycle irreversible capacity (ΔQ_1), the capacity after N cycles (Q_N), the voltage window used (V_{min} to V_{max}), the current used (I), the hysteresis (extracted at both high and low voltage as shown in Fig. 26a), and the capacity fade per cycle as a percent of the first discharge capacity ($\Delta Q/\Delta N$). When average voltage is reported, these are used for hysteresis calculation[a]

Formula	Q_1 (mA h g^{-1})	ΔQ_1 (mA h g^{-1})	Q_N (mA h g^{-1})	N	V_{min} (V)	V_{max} (V)	I (mA g^{-1})	Hysteresis (HV-LV)	$\Delta Q/\Delta N$ (%)	Ref.
$Li_{1.18}Fe_{0.34}Ti_{0.45}O_2$	223	41	142	50	1.5	5	10	1.6–0.8	0.73	347
$Li_{1.17}Mn_{0.34}V_{0.49}O_{1.8}F_{0.2}$	290	23	175	20	1.5	4.6	10	0.8–1.1	1.98	340
$Li_2V_{0.5}Ti_{0.5}O_2F$	280	−45	190	50	1.3	4.1	66	0.59 (2.31)[a]	0.64	348
Li_2VO_2F	330	−10	130	50	1.3	4.1	66	0.51 (2.53)[a]	1.21	348
$Li_{1.2}Ni_{0.3}Ti_{0.3}Nb_{0.2}O_2$	221	44	180	50	1.5	4.5	40	0.4–2.2	0.37	349
$Li_{1.25}Nb_{0.25}Mn_{0.5}O_2$	200	125	150	26	1.5	4.8	6.4	0.9–0.5	0.96	350
$Li_{1.3}Ta_{0.3}Mn_{0.4}O_2$	248	77	85	30	1.5	4.8	10	0.9–1.5	2.19	351
$Li_{1.2}Mn_{5/8}Nb_{7/40}O_{1.95}F_{0.05}$	330	20	200	20	1.5	4.8	15	0.75 (3.2 V)[a]	1.97	346
$LiNi_{0.5}V_{0.5}O_2$	264	10	160	50	1.3	4.5	10	0.8–1.0	0.79	339
$Li_2Mn_{2/3}Nb_{1/3}O_2F$	238	22	205	25	1.5	4.6	20	0.5–1.0	0.55	352
$Li_{1.3}Nb_{0.3}Mn_{0.4}O_2$	300	20	180	20	1.5	4.8	25	1.5–2.5	2.00	353

[a] Hysteresis is the difference between average charge and discharge voltage. In brackets is the average discharge voltage.

efforts concerned with the other metrics. The two main metrics of concern in Table 2 are the hysteresis that is high for all materials, and the poor long-term cycling. The long-term cycling is extremely poor, but this is in no small part due to the very large voltage window used, which is well beyond the stability window of the carbonate-based electrolytes and, again, this becomes exaggerated by the high surface area cathodes. As a result, it is impossible to conclude whether any improvements seen are due to substitutions in the cathodes or variants of electrolyte formulation between different articles. This provides an opportunity to develop this literature further to see if there is real potential for commercialization. A smaller window of 3–4.6 V would be of high interest as liquid electrolytes react with oxygen gas evolved from the cathode at high voltages in both Li–air batteries and in Li-rich layered oxides, so avoiding the <3 V region may be informative and useful.[295,343–345] We therefore consider it impossible to determine the impact of the cathode on long-term cycling when it is operating in liquid electrolytes up to voltages above 4.4 V where the electrolytes are highly reactive, especially when the materials have extremely

high surface areas due to nanometric particle sizes. This is therefore the first class of cathodes discussed herein that necessitates improved electrolytes that are stable at higher voltages than the current carbonate electrolytes, and we refer the reader to part II of this review article to discuss solid electrolytes that have the potential to make such cathodes viable.

Despite the limitation of needing a high-voltage electrolyte, continued studies on the impact of substitutions into DRX are expected to be plentiful given the wide compositional freedom this class of materials permits. Most importantly, the mitigation of the large overpotential will be essential to make these materials competitive with the state-of-the-art layered oxide cathodes. Focus should be directed to mitigating this property, with the hope that progress in the electrolytes will be made co-incidentally.

6. High voltage spinel: $LiNi_{1.5}Ni_{0.5}O_4$ spinel

The final class of oxide cathodes that will be considered here are spinel structures. Although low-voltage spinels have been commercialized, there is little progress to be made. We focus here on high-voltage spinels which continue to be quite promising, though facing the same limitations with electrolyte stabilities as other cathodes operating about 4.3 V *vs.* Li.

$LiNi_{0.5}Mn_{1.5}O_4$ (LNMO) is another heavily-studied high-voltage cathode material with an operational voltage of around 4.7 V. It crystallizes into two different cubic structures (Fig. 28), with the formation of the phases is highly dependent on temperature. The ordered $P4_332$ structure is formed near 700 °C and the disordered $Fd\bar{3}m$ structure is formed at higher temperatures.[354] Generally, the disordered structure demonstrates higher stability and energy density. Like other high-voltage cathodes, the nominal voltage of LNMO is outside the window of stability of contemporary electrolytes restricting its practical application. At this voltage range, the material reacts with the electrolyte and significant Mn dissolution occurs.[355,356] Many protective coatings have been tried to reduce the degree of reaction with the electrolyte.[357] However, surface reactions and Mn dissolution are not the only mechanisms of failure for Mn cathodes. Mn^{3+} is Jahn–Teller active and can lead to the transformation of tetragonal to cubic phases within the material. This increases the volume change during cycling and causes irreversible phase transitions that degrade the structural integrity of the particle.[358] Partial metal substitution has been implemented to improve the structural stability of the bulk material.

LNMO also displays poor rate capability due to its relatively poor electronic and ionic conductivity.[359] Research has focused on controlling particle morphology to address these issues by reducing the length of diffusion pathways. However, it remains critical that the surface be protected when synthesizing smaller particles, as the increased surface area results in more rapid Mn dissolution.

Many metals have been substituted into LNMO to stabilize the structure and improve electrochemical performance. Mg, for instance, has been shown to increase the electronic conductivity while stabilizing the structure, improving rate performance and reducing capacity fade during long-term cycling.[361] Na has also been shown to decrease particle size and cation ordering, resulting in a more conductive and more rate-performant material with a higher capacity.[362] Al substitution for either Ni or Mn has been shown to improve the electrochemical properties of LNMO. Substitution for Mn reduces capacity, but increase stability, while substitution for Ni has a higher capacity but also a larger capacity fade. It was shown that co-substitution was the optimal approach in the case of Al.[363,364] With Cr substitution, LNMO can retain more than 82% capacity after 1000 cycles at 1C at an initial discharge capacity of 130 mA h g^{-1} in a traditional $LiPF_6$ EC:DMC electrolyte (Fig. 29).[364] Thus, it appears that metal substitution is an effective method for improving the electrochemical properties of LNMO spinel cathode materials and may prove critical to their realization as commercial materials. Though they could still benefit from improved electrolyte stability and further structural stabilization.

7. Polyanion cathode materials

7.1 $LiFePO_4$

Polyanion cathodes are another broad class of intensely studied cathode materials. Of the polyanions, phosphates are the most

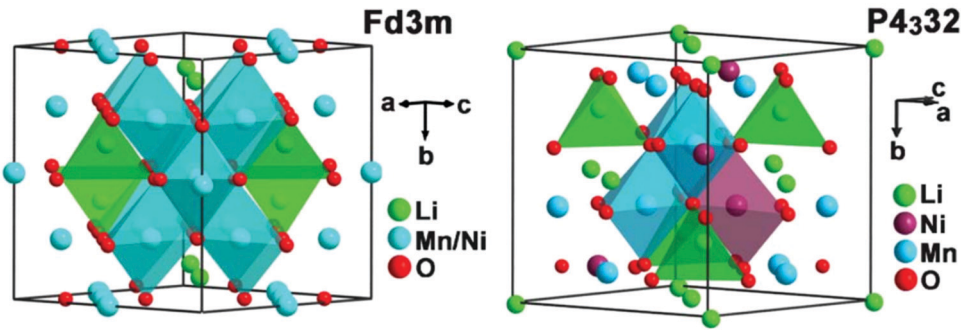

Fig. 28 Ordered (left) and disordered (right) structure of LNMO. Reproduced with permission from ref. 360. Copyright (2012) Royal Society of Chemistry.

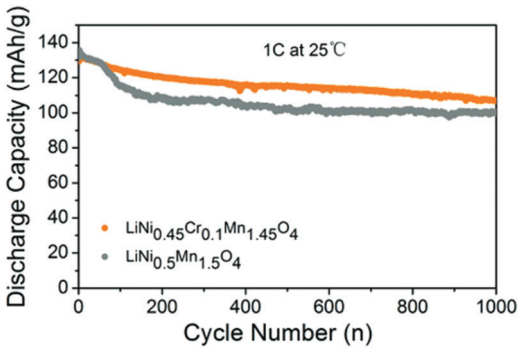

Fig. 29 Long-term cycling of Cr-substituted LNMO. Reproduced with permission from ref. 364. Copyright (2018) Wiley.

common. $LiFePO_4$ (LFP) was first published by Goodenough in 1997 and entered commercial use shortly after.[365] Typically synthesized mechanochemically or through carbothermal reduction at mass-production scale, but also by co-precipitation and solid-state reactions among other techniques,[366] LFP has an olivine structure (Fig. 30) and can be represented in the *Pnma* space group (Fig. 30).[367] Lithium intercalates and deintercalates through 1D channels along the *c*-axis. This 3D interlaced structure gives LFP a high thermal stability. It is stable up to 350 °C in N_2 atmosphere[365] due to the strong bonding of oxygen to both Fe and P compared to layered oxide materials where the oxygen is only strongly bound to the transition metal. A high thermal stability also results in a safer battery with less risk of thermal runaway.[368] Upon cycling, the volume change of LFP is less than 7%,[366] thus there is low strain on the material during cycling contributing to its long cycle life. The structure of LFP, while stable, does not lend itself well to cathode performance as it has intrinsically low electrical conductivity and reduced Li^+ conductivity compared to layered cathode materials.[369] These deficiencies combine to result in poor rate performance. An effective strategy to solve this problem is applying conductive coatings to the active material while nanosizing the particles.[370] While many different conductive coatings have been explored, carbon coatings have become the standard. Carbon coating has been shown to increase the conductivity from 10^{-9} S cm^{-1} to 10^{-5} S cm^{-1}, within an order of magnitude of commercial layered oxides.[371] The poor Li transport properties of LFP have been somewhat addressed synthetically by tailoring synthesis to yield smaller particles, reducing the length of Li diffusion pathways.[372] The dramatic improvement in cycling due to nanosizing and carbon coating is shown in Fig. 30. Therefore, through synthetic optimization, contemporary LFP has a capacity near its theoretical capacity of 170 mA g^{-1} and can cycle for thousands of cycles at 1C while retaining over 95% capacity.[373] However, LFP has a low operating voltage of 3.45 V *vs.* Li and thus a relatively low energy density of 590 W h kg^{-1}.[374]

7.2 Substitution into LFP: LMP (M = Mn, Co, Ni)

In addition to coating, many metals have been substituted into LFP in an attempt to increase capacity, operating voltage, and rate capability. However, there has been limited success with some claims of increased electronic conductivity, and other attributing increased in conductivity to impurities formed on the surface. LFP substituted with Mg has shown a decrease in capacity, but better rate performance. However, this is likely attributable to the smaller particle size of the Mg-substituted material.[375] Vanadium and nickel, for example, have been co-substituted into LFP and increased the capacity by up to 15% at a 1C rate and at a rate of 10C maintains 75% of the 0.1C capacity, demonstrating good rate performance.[376] Again, the particles of the substituted material are a smaller and more uniform particle size, which may partially explain the increase in rate capability. There have been reports of metal substitution

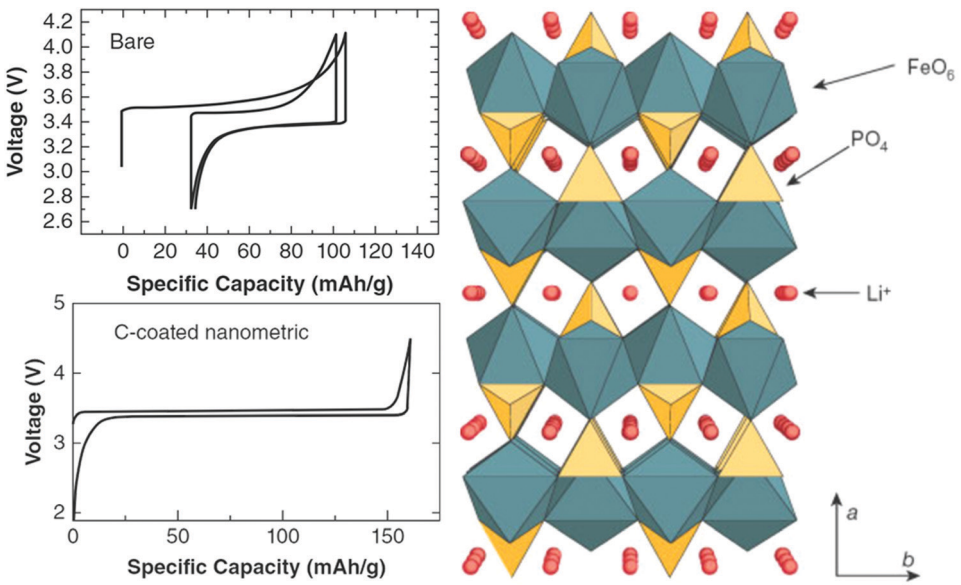

Fig. 30 Charge/discharge curves of bare and C/coated LFP (left). Olivine structure of LFP (right). Reproduced with permission from ref. 127 and 367. Copyright (2017) Wiley and copyright (2001) Nature.

increasing electronic conductivity. For instance, Mn substituted into Fe sites has been shown to decrease charge transfer resistance and increase Li diffusion. However, the substituted material showed increased capacity fade, implying a reduced structural stability.[377] Ni substitution has been shown to achieve similar results, increasing capacity and rate capability of unsubstituted LFP, but at the cost of reduced cycle life.[378] Improved conductivity through bulk substitution was called into question when Nazar *et al.* explained increased conductivity through the formation of connected carbon networks and conductive metal phosphides impurities at the surface of the particles.[379] However, Molenda *et al.*[380] observed small increases in conductivity with Al^{3+}, Zr^{4+}, and W^{6+} substitution of 25% atom and recently, a small increase in conductivity (less than one order of magnitude) was observed by gadolinium substitution into LFP.[381] Overall, there is evidence that partial metal substitutions can effectively enhance the electrochemical performance of LFP, specifically increasing the reversible capacity and rate performance, but often at the cost of reduced long-term stability and the particles must be coated with a conductive material to cycle effectively. Complete metal substitution has been shown to yield materials of high theoretical energy densities. Substituting Fe for another metal entirely, such as Mn, Co, or Ni, gives materials with much higher operating voltages (Fig. 31) with similar theoretical capacities, and thus higher theoretical energy densities. However, these materials come with their own challenges. Changing the Fe for a different metal has led to higher voltage materials that maintain the stable olivine structure. Mn, Co, and Ni phosphate cathodes have been made with varying degrees of success.

$LiMnPO_4$ (LMP) exhibits an operating voltage of 4.1 V, giving it a higher theoretical energy (679 W h kg^{-1}) density than LFP.[383] However, the cyclability of LMP is far inferior to that of LFP due to instability caused by the presence of Mn. As LMP is delithiated, Mn^{2+} is oxidized to Mn^{3+} which is Jahn–Teller active and causes distortion in the lattice which leads to the formation of defect phases and reduced Li diffusivity. Another deficiency with pristine LMP is electrical conductivity. LMP has an electronic conductivity significantly lower than that of LFP, making it impractical without modification.[384] Like LFP, conductive carbon coating can improve the conductivity of LMP. However, carbon coating on LMP proves to be less stable than that on LFP. Many metals have been substituted into LMP in an attempt to improve its electrochemical properties. Cr, Fe, Mg, V and Na have all been shown to improve the reversible capacity of LMP (Fig. 34) and significantly improve structural stability. Mixed results have been found using Zn as a substituent.[385] This is attributed to differences in synthetic conditions, which have a large influence on the effectiveness of metal substitution, with Fang and Wang[386] reporting improved electrochemical performance using a sol–gel and solid-state methods respectfully, while Wang *et al.*[386] reported decreased performance using a hydrothermal technique. There is also evidence that partial substitution of Na for Li can improve the charge transfer properties and lithium diffusion coefficient, likely due to the expansion of Li diffusion channels caused by the large Na ions.[387] DFT calculations have supported transition metal substitution at the Mn site increasing electronic conductivity by narrowing the band gap and increasing structural stability through stronger metal–oxygen bonding.[388] Recently, Mg substitution of Mn has been shown to achieve 400 cycles with 100% capacity retention at 1C, showing that LMP may have potential as a commercial high-voltage cathode (Fig. 32).[389]

$LiCoPO_4$ (LCP) is an attractive alternative to LFP and LMP due to its high operating voltage of 4.8 V and theoretical capacity near 167 mA h g^{-1}, yielding a high theoretical energy density of ~800 W h kg^{-1} due to the higher operating potential than any commercialized cathode.[390] While the theoretical energy of these materials is high, in practice they are plagued by a lack of stability and aggressive electrolyte decomposition due to the high operating potentials. This complicates studying these materials, as there is significant electrolyte degradation upon repeated cycling.[391] Despite this severe electrolyte degradation, a significant amount of work has been conducted on these materials to optimize their capacities and better stabilize the interface such that they may be studied while high-voltage electrolyte materials are developed. Like LMP, LCP exhibits much lower electrical conductivity than LFP making and thus requires a conductive coating and reduced particle size to cycle effectively.[392] LTO has been shown to significantly prevent electrolyte decomposition with a capacity retention of 93% after 100 cycles when coated on unsubstituted LCP. Other than coating, metal substitutions have been shown to increase the reversible capacity of LCP, these include Fe, V, Y, and Ca.[393–396] However, these substituents do not significantly address the cyclability issues of the material. Fe substitution has been shown to decrease antisite defects during cycling, decreasing structural instability and increasing the cycle life of the material.[393] It is also clear that synthesis technique is critical in the effect of substituent metals, as Di Lecce *et al.* report a decrease in electrochemical performance and less spherical particle morphology using a higher annealing temperature.[397] Thus far, theses substitutions do not address the cyclability

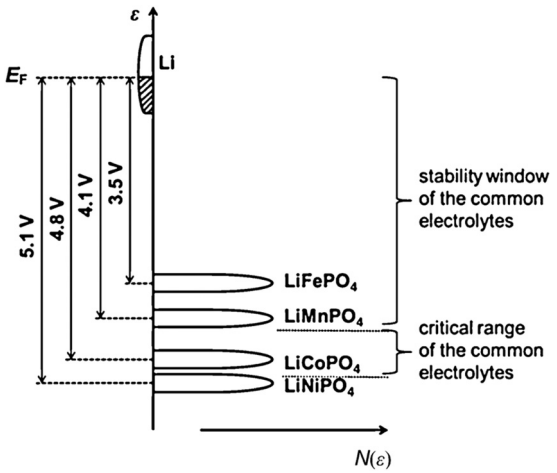

Fig. 31 Relative energies of $LiMPO_4$ cathode materials *vs.* Li/Li^+. Figure reproduced with permission of ref. 382. Copyright (2014) Springer.

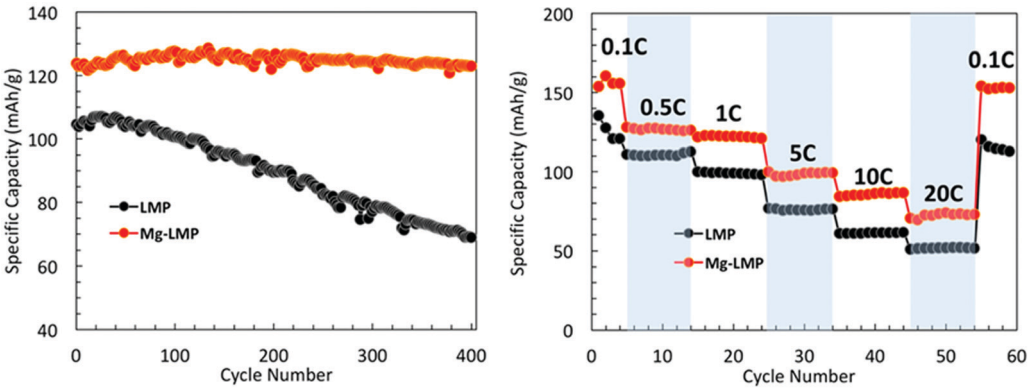

Fig. 32 Long-term cycling (left) and rate performance of Mn-substituted LMP (right). Figure reproduced with the permission of ref. 389. Copyright (2018) American Chemical Society.[389]

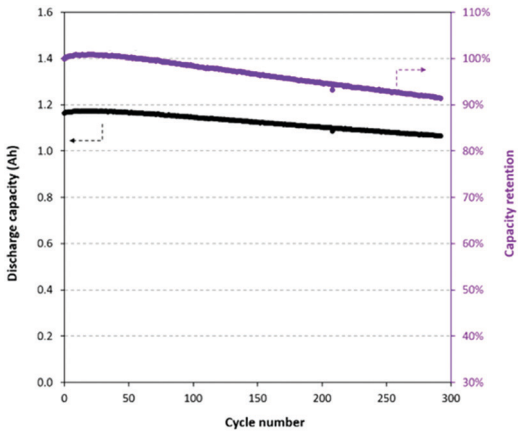

Fig. 33 Capacity retention of Fe, Cr, Si co-substituted LCP full cell in LiFSi/Py_{13}FSI electrolyte cycled at 0.2C from 3.5 to 4.9 V. Reproduced with permission from ref. 398. Copyright (2020) Multidisciplinary Digital Publishing Institute.

issue with LCP. Recently, an impressive multi-substituted material was achieved by Liu *et al.* where Fe, Cr, and Si were co-substituted into LCP. This material maintained a >90% capacity after 290 cycles at a 0.2C rate with a LiFSi/Py_{13}FSI electrolyte (Fig. 33).[398] While the initial reversible capacity was only 120, the energy was over 570 W h kg^{-1}. Progress on LCP as a high-energy cathode is promising, but there is still much work to be done on electrolyte/cathode interface stability before it may be used commercially. Additionally, LCP has a substantial drawback that cannot be solved: the high cobalt content. Like layered oxides, reducing Co content in cathode materials is important, due to its price, environmental impact and socio-economic consequences, as discussed previously in this article.

$LiNiPO_4$ (LNP) is an alternative to LFP with a nominal voltage higher than that of LCP at 5.1 V. This has made the material impractical in virtually all common liquid electrolytes and has made study of the material extremely difficult due to electrolyte decomposition. It has a theoretical capacity of 170 mA h g^{-1} and energy of over 860 W h kg^{-1}.[409] Like the other phosphates, conductive surface coatings are necessary to increase conductivity and is necessary to attempt to reduce electrolyte degradation. In addition, it is difficult to synthesize LNP without impurity phases, or significant antisite defects.[382] Partial metal substitution has been used to improve the quality of the synthesized material, reducing antisite defect, where Ni occupies Li sites, and increasing overall structural stability. In practice, many synthesized LNP cathodes with coating and metal substitution break 100 mA h g^{-1}. Mg^{2+} substitution has been shown to increase structural stability,[410] while Nd^{3+} substitution was able to achieve a capacity of 95 mA h g^{-1} at 0.1C and retained 85% capacity after 50 cycles at 2C.[411] Recently, Co-substituted LNP nanosheets were able to be cycled for 200 cycles at 0.1C with 98% capacity retention and an initial reversible capacity of 133 mA h g^{-1} at that rate using an LNP/$Li_4Ti_5O_{12}$ full cell with solid polymer electrolyte.[412] Thus, it appears through structural control and metal substitution that LNP may be realized as a high-energy cathode material if combined with a highly stable solid electrolyte. There may therefore be a future for LNO based batteries, but this relies on the development of electrolytes.

There are other high-voltage cathode compositions such as some pyrophosphates that may show promise, but have not yet been demonstrated appreciable cyclability at high voltage in full cells as LCP has. A range of pyrophosphate cathodes and other high voltage cathodes have been summarized elsewhere[413,414]

High-voltage lithium metal phosphate cathode materials do show promise for future battery technology if their structural and electronic challenges can be overcome. Metal substitutions can certainly be used to improve material stability and also improve both the electronic and ionic conductivities. Though much work remains to be done, as many elements have not yet been attempted in published partial metal substitutions. Additionally, there appears to be benefit in multi-element substitution as shown in LCP, given the multiple properties that require improvement.[398] Multi-element substitutions are poorly explored due to the increased dimensionality of the composition space. However, novel high-throughput experimental techniques pave the way for meaningful screening and optimization of multi-metal substitutions.[149]

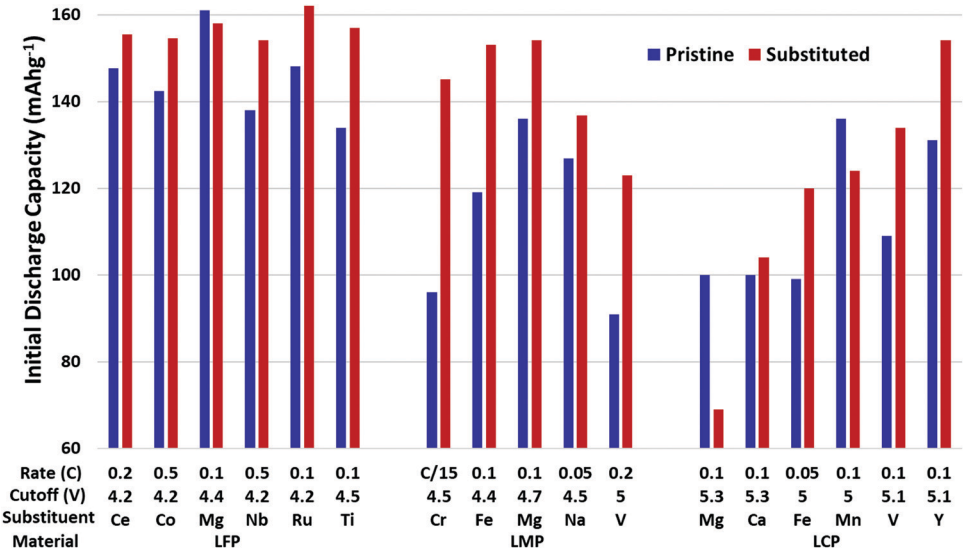

Fig. 34 Discharge capacities of substituted phosphate cathodes. Data collected from ref. 375, 387, 389, 393, 395, 396 and 399–408.

8. Conclusions and outlook

Cathodes for Li-ion batteries are diverse with many compositions having been studied under the broad classes of layered oxides, olivine polyanion, spinel, and disordered rocksalt, each with deficiencies that can be improved. Stoichiometric layered oxides stand to improve their accessible capacity while reducing the cobalt content. This can be achieved by substituting Ni for Co. However, this introduces structural instability as Li/Ni mixing, surface reactions, and structural degradation become more prevalent. Partial metal substitution can reduce the severity of these problems; either acting to stabilize the structure through stronger M–O bonds or by acting as ''pillars'' to prevent Mn migration and layer collapse. This has the added benefit of increasing rate capability in many cases. Compared to coatings, it seems partial metal substitution is similarly effective on average, though coatings often come at the cost of rate performance. Thus far, it appears neither single metal substitutions, nor coatings alone, are ''miracle'' solutions for the problems facing these materials, but they do yield significant improvements.

In Li-rich cathodes (both ordered and disordered rocksalt), structural stability is an even larger problem, plaguing the materials with a high degree of voltage fade and capacity loss. Metal substitutions have been shown to be an effective strategy to help mitigate both these issues. Like in their stoichiometric counterparts, partial metal substitution may occur on TM sites or Li sites. The former improving structural stability through stronger bonding, while the latter improves structural stability by increasing the interlayer distance and discouraging metal migration through repulsion. These electrochemically inactive metal substitutions often come with the cost of reduced capacity, a larger reduction than in stoichiometric layered materials, as they can suppress the activation of Li-rich cathode materials. Coatings are also an effective strategy to increase cycle life, but in general are not as effective at suppressing voltage fade as metal substitution. However, substitutions and coatings are not exclusive, they can be used in conjunction to maximize performance. Further work in Li-rich oxides is sorely needed to make them viable as next-generation cathodes.

Finally, for high-voltage materials, electrolyte reactions at the material interface are a large issue, obscuring the origins of capacity during cycling. Despite this, it is clear that these materials can benefit from improved structural and interfacial stability. Partial metal substitutions are effective, especially in the case of $LiCoPO_4$ where Fe, Cr, Si co-substitution has been shown to yield a cathode that has the potential to make a marked leap in Li-ion energy density.

Metal substitutions undeniably have a role to play in the development of next-generation cathode materials. While many single element substitutions have been explored, the next steps are to investigate and optimize multi-element substitutions in layered and polyanion cathode materials. Currently, multi-element substitutions are poorly explored largely due to the experimental demand of adding extra dimensionality to the composition space. This limitation can be remedied, in part, using novel high-throughput experimental techniques to screen many perspective materials simultaneously. Combined with computational modelling to better direct experimental efforts, materials discovery can be significantly accelerated. Additionally, there are many elements that have not been substituted into the materials here that should be investigated for their potential in improving battery performance, such as many of the lanthanides as well as heavier d-block elements. As shown earlier in this work, there is potential for these d- and f-block elements to positively impact material performance. Thus, there is worth exploring their impact across all classes of cathode discussed in this work. Concerning high-voltage materials though, the stability window of the electrolyte becomes problematic in investigating the effects of metal substitution in detail. Thus, it is imperative that electrolytes with a larger

stability window be developed to significantly move development of high voltage cathodes forward. Solid electrolytes are promising in this respect, and these will be reviewed in part II of this review.

Conflicts of interest

There are no conflicts to declare.

Acknowledgements

This work was supported by a Natural Sciences and Engineering Research Council of Canada (NSERC) discovery grant. AH further acknowledges support from NSERC in the form of a graduate student scholarship and from McGill University in the form of a graduate student fellowship.

References

1 F. Habashi, *Alloys: preparation, properties, applications*, John Wiley & Sons, 2008.
2 C. Veiga, J. Davim and A. Loureiro, Properties and applications of titanium alloys: a brief review, *Rev. Adv. Mater. Sci.*, 2012, **32**(2), 133–148.
3 H. Chen, C. Zhang, D. Jia, D. Wellmann and W. Liu, Corrosion behaviors of selective laser melted aluminum alloys: a review, *Metals*, 2020, **10**(1), 102.
4 J. Gao, Y. D. Kim, L. Liang, J. C. Idrobo, P. Chow, J. Tan, B. Li, L. Li, B. G. Sumpter, T.-M. Lu, V. Meunier, J. Hone and N. Koratkar, Transition-Metal Substitution Doping in Synthetic Atomically Thin Semiconductors, *Adv. Mater.*, 2016, **28**(44), 9735–9743.
5 J. Zhang, L. Zhang, P. Cai, X. Xue, M. Wang, J. Zhang and G. Tu, Enhancing stability of red perovskite nanocrystals through copper substitution for efficient light-emitting diodes, *Nano Energy*, 2019, **62**, 434–441.
6 P. P. Boix, S. Agarwala, T. M. Koh, N. Mathews and S. G. Mhaisalkar, Perovskite Solar Cells: Beyond Methylammonium Lead Iodide, *J. Phys. Chem. Lett.*, 2015, **6**(5), 898–907.
7 S. Chatterjee and A. J. Pal, Influence of metal substitution on hybrid halide perovskites: towards lead-free perovskite solar cells, *J. Mater. Chem. A*, 2018, **6**(9), 3793–3823.
8 M. A. Syzgantseva, C. P. Ireland, F. M. Ebrahim, B. Smit and O. A. Syzgantseva, Metal Substitution as the Method of Modifying Electronic Structure of Metal–Organic Frameworks, *J. Am. Chem. Soc.*, 2019, **141**(15), 6271–6278.
9 J. Park, H. Kim, S. S. Han and Y. Jung, Tuning Metal–Organic Frameworks with Open-Metal Sites and Its Origin for Enhancing CO2 Affinity by Metal Substitution, *J. Phys. Chem. Lett.*, 2012, **3**(7), 826–829.
10 M. A. Melliger, O. P. Van Vliet and H. Liimatainen, Anxiety vs reality–Sufficiency of battery electric vehicle range in Switzerland and Finland, *Transp. Res. D: Transp. Environ.*, 2018, **65**, 101–115.
11 M. Li, J. Lu, Z. Chen and K. Amine, 30 years of lithium-ion batteries, *Adv. Mater.*, 2018, **30**(33), 1800561.
12 N. Nitta, F. Wu, J. T. Lee and G. Yushin, Li-ion battery materials: present and future, *Mater. Today*, 2015, **18**(5), 252–264.
13 S. H. Farjana, N. Huda and M. P. Mahmud, Life cycle assessment of cobalt extraction process, *J. Sustain. Min.*, 2019, **18**(3), 150–161.
14 D. H. P. Kang, M. Chen and O. A. Ogunseitan, Potential environmental and human health impacts of rechargeable lithium batteries in electronic waste, *Environ. Sci. Technol.*, 2013, **47**(10), 5495–5503.
15 M. Winter, B. Barnett and K. Xu, Before Li ion batteries, *Chem. Rev.*, 2018, **118**(23), 11433–11456.
16 T. Ohzuku and Y. Makimura, Layered lithium insertion material of LiCo1/3Ni1/3Mn1/3O2 for lithium-ion batteries, *Chem. Lett.*, 2001, (7), 642–643.
17 D. D. Macneil, Z. Lu and J. R. Dahn, Structure and Electrochemistry of Li[Ni[sub x]Co[sub 1 − 2x]Mn[sub x]]O[sub 2] ($0 \leq x \leq 1/2$), *J. Electrochem. Soc.*, 2002, **149**(10), A1332.
18 P. Guan, L. Zhou, Z. Yu, Y. Sun, Y. Liu, F. Wu, Y. Jiang and D. Chu, Recent progress of surface coating on cathode materials for high-performance lithium-ion batteries, *J. Energy Chem.*, 2020, **43**, 220–235.
19 M. Jeong, H. Kim, W. Lee, S.-J. Ahn, E. Lee and W.-S. Yoon, Stabilizing effects of Al-doping on Ni-rich LiNi0. 80Co0. 15Mn0. 05O2 cathode for Li rechargeable batteries, *J. Power Sources*, 2020, **474**, 228592.
20 M. S. Palagonia, C. Erinmwingbovo, D. Brogioli and F. La Mantia, Comparison between cyclic voltammetry and differential charge plots from galvanostatic cycling, *J. Electroanal. Chem.*, 2019, **847**, 113170.
21 M. D. Radin, S. Hy, M. Sina, C. Fang, H. Liu, J. Vinckeviciute, M. Zhang, M. S. Whittingham, Y. S. Meng and A. Van der Ven, Narrowing the gap between theoretical and practical capacities in Li-ion layered oxide cathode materials, *Adv. Energy Mater.*, 2017, **7**(20), 1602888.
22 T. Ohzuku, A. Ueda, M. Nagayama, Y. Iwakoshi and H. Komori, Comparative study of LiCoO2, LiNi12Co12O2 and LiNiO2 for 4 volt secondary lithium cells, *Electrochim. Acta*, 1993, **38**(9), 1159–1167.
23 J. Li, R. Klöpsch, M. Stan, S. Nowak, M. Kunze, M. Winter and S. Passerini, Synthesis and electrochemical performance of the high voltage cathode material Li [Li0. 2Mn0. 56Ni0. 16Co0. 08] O2 with improved rate capability, *J. Power Sources*, 2011, **196**(10), 4821–4825.
24 Y. Ji, Y. Zhang and C.-Y. Wang, Li-ion cell operation at low temperatures, *J. Electrochem. Soc.*, 2013, **160**(4), A636.
25 B. Song, Z. Liu, M. O. Lai and L. Lu, Structural evolution and the capacity fade mechanism upon long-term cycling in Li-rich cathode material, *Phys. Chem. Chem. Phys.*, 2012, **14**(37), 12875–12883.
26 F. La Mantia, C. Wessells, H. Deshazer and Y. Cui, Reliable reference electrodes for lithium-ion batteries, *Electrochem. Commun.*, 2013, **31**, 141–144.

27 R. Dugas, J. D. Forero-Saboya and A. Ponrouch, Methods and protocols for reliable electrochemical testing in post-Li batteries (Na, K, Mg, and Ca), *Chem. Mater.*, 2019, **31**(21), 8613–8628.
28 Y. Huang, X. Liu, R. Yu, S. Cao, Y. Pei, Z. Luo, Q. Zhao, B. Chang, Y. Wang and X. Wang, Tellurium Surface Doping to Enhance the Structural Stability and Electrochemical Performance of Layered Ni-Rich Cathodes, *ACS Appl. Mater. Interfaces*, 2019, **11**(43), 40022–40033.
29 A. Mauger and C. M. Julien, Olivine positive electrodes for Li-ion batteries: Status and perspectives, *Batteries*, 2018, **4**(3), 39.
30 J. Groot, *State-of-health estimation of li-ion batteries: Cycle life test methods*, 2012.
31 J. Burns, A. Kassam, N. Sinha, L. Downie, L. Solnickova, B. Way and J. Dahn, Predicting and extending the lifetime of Li-ion batteries, *J. Electrochem. Soc.*, 2013, **160**(9), A1451.
32 A. Smith, J. C. Burns, X. Zhao, D. Xiong and J. Dahn, A high precision coulometry study of the SEI growth in Li/graphite cells, *J. Electrochem. Soc.*, 2011, **158**(5), A447.
33 M. Zhang, H. Zhao, M. Tan, J. Liu, Y. Hu, S. Liu, X. Shu, H. Li, Q. Ran, J. Cai and X. Liu, Yttrium modified Ni-rich LiNi0.8Co0.1Mn0.1O2 with enhanced electrochemical performance as high energy density cathode material at 4.5 V high voltage, *J. Alloys Compd.*, 2019, **774**, 82–92.
34 L. Ellis, J. Allen, I. Hill and J. Dahn, High-precision coulometry studies of the impact of temperature and time on SEI formation in Li-ion cells, *J. Electrochem. Soc.*, 2018, **165**(7), A1529.
35 J. Burns, N. Sinha, G. Jain, H. Ye, C. M. VanElzen, W. Lamanna, A. Xiao, E. Scott, J. Choi and J. Dahn, Impedance Reducing Additives and Their Effect on Cell Performance: II. C3H9B3O6, *J. Electrochem. Soc.*, 2012, **159**(7), A1105.
36 J. Xia, M. Nie, L. Ma and J. Dahn, Variation of coulombic efficiency versus upper cutoff potential of Li-ion cells tested with aggressive protocols, *J. Power Sources*, 2016, **306**, 233–240.
37 F. Yang, D. Wang, Y. Zhao, K.-L. Tsui and S. J. Bae, A study of the relationship between coulombic efficiency and capacity degradation of commercial lithium-ion batteries, *Energy*, 2018, **145**, 486–495.
38 C. Mao, R. E. Ruther, J. Li, Z. Du and I. Belharouak, Identifying the limiting electrode in lithium ion batteries for extreme fast charging, *Electrochem. Commun.*, 2018, **97**, 37–41.
39 Y. Nishida, N. Maruno and S. Komoda, Battery Control Technology of Li-ion Battery System for HEV, *IFAC Proc. Vol.*, 2013, **46**(21), 295–300.
40 M. S. H. Lipu, M. A. Hannan, A. Hussain, M. M. Hoque, P. J. Ker, M. H. M. Saad and A. Ayob, A review of state of health and remaining useful life estimation methods for lithium-ion battery in electric vehicles: Challenges and recommendations, *J. Cleaner Prod.*, 2018, **205**, 115–133.
41 L. Kong, C. Li, J. Jiang and M. G. Pecht, Li-ion battery fire hazards and safety strategies, *Energies*, 2018, **11**(9), 2191.
42 Q. Wang, P. Ping, X. Zhao, G. Chu, J. Sun and C. Chen, Thermal runaway caused fire and explosion of lithium ion battery, *J. Power Sources*, 2012, **208**, 210–224.
43 H. Maleki, G. Deng, A. Anani and J. Howard, Thermal stability studies of Li-ion cells and components, *J. Electrochem. Soc.*, 1999, **146**(9), 3224.
44 S. Zheng, L. Wang, X. Feng and X. He, Probing the heat sources during thermal runaway process by thermal analysis of different battery chemistries, *J. Power Sources*, 2018, **378**, 527–536.
45 X. Feng, S. Zheng, D. Ren, X. He, L. Wang, H. Cui, X. Liu, C. Jin, F. Zhang and C. Xu, Investigating the thermal runaway mechanisms of lithium-ion batteries based on thermal analysis database, *Appl. Energy*, 2019, **246**, 53–64.
46 X. Liu, D. Ren, H. Hsu, X. Feng, G.-L. Xu, M. Zhuang, H. Gao, L. Lu, X. Han and Z. Chu, Thermal runaway of lithium-ion batteries without internal short circuit, *Joule*, 2018, **2**(10), 2047–2064.
47 Z. Zhang, D. Fouchard and J. Rea, Differential scanning calorimetry material studies: implications for the safety of lithium-ion cells, *J. Power Sources*, 1998, **70**(1), 16–20.
48 J. Gnanaraj, E. Zinigrad, L. Asraf, H. Gottlieb, M. Sprecher, D. Aurbach and M. Schmidt, The use of accelerating rate calorimetry (ARC) for the study of the thermal reactions of Li-ion battery electrolyte solutions, *J. Power Sources*, 2003, **119**, 794–798.
49 W. Fenlon, A comparison of ARC and other thermal stability test methods, *Plant/Oper. Prog.*, 1984, **3**(4), 197–202.
50 D. H. Doughty and E. P. Roth, A general discussion of Li ion battery safety, *Electrochem. Soc. Interface*, 2012, **21**(2), 37.
51 K.-S. Lee, S.-T. Myung, D.-W. Kim and Y.-K. Sun, AlF3-coated LiCoO2 and Li [Ni1/3Co1/3Mn1/3] O2 blend composite cathode for lithium ion batteries, *J. Power Sources*, 2011, **196**(16), 6974–6977.
52 M. Broussely, P. Biensan, F. Bonhomme, P. Blanchard, S. Herreyre, K. Nechev and R. Staniewicz, Main aging mechanisms in Li ion batteries, *J. Power Sources*, 2005, **146**(1–2), 90–96.
53 J. Zheng, J. A. Lochala, A. Kwok, Z. D. Deng and J. Xiao, Research progress towards understanding the unique interfaces between concentrated electrolytes and electrodes for energy storage applications, *Adv. Sci.*, 2017, **4**(8), 1700032.
54 A. Lasia, Electrochemical impedance spectroscopy and its applications, *Modern aspects of electrochemistry*, Springer, 2002, pp. 143–248.
55 G. Assat, C. Delacourt, D. A. Dalla Corte and J.-M. Tarascon, Practical assessment of anionic redox in Li-rich layered oxide cathodes: a mixed blessing for high energy Li-ion batteries, *J. Electrochem. Soc.*, 2016, **163**(14), A2965.
56 D. Wang, X. Wu, Z. Wang and L. Chen, Cracking causing cyclic instability of LiFePO4 cathode material, *J. Power Sources*, 2005, **140**(1), 125–128.
57 G. Sun, T. Sui, B. Song, H. Zheng, L. Lu and A. M. Korsunsky, On the fragmentation of active material

secondary particles in lithium ion battery cathodes induced by charge cycling, *Extreme Mech. Lett.*, 2016, **9**, 449–458.

58 S. Hashigami, Y. Kato, K. Yoshimi, H. Yoshida, T. Inagaki, M. Hashinokuchi, T. Doi and M. Inaba, Influence of lithium silicate coating on retarding crack formation in LiNi0. 5Co0. 2Mn0. 3O2 cathode particles, *Electrochim. Acta*, 2018, **291**, 304–310.

59 S. Watanabe, M. Kinoshita, T. Hosokawa, K. Morigaki and K. Nakura, Capacity fading of LiAlyNi1− x− yCoxO2 cathode for lithium-ion batteries during accelerated calendar and cycle life tests (effect of depth of discharge in charge–discharge cycling on the suppression of the micro-crack generation of LiAlyNi1− x− yCoxO2 particle), *J. Power Sources*, 2014, **260**, 50–56.

60 B. Song, T. Sui, S. Ying, L. Li, L. Lu and A. M. Korsunsky, Nano-structural changes in Li-ion battery cathodes during cycling revealed by FIB-SEM serial sectioning tomography, *J. Mater. Chem. A*, 2015, **3**(35), 18171–18179.

61 R. Scipioni, P. S. Jørgensen, D.-T. Ngo, S. B. Simonsen, Z. Liu, K. J. Yakal-Kremski, H. Wang, J. Hjelm, P. Norby and S. A. Barnett, Electron microscopy investigations of changes in morphology and conductivity of LiFePO4/C electrodes, *J. Power Sources*, 2016, **307**, 259–269.

62 M. Ender, J. Joos, T. Carraro and E. Ivers-Tiffée, Quantitative characterization of LiFePO4 cathodes reconstructed by FIB/SEM tomography, *J. Electrochem. Soc.*, 2012, **159**(7), A972.

63 Z. Liu, K. Yu-chen, J. Wang, S. A. Barnett and K. T. Faber, Three-Phase 3D Reconstruction of a LiCoO 2 Cathode via FIB-SEM Tomography, *Microsc. Microanal.*, 2016, **22**(1), 140–148.

64 Z. Wu, S. Ji, T. Liu, Y. Duan, S. Xiao, Y. Lin, K. Xu and F. Pan, Aligned Li+ Tunnels in Core–Shell Li (Ni x Mn y Co z) O2@ LiFePO4 Enhances Its High Voltage Cycling Stability as Li-ion Battery Cathode, *Nano Lett.*, 2016, **16**(10), 6357–6363.

65 X. Ju, X. Hou, T. Beuse, Z. Liu, L. Du, J.-P. Brinkmann, E. Paillard, T. Wang, M. Winter and J. Li, Tailoring of Gradient Particles of Li-Rich Layered Cathodes with Mitigated Voltage Decay for Lithium-Ion Batteries, *ACS Appl. Mater. Interfaces*, 2020, **12**(39), 43596–43604.

66 Y. Zhang, H. Li, J. Liu, J. Zhang, F. Cheng and J. Chen, LiNi 0.90 Co 0.07 Mg 0.03 O 2 cathode materials with Mg-concentration gradient for rechargeable lithium-ion batteries, *J. Mater. Chem. A*, 2019, **7**(36), 20958–20964.

67 H. S. Ko, J. H. Kim, J. Wang and J. D. Lee, Co/Ti co-substituted layered LiNiO2 prepared using a concentration gradient method as an effective cathode material for Li-ion batteries, *J. Power Sources*, 2017, **372**, 107–115.

68 P. Yan, J. Zheng, M. Gu, J. Xiao, J.-G. Zhang and C.-M. Wang, Intragranular cracking as a critical barrier for high-voltage usage of layer-structured cathode for lithium-ion batteries, *Nat. Commun.*, 2017, **8**(1), 1–9.

69 G. Fan, Y. Wen, B. Liu and W. Yang, An insight into the influence of crystallite size on the performances of microsized spherical Li (Ni 0.5 Co 0.2 Mn 0.3) O 2 cathode material composed of aggregated nanosized particles, *J. Nanopart. Res.*, 2018, **20**(2), 43.

70 F. Zhou, X. Zhao, A. van Bommel, X. Xia and J. Dahn, Comparison of Li [Li1/9Ni1/3Mn5/9] O2, Li [Li1/5Ni1/5Mn3/5] O2, LiNi0. 5Mn1. 5O4, and LiNi2/3Mn1/3O2 as High Voltage Positive Electrode Materials, *J. Electrochem. Soc.*, 2010, **158**(2), A187.

71 Y. Liu, J. Wang, J. Liu, M. N. Banis, B. Xiao, A. Lushington, W. Xiao, R. Li, T.-K. Sham and G. Liang, Origin of phase inhomogeneity in lithium iron phosphate during carbon coating, *Nano Energy*, 2018, **45**, 52–60.

72 E. Ershenko, A. Bobyl, M. Boiko, Y. Zubavichus, V. Runov, M. Trenikhin and M. Sharkov, Fe 3 P impurity phase in high-quality LiFePO 4: X-ray diffraction and neutron-graphical studies, *Ionics*, 2017, **23**(9), 2293–2300.

73 R. Zhang, Z. Meng, X. Ma, M. Chen, B. Chen, Y. Zheng, Z. Yao, P. Vanaphuti, S. Bong and Z. Yang, Understanding fundamental effects of Cu impurity in different forms for recovered LiNi0. 6Co0. 2Mn0. 2O2 cathode materials, *Nano Energy*, 2020, **78**, 105214.

74 G. Liu, L. Wen, X. Wang and B. Ma, Effect of the impurity LixNi1− xO on the electrochemical properties of 5 V cathode material LiNi0. 5Mn1. 5O4, *J. Alloys Compd.*, 2011, **509**(38), 9377–9381.

75 E. Levi, E. Zinigrad, H. Teller, M. Levi, D. Aurbach, E. Mengeritsky, E. Elster, P. Dan, E. Granot and H. Yamin, Structural and Electrochemical Studies of 3 V Li x MnO2 Cathodes for Rechargeable Li Batteries, *J. Electrochem. Soc.*, 1997, **144**(12), 4133.

76 D. Mohanty, S. Kalnaus, R. A. Meisner, K. J. Rhodes, J. Li, E. A. Payzant, D. L. Wood III and C. Daniel, Structural transformation of a lithium-rich Li1. 2Co0. 1Mn0. 55Ni0. 15O2 cathode during high voltage cycling resolved by in situ X-ray diffraction, *J. Power Sources*, 2013, **229**, 239–248.

77 M. Balasubramanian, X. Sun, X. Yang and J. McBreen, In situ X-ray diffraction and X-ray absorption studies of high-rate lithium-ion batteries, *J. Power Sources*, 2001, **92**(1–2), 1–8.

78 X.-Q. Yang, J. McBreen, W.-S. Yoon and C. P. Grey, Crystal structure changes of LiMn0. 5Ni0. 5O2 cathode materials during charge and discharge studied by synchrotron based in situ XRD, *Electrochem. Commun.*, 2002, **4**(8), 649–654.

79 J. N. Reimers and J. Dahn, Electrochemical and in situ X-ray diffraction studies of lithium intercalation in Li x CoO2, *J. Electrochem. Soc.*, 1992, **139**(8), 2091.

80 W. Li, J. Reimers and J. Dahn, In situ x-ray diffraction and electrochemical studies of Li1 − xNiO2, *Solid State Ionics*, 1993, **67**(1–2), 123–130.

81 D. Ye, G. Zeng, K. Nogita, K. Ozawa, M. Hankel, D. J. Searles and L. Wang, Understanding the Origin of Li2MnO3 Activation in Li-Rich Cathode Materials for Lithium-Ion Batteries, *Adv. Funct. Mater.*, 2015, **25**(48), 7488–7496.

82 H.-H. Ryu, G.-T. Park, C. S. Yoon and Y.-K. Sun, Suppressing detrimental phase transitions via tungsten doping of

LiNiO 2 cathode for next-generation lithium-ion batteries, *J. Mater. Chem. A*, 2019, 7(31), 18580–18588.

83 Y. Mo, L. Guo, B. Cao, Y. Wang, L. Zhang, X. Jia and Y. Chen, Correlating structural changes of the improved cyclability upon Nd-substitution in LiNi0. 5Co0. 2Mn0. 3O2 cathode materials, *Energy Storage Mater.*, 2019, **18**, 260–268.

84 G. Chen, J. An, Y. Meng, C. Yuan, B. Matthews, F. Dou, L. Shi, Y. Zhou, P. Song and G. Wu, Cation and anion Co-doping synergy to improve structural stability of Li-and Mn-rich layered cathode materials for lithium-ion batteries, *Nano Energy*, 2019, **57**, 157–165.

85 H. Li, P. Zhou, F. Liu, H. Li, F. Cheng and J. Chen, Stabilizing nickel-rich layered oxide cathodes by magnesium doping for rechargeable lithium-ion batteries, *Chem. Sci.*, 2019, **10**(5), 1374–1379.

86 M. A. Krivoglaz, *X-ray and neutron diffraction in nonideal crystals*, Springer Science & Business Media, 2012.

87 D. Zeng, J. Cabana, J. Bréger, W.-S. Yoon and C. P. Grey, Cation Ordering in Li [Ni x Mn x Co (1–2 x)] O2-Layered Cathode Materials: A Nuclear Magnetic Resonance (NMR), Pair Distribution Function, X-ray Absorption Spectroscopy, and Electrochemical Study, *Chem. Mater.*, 2007, **19**(25), 6277–6289.

88 E. Zhao, L. Fang, M. Chen, D. Chen, Q. Huang, Z. Hu, Q.-B. Yan, M. Wu and X. Xiao, New insight into Li/Ni disorder in layered cathode materials for lithium ion batteries: a joint study of neutron diffraction, electrochemical kinetic analysis and first-principles calculations, *J. Mater. Chem. A*, 2017, **5**(4), 1679–1686.

89 H. Liu, C. R. Fell, K. An, L. Cai and Y. S. Meng, In-situ neutron diffraction study of the xLi2MnO3·(1 − x)LiMO2 (x = 0, 0.5; M = Ni, Mn, Co) layered oxide compounds during electrochemical cycling, *J. Power Sources*, 2013, **240**, 772–778.

90 D. Goonetilleke, N. Sharma, W. K. Pang, V. K. Peterson, R. Petibon, J. Li and J. Dahn, Structural Evolution and High-Voltage Structural Stability of Li (Ni x Mn y Co z) O2 Electrodes, *Chem. Mater.*, 2018, **31**(2), 376–386.

91 S. Sallis, N. Pereira, P. Mukherjee, N. Quackenbush, N. Faenza, C. Schlueter, T.-L. Lee, W. Yang, F. Cosandey and G. Amatucci, Surface degradation of Li1–x Ni0. 80Co0. 15Al0. 05O2 cathodes: Correlating charge transfer impedance with surface phase transformations, *Appl. Phys. Lett.*, 2016, **108**(26), 263902.

92 C. Xu, K. Märker, J. Lee, A. Mahadevegowda, P. J. Reeves, S. J. Day, M. F. Groh, S. P. Emge, C. Ducati and B. L. Mehdi, Bulk fatigue induced by surface reconstruction in layered Ni-rich cathodes for Li-ion batteries, *Nat. Mater.*, 2021, **20**(1), 84–92.

93 A. Tornheim, S. Sharifi-Asl, J. C. Garcia, J. Bareño, H. Iddir, R. Shahbazian-Yassar and Z. Zhang, Effect of electrolyte composition on rock salt surface degradation in NMC cathodes during high-voltage potentiostatic holds, *Nano Energy*, 2019, **55**, 216–225.

94 J. Li, H. Liu, J. Xia, A. R. Cameron, M. Nie, G. A. Botton and J. Dahn, The impact of electrolyte additives and upper cut-off voltage on the formation of a rocksalt surface layer in LiNi0. 8Mn0. 1Co0. 1O2 electrodes, *J. Electrochem. Soc.*, 2017, **164**(4), A655.

95 J. Xu, Y. Hu and X. Wu, Improvement of cycle stability for high-voltage lithium-ion batteries by in-situ growth of SEI film on cathode, *Nano Energy*, 2014, **5**, 67–73.

96 D.-S. Ko, J.-H. Park, S. Park, Y. N. Ham, S. J. Ahn, J.-H. Park, H. N. Han, E. Lee, W. S. Jeon and C. Jung, Microstructural visualization of compositional changes induced by transition metal dissolution in Ni-rich layered cathode materials by high-resolution particle analysis, *Nano Energy*, 2019, **56**, 434–442.

97 J. Lu, C. Zhan, T. Wu, J. Wen, Y. Lei, A. J. Kropf, H. Wu, D. J. Miller, J. W. Elam and Y.-K. Sun, Effectively suppressing dissolution of manganese from spinel lithium manganate via a nanoscale surface-doping approach, *Nat. Commun.*, 2014, **5**(1), 1–8.

98 B. Song, W. Li, S.-M. Oh and A. Manthiram, Long-life nickel-rich layered oxide cathodes with a uniform Li2ZrO3 surface coating for lithium-ion batteries, *ACS Appl. Mater. Interfaces*, 2017, **9**(11), 9718–9725.

99 Z. Chen and J. Dahn, Effect of a ZrO2 coating on the structure and electrochemistry of Li x CoO2 when cycled to 4.5 V, *Electrochem. Solid-State Lett.*, 2002, **5**(10), A213.

100 J. Zheng, M. Gu, J. Xiao, B. J. Polzin, P. Yan, X. Chen, C. Wang and J.-G. Zhang, Functioning mechanism of AlF3 coating on the Li-and Mn-rich cathode materials, *Chem. Mater.*, 2014, **26**(22), 6320–6327.

101 X. Cheng, J. Zheng, J. Lu, Y. Li, P. Yan and Y. Zhang, Realizing superior cycling stability of Ni-Rich layered cathode by combination of grain boundary engineering and surface coating, *Nano Energy*, 2019, **62**, 30–37.

102 X. Liu, H. Li, E. Yoo, M. Ishida and H. Zhou, Fabrication of FePO4 layer coated LiNi1/3Co1/3Mn1/3O2: Towards high-performance cathode materials for lithium ion batteries, *Electrochim. Acta*, 2012, **83**, 253–258.

103 E. McCalla, A. Abakumov, G. Rousse, M. Reynaud, M. T. Sougrati, B. Budic, A. Mahmoud, R. Dominko, G. Van Tendeloo and R. P. Hermann, Novel complex stacking of fully-ordered transition metal layers in Li4FeSbO6 materials, *Chem. Mater.*, 2015, **27**(5), 1699–1708.

104 Q. D. Truong, M. K. Devaraju, T. Tomai and I. Honma, Direct observation of antisite defects in LiCoPO4 cathode materials by annular dark-and bright-field electron microscopy, *ACS Appl. Mater. Interfaces*, 2013, **5**(20), 9926–9932.

105 Q. Li, Z. Yao, E. Lee, Y. Xu, M. M. Thackeray, C. Wolverton, V. P. Dravid and J. Wu, Dynamic imaging of crystalline defects in lithium-manganese oxide electrodes during electrochemical activation to high voltage, *Nat. Commun.*, 2019, **10**(1), 1–7.

106 Y. Shi, G. Chen, F. Liu, X. Yue and Z. Chen, Resolving the Compositional and Structural Defects of Degraded LiNi x Co y Mn z O2 Particles to Directly Regenerate High-Performance Lithium-Ion Battery Cathodes, *ACS Energy Lett.*, 2018, **3**(7), 1683–1692.

107 E. McCalla, A. M. Abakumov, M. Saubanère, D. Foix, E. J. Berg, G. Rousse, M.-L. Doublet, D. Gonbeau, P. Novák

and G. Van Tendeloo, Visualization of OO peroxo-like dimers in high-capacity layered oxides for Li-ion batteries, *Science*, 2015, **350**(6267), 1516–1521.

108 B. Wei, X. Lu, F. Voisard, H. Wei, H.-C. Chiu, Y. Ji, X. Han, M. L. Trudeau, K. Zaghib, G. P. Demopoulos and R. Gauvin, In Situ TEM Investigation of Electron Irradiation Induced Metastable States in Lithium-Ion Battery Cathodes: Li2FeSiO4 versus LiFePO4, *ACS Appl. Energy Mater.*, 2018, **1**(7), 3180–3189.

109 A. Ito, Y. Sato, T. Sanada, M. Hatano, H. Horie and Y. Ohsawa, In situ X-ray absorption spectroscopic study of Li-rich layered cathode material Li[Ni0.17Li0.2Co0.07Mn0.56]O2, *J. Power Sources*, 2011, **196**(16), 6828–6834.

110 R. Dominko, I. Arčon, A. Kodre, D. Hanžel and M. Gaberšček, In-situ XAS study on Li2MnSiO4 and Li2FeSiO4 cathode materials, *J. Power Sources*, 2009, **189**(1), 51–58.

111 Y.-C. Chen, J.-M. Chen, C.-H. Hsu, J.-F. Lee, J.-W. Yeh and H. C. Shih, In-situ synchrotron X-ray absorption studies of LiMn0.25Fe0.75PO4 as a cathode material for lithium ion batteries, *Solid State Ionics*, 2009, **180**(20–22), 1215–1219.

112 M. Ting, M. Burigana, L. Zhang, Y. Z. Finfrock, S. Trabesinger, A. Jonderian and E. McCalla, Impact of Nickel Substitution into Model Li-Rich Oxide Cathode Materials for Li-Ion Batteries, *Chem. Mater.*, 2020, **32**(2), 849–857.

113 S. Oswald, K. Nikolowski and H. Ehrenberg, XPS investigations of valence changes during cycling of LiCrMnO4-based cathodes in Li-ion batteries, *Surf. Interface Anal.*, 2010, **42**(6–7), 916–921.

114 J. L. White, F. S. Gittleson, M. Homer and F. El Gabaly, Nickel and Cobalt Oxidation State Evolution at Ni-Rich NMC Cathode Surfaces during Treatment, *J. Phys. Chem. C*, 2020, **124**(30), 16508–16514.

115 Z. Fu, J. Hu, W. Hu, S. Yang and Y. Luo, Quantitative analysis of Ni2 +/Ni3+ in Li[NixMnyCoz]O2 cathode materials: Non-linear least-squares fitting of XPS spectra, *Appl. Surf. Sci.*, 2018, **441**, 1048–1056.

116 N. Schulz, R. Hausbrand, L. Dimesso and W. Jaegermann, XPS-Surface Analysis of SEI Layers on Li-Ion Cathodes: Part I. Investigation of Initial Surface Chemistry, *J. Electrochem. Soc.*, 2018, **165**(5), A819–A832.

117 N. Schulz, R. Hausbrand, C. Wittich, L. Dimesso and W. Jaegermann, XPS-Surface Analysis of SEI Layers on Li-Ion Cathodes: Part II. SEI-Composition and Formation inside Composite Electrodes, *J. Electrochem. Soc.*, 2018, **165**(5), A833–A846.

118 M. Hekmatfar, A. Kazzazi, G. G. Eshetu, I. Hasa and S. Passerini, Understanding the Electrode/Electrolyte Interface Layer on the Li-Rich Nickel Manganese Cobalt Layered Oxide Cathode by XPS, *ACS Appl. Mater. Interfaces*, 2019, **11**(46), 43166–43179.

119 L. Baggetto, N. J. Dudney and G. M. Veith, Surface chemistry of metal oxide coated lithium manganese nickel oxide thin film cathodes studied by XPS, *Electrochim. Acta*, 2013, **90**, 135–147.

120 Y. Fan, J. Wang, Z. Tang, W. He and J. Zhang, Effects of the nanostructured SiO2 coating on the performance of LiNi0.5Mn1.5O4 cathode materials for high-voltage Li-ion batteries, *Electrochim. Acta*, 2007, **52**(11), 3870–3875.

121 S. Verdier, L. El Ouatani, R. DedryvèRe, F. Bonhomme, P. Biensan and D. Gonbeau, XPS Study on Al[sub 2]O[sub 3]- and AlPO[sub 4]-Coated LiCoO[sub 2] Cathode Material for High-Capacity Li Ion Batteries, *J. Electrochem. Soc.*, 2007, **154**(12), A1088.

122 K. Mizushima, P. C. Jones, P. J. Wiseman and J. B. Goodenough, LixCoO2 (0 < x < -1): A new cathode material for batteries of high energy density, *Mater. Res. Bull.*, 1980, **15**(6), 783–789.

123 A. Yoshino, *Development of the Lithium-Ion Battery and Recent Technological Trends*, Elsevier, 2014, pp. 1–20.

124 C. Julien, M. A. Camacho-Lopez, L. Escobar-Alarcon and E. Haro-Poniatowski, Fabrication of LiCoO2 thin-film cathodes for rechargeable lithium microbatteries, *Mater. Chem. Phys.*, 2001, **68**(1–3), 210–216.

125 T. Ohzuku and A. Ueda, Solid-State Redox Reactions of LiCoO2 (R3m) for 4 Volt Secondary Lithium Cells, *J. Electrochem. Soc.*, 1994, **141**(11), 2972–2977.

126 T. Okumura, Y. Yamaguchi, M. Shikano and H. Kobayashi, Correlation of lithium ion distribution and X-ray absorption near-edge structure in O3- and O2-lithium cobalt oxides from first-principle calculation, *J. Mater. Chem.*, 2012, **22**(33), 17340.

127 E. McCalla, Electrical Energy Storage: Batteries, *Handbook of Solid State Chemistry*, Wiley, 2017, vol. 6, pp. 1–24.

128 T. Ohzuku, A. Ueda and M. Nagayama, Electrochemistry and Structural Chemistry of LiNiO2 (R3m) for 4 Volt Secondary Lithium Cells, *J. Electrochem. Soc.*, 1993, **140**(7), 1862–1870.

129 J. Molenda, Structural, electrical and electrochemical properties of LiNiO2, *Solid State Ionics*, 2002, **146**(1–2), 73–79.

130 S. N. Kwon, J. Song and D. R. Mumm, Effects of cathode fabrication conditions and cycling on the electrochemical performance of LiNiO2 synthesized by combustion and calcination, *Ceram. Int.*, 2011, **37**(5), 1543–1548.

131 L. Fang, M. Wang, Q. Zhou, H. Xu, W. Hu and H. Li, Suppressing cation mixing and improving stability by F doping in cathode material LiNiO2 for Li-ion batteries: First-principles study, *Colloids Surf., A*, 2020, **600**, 124940.

132 H. Chen, J. A. Dawson and J. H. Harding, Effects of cationic substitution on structural defects in layered cathode materials LiNiO2, *J. Mater. Chem. A*, 2014, **2**(21), 7988.

133 T. Uyama, K. Mukai and I. Yamada, High-pressure synthesis and electrochemical properties of tetragonal LiMnO2, *RSC Adv.*, 2018, **8**(46), 26325–26334.

134 Y. Jiang, C. Qin, P. Yan and M. Sui, Origins of capacity and voltage fading of LiCoO2 upon high voltage cycling, *J. Mater. Chem. A*, 2019, **7**(36), 20824–20831.

135 J. Cho, Y. J. Kim and B. Park, Novel LiCoO2Cathode Material with Al2O3Coating for a Li Ion Cell, *Chem. Mater.*, 2000, **12**(12), 3788–3791.

136 J. M. Paulsen, J. R. Mueller-Neuhaus and J. R. Dahn, Layered LiCoO[sub 2] with a Different Oxygen Stacking (O2 Structure) as a Cathode Material for Rechargeable Lithium Batteries, *J. Electrochem. Soc.*, 2000, **147**(2), 508.

137 A. Mesnier and A. Manthiram, Synthesis of LiNiO2 at Moderate Oxygen Pressure and Long-Term Cyclability in Lithium-Ion Full Cells, *ACS Appl. Mater. Interfaces*, 2020, **12**(47), 52826–52835.

138 C. S. Yoon, D.-W. Jun, S.-T. Myung and Y.-K. Sun, Structural Stability of LiNiO2 Cycled above 4.2 V, *ACS Energy Lett.*, 2017, **2**(5), 1150–1155.

139 S. Komaba, S.-T. Myung, N. Kumagai, T. Kanouchi, K. Oikawa and T. Kamiyama, Hydrothermal synthesis of high crystalline orthorhombic LiMnO2 as a cathode material for Li-ion batteries, *Solid State Ionics*, 2002, **152**, 311–318.

140 S.-H. Wu and M.-T. Yu, Preparation and characterization of *o*-$LiMnO_2$ cathode materials, *J. Power Sources*, 2007, **165**(2), 660–665.

141 C. Delmas, Electrochemical and physical properties of the LixNi1$minus;yCoyO2 phases, *Solid State Ionics*, 1992, **53-56**, 370–375.

142 M. Wohlfahrt-Mehrens, C. Vogler and J. Garche, Aging mechanisms of lithium cathode materials, *J. Power Sources*, 2004, **127**(1–2), 58–64.

143 E. Levi, M. D. Levi, G. Salitra, D. Aurbach, R. Oesten, U. Heider and L. Heider, Electrochemical and in-situ XRD characterization of LiNiO2 and LiCo0.2Ni0.8O2 electrodes for rechargeable lithium cells, *Solid State Ionics*, 1999, **126**(1–2), 97–108.

144 H.-J. Noh, S. Youn, C. S. Yoon and Y.-K. Sun, Comparison of the structural and electrochemical properties of layered Li[NixCoyMnz]O2 (x = 1/3, 0.5, 0.6, 0.7, 0.8 and 0.85) cathode material for lithium-ion batteries, *J. Power Sources*, 2013, **233**, 121–130.

145 C. M. Julien and A. Mauger, Functional behavior of AlF 3 coatings for high-performance cathode materials for lithium-ion batteries, *AIMS Mater. Sci.*, 2019, **6**(3), 406.

146 E. McCalla, A. W. Rowe, R. Shunmugasundaram and J. R. Dahn, Structural Study of the Li–Mn–Ni Oxide Pseudoternary System of Interest for Positive Electrodes of Li-Ion Batteries, *Chem. Mater.*, 2013, **25**(6), 989–999.

147 C. R. Brown, E. McCalla, C. Watson and J. R. Dahn, Combinatorial Study of the Li–Ni–Mn–Co Oxide Pseudoquaternary System for Use in Li–Ion Battery Materials Research, *ACS Comb. Sci.*, 2015, **17**(6), 381–391.

148 E. McCalla, A. W. Rowe, C. R. Brown, L. R. P. Hacquebard and J. R. Dahn, How Phase Transformations during Cooling Affect Li-Mn-Ni-O Positive Electrodes in Lithium Ion Batteries, *J. Electrochem. Soc.*, 2013, **160**(8), A1134–A1138.

149 K. P. Potts, E. Grignon and E. McCalla, Accelerated Screening of High-Energy Lithium-Ion Battery Cathodes, *ACS Appl. Energy Mater.*, 2019, **2**(12), 8388–8393.

150 Y. Xia, J. Zheng, C. Wang and M. Gu, Designing principle for Ni-rich cathode materials with high energy density for practical applications, *Nano Energy*, 2018, **49**, 434–452.

151 J. K. Ngala, N. A. Chernova, M. Ma, M. Mamak, P. Y. Zavalij and M. S. Whittingham, The synthesis, characterization and electrochemical behavior of the layered LiNi0.4Mn0.4-Co0.2O2 compound, *J. Mater. Chem.*, 2004, **14**(2), 214.

152 B. J. Hwang, Y. W. Tsai, D. Carlier and G. Ceder, A Combined Computational/Experimental Study on LiNi1/3Co1/3Mn1/3O2, *Chem. Mater.*, 2003, **15**(19), 3676–3682.

153 Y. Koyama, I. Tanaka, H. Adachi, Y. Makimura and T. Ohzuku, Crystal and electronic structures of superstructural Li1 − x [Co1/3Ni1/3Mn1/3] O2 ($0 \leq x \leq 1$), *J. Power Sources*, 2003, **119**, 644–648.

154 S. C. Yin, Y. H. Rho, I. Swainson and L. F. Nazar, X-ray/Neutron Diffraction and Electrochemical Studies of Lithium De/Re-Intercalation in Li1-xCo1/3Ni1/3Mn1/3O2(x= 0 → 1), *Chem. Mater.*, 2006, **18**(7), 1901–1910.

155 J. Xu, F. Lin, M. M. Doeff and W. Tong, A review of Ni-based layered oxides for rechargeable Li-ion batteries, *J. Mater. Chem. A*, 2017, **5**(3), 874–901.

156 Y. Jiang, P. Yan, M. Yu, J. Li, H. Jiao, B. Zhou and M. Sui, Atomistic mechanism of cracking degradation at twin boundary of LiCoO2, *Nano Energy*, 2020, **78**, 105364.

157 K. Min and E. Cho, Intrinsic origin of intra-granular cracking in Ni-rich layered oxide cathode materials, *Phys. Chem. Chem. Phys.*, 2018, **20**(14), 9045–9052.

158 H. Liu, M. Wolf, K. Karki, Y.-S. Yu, E. A. Stach, J. Cabana, K. W. Chapman and P. J. Chupas, Intergranular Cracking as a Major Cause of Long-Term Capacity Fading of Layered Cathodes, *Nano Lett.*, 2017, **17**(6), 3452–3457.

159 J. Jiang and J. R. Dahn, ARC studies of the thermal stability of three different cathode materials: LiCoO2; Li[Ni0.1Co-0.8Mn0.1]O2; and LiFePO4, in LiPF6 and LiBoB EC/DEC electrolytes, *Electrochem. Commun.*, 2004, **6**(1), 39–43.

160 C. Banza Lubaba Nkulu, L. Casas, V. Haufroid, T. De Putter, N. D. Saenen, T. Kayembe-Kitenge, P. Musa-Obadia, D. Kyanika Wa Mukoma, J.-M. Lunda Ilunga, T. S. Nawrot, O. Luboya Numbi, E. Smolders and B. Nemery, Sustainability of artisanal mining of cobalt in DR Congo, *Nat. Sustain.*, 2018, **1**(9), 495–504.

161 B. Cheruga, R. Liron and M. Canavera, Ensuring children's social protection in the Democratic Republic of the Congo: A case study of combating child labour in the copper-cobalt belt, *What Works for Africa's Poorest Children: From measurement to action*, 2020, p. 273.

162 B. K. Sovacool, The precarious political economy of cobalt: Balancing prosperity, poverty, and brutality in artisanal and industrial mining in the Democratic Republic of the Congo, *Extr. Ind. Soc.*, 2019, **6**(3), 915–939.

163 W. Liu, P. Oh, X. Liu, M.-J. Lee, W. Cho, S. Chae, Y. Kim and J. Cho, Nickel-Rich Layered Lithium Transition-Metal Oxide for High-Energy Lithium-Ion Batteries, *Angew. Chem., Int. Ed.*, 2015, **54**(15), 4440–4457.

164 M. Tang, J. Yang, N. Chen, S. Zhu, X. Wang, T. Wang, C. Zhang and Y. Xia, Overall structural modification of a layered Ni-rich cathode for enhanced cycling stability and rate capability at high voltage, *J. Mater. Chem. A*, 2019, **7**(11), 6080–6089.

165 S. S. Zhang, Problems and their origins of Ni-rich layered oxide cathode materials. *Energy Storage*, *Materials*, 2020, **24**, 247–254.

166 Z. Li, N. A. Chernova, M. Roppolo, S. Upreti, C. Petersburg, F. M. Alamgir and M. S. Whittingham, Comparative Study of the Capacity and Rate Capability of LiNiyMnyCo1–2yO2 (y = 0.5, 0.45, 0.4, 0.33), *J. Electrochem. Soc.*, 2011, **158**(5), A516.

167 C. Julien, A. Mauger, K. Zaghib and H. Groult, Optimization of Layered Cathode Materials for Lithium-Ion Batteries, *Materials*, 2016, **9**(7), 595.

168 M. M. Doeff, T. Conry and J. Wilcox, *Improved layered mixed transition metal oxides for Li-ion batteries*, SPIE, 2010, p. 2010.

169 T. Pan, J. Alvarado, J. Zhu, Y. Yue, H. L. Xin, D. Nordlund, F. Lin and M. M. Doeff, Structural Degradation of Layered Cathode Materials in Lithium-Ion Batteries Induced by Ball Milling, *J. Electrochem. Soc.*, 2019, **166**(10), A1964–A1971.

170 C. Tian, F. Lin and M. M. Doeff, Electrochemical Characteristics of Layered Transition Metal Oxide Cathode Materials for Lithium Ion Batteries: Surface, Bulk Behavior, and Thermal Properties, *Acc. Chem. Res.*, 2018, **51**(1), 89–96.

171 H. Ronduda, M. Zybert, A. Szczęsna-Chrzan, T. Trzeciak, A. Ostrowski, D. Szymański, W. Wieczorek, W. Raróg-Pilecka and M. Marcinek, On the Sensitivity of the Ni-rich Layered Cathode Materials for Li-ion Batteries to the Different Calcination Conditions, *Nanomaterials*, 2020, **10**(10), 2018.

172 M. R. Laskar, D. H. K. Jackson, S. Xu, R. J. Hamers, D. Morgan and T. F. Kuech, Atomic Layer Deposited MgO: A Lower Overpotential Coating for Li[Ni0.5Mn0.3Co0.2]O2 Cathode, *ACS Appl. Mater. Interfaces*, 2017, **9**(12), 11231–11239.

173 S.-K. Jung, H. Gwon, J. Hong, K.-Y. Park, D.-H. Seo, H. Kim, J. Hyun, W. Yang and K. Kang, Understanding the Degradation Mechanisms of LiNi0.5 Co0.2 Mn0.3 O2 Cathode Material in Lithium Ion Batteries, *Adv. Energy Mater.*, 2014, **4**(1), 1300787.

174 Z. Khodr, C. Mallet, J.-C. Daigle, Z. Feng, K. Amouzegar, J. Claverie and K. Zaghib, Electrochemical Study of Functional Additives for Li-Ion Batteries, *J. Electrochem. Soc.*, 2020, **167**(12), 120535.

175 A. L. Lipson, J. L. Durham, M. Leresche, I. Abu-Baker, M. J. Murphy, T. T. Fister, L. Wang, F. Zhou, L. Liu, K. Kim and D. Johnson, Improving the Thermal Stability of NMC 622 Li-Ion Battery Cathodes through Doping During Coprecipitation, *ACS Appl. Mater. Interfaces*, 2020, **12**(16), 18512–18518.

176 L. Xu, F. Zhou, H. Zhou, J. Kong, Q. Wang and G. Yan, Ti3C2(OH)2 coated Li(Ni0.6Co0.2Mn0.2)O2 cathode material with enhanced electrochemical properties for lithium ion battery, *Electrochim. Acta*, 2018, **289**, 120–130.

177 L. Liang, K. Du, W. Lu, Z. Peng, Y. Cao and G. Hu, Synthesis and characterization of LiNi 0.6 Co x Mn 0.4-x O 2 (x = 0.05, 0.1, 0.15, 0.2, 0.25 and 0.3) with high-electrochemical performance for lithium-ion batteries, *Electrochim. Acta*, 2014, **146**, 207–217.

178 Y.-C. Li, W. Xiang, Y. Xiao, Z.-G. Wu, C.-L. Xu, W. Xu, Y.-D. Xu, C. Wu, Z.-G. Yang and X.-D. Guo, Synergy of doping and coating induced heterogeneous structure and concentration gradient in Ni-rich cathode for enhanced electrochemical performance, *J. Power Sources*, 2019, **423**, 144–151.

179 S.-H. Lee, G.-J. Park, S.-J. Sim, B.-S. Jin and H.-S. Kim, Improved electrochemical performances of LiNi0.8-Co0.1Mn0.1O2 cathode via SiO2 coating, *J. Alloys Compd.*, 2019, **791**, 193–199.

180 M. Wood, J. Li, R. E. Ruther, Z. Du, E. C. Self, H. M. Meyer, C. Daniel, I. Belharouak and D. L. Wood, Chemical stability and long-term cell performance of low-cobalt, Ni-Rich cathodes prepared by aqueous processing for high-energy Li-Ion batteries, *Energy Storage Mater.*, 2020, **24**, 188–197.

181 A. Purwanto, C. S. Yudha, U. Ubaidillah, H. Widiyandari, T. Ogi and H. Haerudin, NCA cathode material: synthesis methods and performance enhancement efforts, *Mater. Res. Express*, 2018, **5**(12), 122001.

182 K. Zhou, Q. Xie, B. Li and A. Manthiram, An in-depth understanding of the effect of aluminum doping in high-nickel cathodes for lithium-ion batteries. *Energy Storage*, *Materials*, 2021, **34**, 229–240.

183 F. Dogan, J. T. Vaughey, H. Iddir and B. Key, Direct Observation of Lattice Aluminum Environments in Li Ion Cathodes LiNi1–y–zCoyAlzO2 and Al-Doped LiNixMny-CozO2 via 27Al MAS NMR Spectroscopy, *ACS Appl. Mater. Interfaces*, 2016, **8**(26), 16708–16717.

184 D. Wang, W. Liu, X. Zhang, Y. Huang, M. Xu and W. Xiao, Review of Modified Nickel-Cobalt Lithium Aluminate Cathode Materials for Lithium-Ion Batteries, *Int. J. Photoenergy*, 2019, **2019**, 1–13.

185 S. Ahmed, P. A. Nelson, K. G. Gallagher, N. Susarla and D. W. Dees, Cost and energy demand of producing nickel manganese cobalt cathode material for lithium ion batteries, *J. Power Sources*, 2017, **342**, 733–740.

186 J. B. Dunn, C. James, L. Gaines, K. Gallagher, Q. Dai and J. C. Kelly, *Material and energy flows in the production of cathode and anode materials for lithium ion batteries*, Argonne National Lab. (ANL), Argonne, IL (United States), 2015.

187 D. Wang, I. Belharouak, L. H. Ortega, X. Zhang, R. Xu, D. Zhou, G. Zhou and K. Amine, Synthesis of high capacity cathodes for lithium-ion batteries by morphology-tailored hydroxide co-precipitation, *J. Power Sources*, 2015, **274**, 451–457.

188 D. Zhang, Y. Liu, L. Wu, L. Feng, S. Jin, R. Zhang and M. Jin, Effect of Ti ion doping on electrochemical performance of Ni-rich LiNi0. 8Co0. 1Mn0. 1O2 cathode material, *Electrochim. Acta*, 2019, **328**, 135086.

189 Q. Sa, J. A. Heelan, Y. Lu, D. Apelian and Y. Wang, Copper Impurity Effects on LiNi1/3Mn1/3Co1/3O2 Cathode Material, *ACS Appl. Mater. Interfaces*, 2015, **7**(37), 20585–20590.

190 V. Subramanian, C. L. Chen, H. S. Chou and G. T. K. Fey, Microwave-assisted solid-state synthesis of LiCoO2and

itselectrochemical properties as a cathode material for lithium batteries, *J. Mater. Chem.*, 2001, **11**(12), 3348–3353.

191 P. Hou, H. Zhang, Z. Zi, L. Zhang and X. Xu, Core–shell and concentration-gradient cathodes prepared via co-precipitation reaction for advanced lithium-ion batteries, *J. Mater. Chem. A*, 2017, **5**(9), 4254–4279.

192 E. Lee, R. Koritala, D. J. Miller and C. S. Johnson, Aluminum and Gallium Substitution into 0.5Li2MnO3·0.5Li(Ni0.375Mn-0.375Co0.25)O2Layered Composite and the Voltage Fade Effect, *J. Electrochem. Soc.*, 2015, **162**(3), A322–A329.

193 B. Pişkin, C. Savaş Uygur and M. K. Aydınol, Mo doping of layered Li (Ni x Mn y Co1-x -y -z M z)O2 cathode materia, *Int. J. Energy Res.*, 2018, **42**(12), 3888–3898.

194 S. Nowak and M. Winter, Elemental analysis of lithium ion batteries, *J. Anal. At. Spectrom.*, 2017, **32**(10), 1833–1847.

195 Y.-Y. Wang, M.-Y. Gao, S. Liu, G.-R. Li and X.-P. Gao, Yttrium Surface Gradient Doping for Enhancing Structure and Thermal Stability of High-Ni Layered Oxide as Cathode for Li–Ion Batteries, *ACS Appl. Mater. Interfaces*, 2021, **13**(6), 7343–7354.

196 U.-H. Kim, S.-T. Myung, C. S. Yoon and Y.-K. Sun, Extending the Battery Life Using an Al-Doped Li[Ni0.76Co0.09Mn-0.15]O2 Cathode with Concentration Gradients for Lithium Ion Batteries, *ACS Energy Lett.*, 2017, **2**(8), 1848–1854.

197 W. Zhao, L. Zou, H. Jia, J. Zheng, D. Wang, J. Song, C. Hong, R. Liu, W. Xu, Y. Yang, J. Xiao, C. Wang and J.-G. Zhang, Optimized Al Doping Improves Both Interphase Stability and Bulk Structural Integrity of Ni-Rich NMC Cathode Materials, *ACS Appl. Energy Mater.*, 2020, **3**(4), 3369–3377.

198 X. Zhao, G. Liang and D. Lin, Synthesis and characterization of Al-substituted LiNi0.5Co0.2Mn0.3O2 cathode materials by a modified co-precipitation method, *RSC Adv.*, 2017, 7(60), 37588–37595.

199 Y. Zhang, Z.-B. Wang, J. Lei, F.-F. Li, J. Wu, X.-G. Zhang, F.-D. Yu and K. Ke, Investigation on performance of Li(Ni0.5Co0.2Mn0.3)1 − Ti O2 cathode materials for lithium-ion battery, *Ceram. Int.*, 2015, **41**(7), 9069–9077.

200 L. Wu, X. Tang, X. Chen, Z. Rong, W. Dang, Y. Wang, X. Li, L. Huang and Y. Zhang, Improvement of electrochemical reversibility of the Ni-Rich cathode material by gallium doping, *J. Power Sources*, 2020, **445**, 227337.

201 F. A. Susai, D. Kovacheva, A. Chakraborty, T. Kravchuk, R. Ravikumar, M. Talianker, J. Grinblat, L. Burstein, Y. Kauffmann, D. T. Major, B. Markovsky and D. Aurbach, Improving Performance of LiNi0.8Co0.1Mn0.1O2 Cathode Materials for Lithium-Ion Batteries by Doping with Molybdenum-Ions: Theoretical and Experimental Studies, *ACS Appl. Energy Mater.*, 2019, **2**(6), 4521–4534.

202 S. Liu, Z. Dang, D. Liu, C. Zhang, T. Huang and A. Yu, Comparative studies of zirconium doping and coating on LiNi0.6Co0.2Mn0.2O2 cathode material at elevated temperatures, *J. Power Sources*, 2018, **396**, 288–296.

203 Y.-D. Xu, J. Zhang, Z.-G. Wu, C.-L. Xu, Y.-C. Li, W. Xiang, Y. Wang, Y.-J. Zhong, X.-D. Guo and H. Chen, Stabilizing the Structure of Nickel-Rich Lithiated Oxides via Cr Doping as Cathode with Boosted High-Voltage/Temperature Cycling Performance for Li-Ion Battery, *Energy Technol.*, 2020, **8**(1), 1900498.

204 M. Eilers-Rethwisch, M. Winter and F. M. Schappacher, Synthesis, electrochemical investigation and structural analysis of doped Li[Ni0.6Mn0.2Co0.2-M]O2 (x = 0, 0.05; M = Al, Fe, Sn) cathode materials, *J. Power Sources*, 2018, **387**, 101–107.

205 L. Li, M. Xu, Q. Yao, Z. Chen, L. Song, Z. Zhang, C. Gao, P. Wang, Z. Yu and Y. Lai, Alleviating Surface Degradation of Nickel-Rich Layered Oxide Cathode Material by Encapsulating with Nanoscale Li-Ions/Electrons Superionic Conductors Hybrid Membrane for Advanced Li-Ion Batteries, *ACS Appl. Mater. Interfaces*, 2016, **8**(45), 30879–30889.

206 H. Gao, X. Zeng, Y. Hu, V. Tileli, L. Li, Y. Ren, X. Meng, F. Maglia, P. Lamp, S.-J. Kim, K. Amine and Z. Chen, Modifying the Surface of a High-Voltage Lithium-Ion Cathode, *ACS Appl. Energy Mater.*, 2018, **1**(5), 2254–2260.

207 M. R. Laskar, D. H. K. Jackson, Y. Guan, S. Xu, S. Fang, M. Dreibelbis, M. K. Mahanthappa, D. Morgan, R. J. Hamers and T. F. Kuech, Atomic Layer Deposition of Al2O3–Ga2O3 Alloy Coatings for Li[Ni0.5Mn0.3Co0.2]O2 Cathode to Improve Rate Performance in Li-Ion Battery, *ACS Appl. Mater. Interfaces*, 2016, **8**(16), 10572–10580.

208 A. M. Wise, C. Ban, J. N. Weker, S. Misra, A. S. Cavanagh, Z. Wu, Z. Li, M. S. Whittingham, K. Xu, S. M. George and M. F. Toney, Effect of Al2O3 Coating on Stabilizing LiNi0.4Mn0.4Co0.2O2 Cathodes, *Chem. Mater.*, 2015, **27**(17), 6146–6154.

209 Q.-Q. Qiu, Z. Shadike, Q.-C. Wang, X.-Y. Yue, X.-L. Li, S.-S. Yuan, F. Fang, X.-J. Wu, A. Hunt, I. Waluyo, S.-M. Bak, X.-Q. Yang and Y.-N. Zhou, Improving the Electrochemical Performance and Structural Stability of the LiNi0.8Co0.15Al0.05O2 Cathode Material at High-Voltage Charging through Ti Substitution, *ACS Appl. Mater. Interfaces*, 2019, **11**(26), 23213–23221.

210 A. Nurpeissova, M. H. Choi, J.-S. Kim, S.-T. Myung, S.-S. Kim and Y.-K. Sun, Effect of titanium addition as nickel oxide formation inhibitor in nickel-rich cathode material for lithium-ion batteries, *J. Power Sources*, 2015, **299**, 425–433.

211 Y. Li, S. Wang, Y. Chen, T. Lei, S. Deng, J. Zhu, J. Zhang and J. Guo, Achieving superior electrochemical performances on LiNi0.8Co0.15Al0.05O2 cathode materials by cadmium oxide modification, *Mater. Chem. Phys.*, 2020, **240**, 122029.

212 S. Jamil, R. Yu, Q. Wang, M. Fasehullah, Y. Huang, Z. Yang, X. Yang and X. Wang, Enhanced cycling stability of nickel-rich layered oxide by tantalum doping, *J. Power Sources*, 2020, **473**, 228597.

213 Y.-Y. Wang, Y.-Y. Sun, S. Liu, G.-R. Li and X.-P. Gao, Na-Doped LiNi0.8Co0.15Al0.05O2 with Excellent Stability of Both Capacity and Potential as Cathode Materials for Li-Ion Batteries, *ACS Appl. Energy Mater.*, 2018, **1**(8), 3881–3889.

214 Z. Xi, Z. Wang, W. Peng, H. Guo and J. Wang, Effect of copper and iron substitution on the structures and

electrochemical properties of LiNi 0.8 Co 0.15 Al 0.05 O 2 cathode materials, *Energy Sci. Eng.*, 2020, **8**(5), 1868–1879.

215 H. He, J. Dong, D. Zhang and C. Chang, Effect of Nb doping on the behavior of NCA cathode: Enhanced electrochemical performances from improved lattice stability towards 4.5V application, *Ceram. Int.*, 2020, **46**(15), 24564–24574.

216 J. Yu, Carbon Nanotubes Coating on LiNi0.8-Co0.15Al0.05O2 as Cathode Materials for Lithium Battery, *Int. J. Electrochem. Sci.*, 2017, 11892–11903.

217 W. Liu, X. Tang, M. Qin, G. Li, J. Deng and X. Huang, FeF3-coated LiNi0.8Co0.15Al0.05O2 cathode materials with improved electrochemical properties, *Mater. Lett.*, 2016, **185**, 96–99.

218 Z.-F. Tang, R. Wu, P.-F. Huang, Q.-S. Wang and C.-H. Chen, Improving the electrochemical performance of Ni-rich cathode material LiNi0.815Co0.15Al0.035O2 by removing the lithium residues and forming Li3PO4 coating layer, *J. Alloys Compd.*, 2017, **693**, 1157–1163.

219 S.-H. Lee, C. S. Yoon, K. Amine and Y.-K. Sun, Improvement of long-term cycling performance of Li[Ni0.8Co0.15-Al0.05]O2 by AlF3 coating, *J. Power Sources*, 2013, **234**, 201–207.

220 P. Liu, L. Xiao, Y. Chen and H. Chen, Highly enhanced electrochemical performances of LiNi0.815Co0.15Al0.035O2 by coating via conductively LiTiO2 for lithium-ion batteries, *Ceram. Int.*, 2019, **45**(15), 18398–18405.

221 P. Zhou, Z. Zhang, H. Meng, Y. Lu, J. Cao, F. Cheng, Z. Tao and J. Chen, SiO2-coated LiNi0.915Co0.075Al0.01O2-cathode material for rechargeable Li-ion batteries, *Nanoscale*, 2016, **8**(46), 19263–19269.

222 L. Croguennec, J. Bains, J. BréGer, C. Tessier, P. Biensan, S. Levasseur and C. Delmas, Effect of Aluminum Substitution on the Structure, Electrochemical Performance and Thermal Stability of Li1 + x(Ni0.40Mn0.40Co0.20 − zAlz)1 − xO2, *J. Electrochem. Soc.*, 2011, **158**(6), A664.

223 D. Liu, Z. Wang and L. Chen, Comparison of structure and electrochemistry of Al- and Fe-doped LiNi1/3Co1/3Mn1/3O2, *Electrochim. Acta*, 2006, **51**(20), 4199–4203.

224 A. M. Hashem, M. Scheuermann, S. Indris, H. Ehrenberg, A. Mauger and C. M. Julien, Doped Nanoscale NMC333 as Cathode Materials for Li-Ion Batteries, *Materials*, 2019, **12**(18), 2899.

225 M. Dixit, B. Markovsky, D. Aurbach and D. T. Major, Unraveling the Effects of Al Doping on the Electrochemical Properties of LiNi0.5Co0.2Mn0.3O2Using First Principles, *J. Electrochem. Soc.*, 2017, **164**(1), A6359–A6365.

226 P. Hou, F. Li, Y. Sun, M. Pan, X. Wang, M. Shao and X. Xu, Improving Li+ Kinetics and Structural Stability of Nickel-Rich Layered Cathodes by Heterogeneous Inactive-Al3+ Doping, *ACS Sustainable Chem. Eng.*, 2018, **6**(4), 5653–5661.

227 Z.-Y. Li, H. Guo, X. Ma, K. Sun, D. Chen, L. He and S. Han, Al Substitution Induced Differences in Materials Structure and Electrochemical Performance of Ni-Rich Layered Cathodes for Lithium-Ion Batteries, *J. Phys. Chem. C*, 2019, **123**(32), 19298–19306.

228 K. C. Kam, A. Mehta, J. T. Heron and M. M. Doeff, Electrochemical and Physical Properties of Ti-Substituted Layered Nickel Manganese Cobalt Oxide (NMC) Cathode Materials, *J. Electrochem. Soc.*, 2012, **159**(8), A1383–A1392.

229 J. H. Kim, H. Kim, W.-J. Kim, Y.-C. Kim, J. Y. Jung, D. Y. Rhee, J. H. Song, W. Cho and M.-S. Park, Incorporation of Titanium into Ni-Rich Layered Cathode Materials for Lithium-Ion Batteries, *ACS Appl. Energy Mater.*, 2020, **3**(12), 12204–12211.

230 I. M. Markus, F. Lin, K. C. Kam, M. Asta and M. M. Doeff, Computational and Experimental Investigation of Ti Substitution in Li1(NixMnxCo1–2x–yTiy)O2for Lithium Ion Batteries, *J. Phys. Chem. Lett.*, 2014, **5**(21), 3649–3655.

231 J. Chen, H. Yang, T. Li, C. Liu, H. Tong, J. Chen, Z. Liu, L. Xia, Z. Chen, J. Duan and L. Li, The Effects of Reversibility of H2-H3 Phase Transition on Ni-Rich Layered Oxide Cathode for High-Energy Lithium-Ion Batteries, *Front. Chem.*, 2019, **7**, 1–10.

232 D. Y. Wan, Z. Y. Fan, Y. X. Dong, E. Baasanjav, H.-B. Jun, B. Jin, E. M. Jin and S. M. Jeong, Effect of Metal (Mn, Ti) Doping on NCA Cathode Materials for Lithium Ion Batteries, *J. Nanomater.*, 2018, **2018**, 1–9.

233 D. Liu, S. Liu, C. Zhang, L. You, T. Huang and A. Yu, Revealing the Effect of Ti Doping on Significantly Enhancing Cyclic Performance at a High Cutoff Voltage for Ni-Rich LiNi0.8Co0.15Al0.05O2 Cathode, *ACS Sustainable Chem. Eng.*, 2019, **7**(12), 10661–10669.

234 F. Schipper, H. Bouzaglo, M. Dixit, E. M. Erickson, T. Weigel, M. Talianker, J. Grinblat, L. Burstein, M. Schmidt, J. Lampert, C. Erk, B. Markovsky, D. T. Major and D. Aurbach, From Surface ZrO2 Coating to Bulk Zr Doping by High Temperature Annealing of Nickel-Rich Lithiated Oxides and Their Enhanced Electrochemical Performance in Lithium Ion Batteries, *Adv. Energy Mater.*, 2018, **8**(4), 1701682.

235 Z. Qiu, Z. Liu, X. Fu, J. Liu and Q. Zeng, Improving the cycling performance of LiNi0.8Co0.15Al0.05O2 cathode materials via zirconium and fluorine co-substitution, *J. Alloys Compd.*, 2019, **806**, 136–145.

236 H.-J. Kweon, J. Park, J. Seo, G. Kim, B. Jung and H. S. Lim, Effects of metal oxide coatings on the thermal stability and electrical performance of LiCoCO2 in a Li-ion cell, *J. Power Sources*, 2004, **126**(1–2), 156–162.

237 B. Han, T. Paulauskas, B. Key, C. Peebles, J. S. Park, R. F. Klie, J. T. Vaughey and F. Dogan, Understanding the Role of Temperature and Cathode Composition on Interface and Bulk: Optimizing Aluminum Oxide Coatings for Li-Ion Cathodes, *ACS Appl. Mater. Interfaces*, 2017, **9**(17), 14769–14778.

238 A. Savina, E. Orlova, A. Morozov, S. Luchkin and A. Abakumov, Sulfate-Containing Composite Based on Ni-Rich Layered Oxide LiNi0.8Mn0.1Co0.1O2 as High-Performance Cathode Material for Li-ion Batteries, *Nanomaterials*, 2020, **10**(12), 2381.

239 J. Chen, L. Zhu, D. Jia, X. Jiang, Y. Wu, Q. Hao, X. Xia, Y. Ouyang, L. Peng, W. Tang and T. Liu, LiNi0.8-Co0.15Al0.05O2 cathodes exhibiting improved capacity

retention and thermal stability due to a lithium iron phosphate coating, *Electrochim. Acta*, 2019, **312**, 179–187.

240 J. Li, L. Wang, Q. Zhang and X. He, Electrochemical performance of SrF2-coated LiNi1/3Co1/3Mn1/3O2 cathode materials for Li-ion batteries, *J. Power Sources*, 2009, **190**(1), 149–153.

241 D. H. K. Jackson, M. R. Laskar, S. Fang, S. Xu, R. G. Ellis, X. Li, M. Dreibelbis, S. E. Babcock, M. K. Mahanthappa, D. Morgan, R. J. Hamers and T. F. Kuech, Optimizing AlF3 atomic layer deposition using trimethylaluminum and TaF5: Application to high voltage Li-ion battery cathodes, *J. Vac. Sci. Technol., A*, 2016, **34**(3), 031503.

242 N. Su, Y. Lyu, R. Gu and B. Guo, Al2O3 coated Li1.2Ni0.2Mn0.2Ru0.4O2 as cathode material for Li-ion batteries, *J. Alloys Compd.*, 2018, **741**, 398–403.

243 T. Zou, W. Qi, X. Liu, X. Wu, D. Fan, S. Guo and L. Wang, Improvement of the electrochemical performance of Li1.2Ni0.13Co0.13Mn0.54O2 cathode material by Al2O3 surface coating, *J. Electroanal. Chem.*, 2020, **859**, 113845.

244 C. Chen, T. Geng, C. Du, P. Zuo, X. Cheng, Y. Ma and G. Yin, Oxygen vacancies in SnO2 surface coating to enhance the activation of layered Li-Rich Li1.2Mn0.54-Ni0.13Co0.13O2 cathode material for Li-ion batteries, *J. Power Sources*, 2016, **331**, 91–99.

245 Y. Yao, H. Liu, G. Li, H. Peng and K. Chen, Synthesis and electrochemical performance of phosphate-coated porous LiNi1/3Co1/3Mn1/3O2 cathode material for lithium ion batteries, *Electrochim. Acta*, 2013, **113**, 340–345.

246 Y. Li, K.-Y. Liu, M.-Y. Lü, L. Wei and J.-J. Zhong, Synthesis, characterization and electrochemical performance of AlF3-coated Li1.2(Mn0.54Ni0.16Co0.08)O2 as cathode for Li-ion battery, *Trans. Nonferrous Met. Soc. China*, 2014, **24**(11), 3534–3540.

247 S. Kalluri, M. Yoon, M. Jo, S. Park, S. Myeong, J. Kim, S. X. Dou, Z. Guo and J. Cho, Surface Engineering Strategies of Layered LiCoO2Cathode Material to Realize High-Energy and High-Voltage Li-Ion Cells, *Adv. Energy Mater.*, 2017, **7**(1), 1601507.

248 B. Han, B. Key, S. H. Lapidus, J. C. Garcia, H. Iddir, J. T. Vaughey and F. Dogan, From Coating to Dopant: How the Transition Metal Composition Affects Alumina Coatings on Ni-Rich Cathodes, *ACS Appl. Mater. Interfaces*, 2017, **9**(47), 41291–41302.

249 C. Chen, W. Yao, Q. He, M. Ashuri, J. Kaduk, Y. Liu and L. Shaw, Tunable LiAlO2/Al2O3 Coating through a Wet-Chemical Method To Improve Cycle Stability of Nano-LiCoO2, *ACS Appl. Energy Mater.*, 2019, **2**(5), 3098–3113.

250 B. Han, B. Key, A. S. Lipton, J. T. Vaughey, B. Hughes, J. Trevey and F. Dogan, Influence of Coating Protocols on Alumina-Coated Cathode Material: Atomic Layer Deposition versus Wet-Chemical Coating, *J. Electrochem. Soc.*, 2019, **166**(15), A3679–A3684.

251 L. Zhao, G. Chen, Y. Weng, T. Yan, L. Shi, Z. An and D. Zhang, Precise Al2O3 Coating on LiNi0.5Co0.2Mn0.3O2 by Atomic Layer Deposition Restrains the Shuttle Effect of Transition Metals in Li-Ion Capacitors, *Chem. Eng. J.*, 2020, **401**, 126138.

252 S. Oh, J. K. Lee, D. Byun, W. I. Cho and B. Won Cho, Effect of Al2O3 coating on electrochemical performance of LiCoO2 as cathode materials for secondary lithium batteries, *J. Power Sources*, 2004, **132**(1–2), 249–255.

253 J. Xiang, C. Chang, L. Yuan and J. Sun, A simple and effective strategy to synthesize Al2O3-coated LiNi0.8-Co0.2O2 cathode materials for lithium ion battery, *Electrochem. Commun.*, 2008, **10**(9), 1360–1363.

254 W. Zhu, X. Huang, T. Liu, Z. Xie, Y. Wang, K. Tian, L. Bu, H. Wang, L. Gao and J. Zhao, Ultrathin Al2O3 Coating on LiNi0.8Co0.1Mn0.1O2 Cathode Material for Enhanced Cycleability at Extended Voltage Ranges, *Coatings*, 2019, **9**(2), 92.

255 L. David, K. Dahlberg, D. Mohanty, R. E. Ruther, A. Huq, M. Chi, S. J. An, C. Mao, D. M. King, L. Stevenson and D. L. Wood, Unveiling the Role of Al2O3 in Preventing Surface Reconstruction During High-Voltage Cycling of Lithium-Ion Batteries, *ACS Appl. Energy Mater.*, 2019, **2**(2), 1308–1313.

256 D. S. Hall, R. Gauthier, A. Eldesoky, V. S. Murray and J. R. Dahn, New Chemical Insights into the Beneficial Role of Al2O3 Cathode Coatings in Lithium-ion Cells, *ACS Appl. Mater. Interfaces*, 2019, **11**(15), 14095–14100.

257 Y. Mo, L. Guo, H. Jin, B. Du, B. Cao, Y. Chen, D. Li and Y. Chen, Improved cycling stability of LiNi0.6Co0.2Mn0.2O2 through microstructure consolidation by TiO2 coating for Li-ion batteries, *J. Power Sources*, 2020, **448**, 227439.

258 S. Hildebrand, C. Vollmer, M. Winter and F. M. Schappacher, Al2O3, SiO2and TiO2as Coatings for Safer LiNi0.8Co0.15Al0.05O2Cathodes: Electrochemical Performance and Thermal Analysis by Accelerating Rate Calorimetry, *J. Electrochem. Soc.*, 2017, **164**(9), A2190–A2198.

259 Q. Fan, K. Lin, S. Yang, S. Guan, J. Chen, S. Feng, J. Liu, L. Liu, J. Li and Z. Shi, Constructing effective TiO2 nanocoating for high-voltage Ni-rich cathode materials for lithium ion batteries by precise kinetic control, *J. Power Sources*, 2020, **477**, 228745.

260 S.-T. Myung, H.-J. Noh, S.-J. Yoon, E.-J. Lee and Y.-K. Sun, Progress in High-Capacity Core–Shell Cathode Materials for Rechargeable Lithium Batteries, *J. Phys. Chem. Lett.*, 2014, **5**(4), 671–679.

261 H.-J. Noh, S.-T. Myung, Y. J. Lee and Y.-K. Sun, High-Energy Layered Oxide Cathodes with Thin Shells for Improved Surface Stability, *Chem. Mater.*, 2014, **26**(20), 5973–5979.

262 D.-W. Jun, C. S. Yoon, U.-H. Kim and Y.-K. Sun, High-Energy Density Core–Shell Structured Li[Ni0.95Co0.025Mn-0.025]O2 Cathode for Lithium-Ion Batteries, *Chem. Mater.*, 2017, **29**(12), 5048–5052.

263 H. Tong, Q. Zhou, B. Zhang, X. Wang, Y. Yao, Z. Ding, H. Chen, J. Zheng and W. Yu, A Novel Core–shell Structured Nickel-rich Layered Cathode Material for High-energy Lithium-ion Batteries, *Eng. Sci.*, 2020, 25–32.

264 Y. Sun, W. Lv, P. Fu, Y. Song, D. Song, X. Shi, H. Zhang, C. Li, L. Zhang and D. Wang, Influence of core and shell components on the Ni-rich layered oxides with core–shell and dual-shell structures, *Chem. Eng. J.*, 2020, **400**, 125821.

265 Y.-K. Sun, B.-R. Lee, H.-J. Noh, H. Wu, S.-T. Myung and K. Amine, A novel concentration-gradient Li[Ni0.83Co0.07Mn-0.10]O2 cathode material for high-energy lithium-ion batteries, *J. Mater. Chem.*, 2011, **21**(27), 10108.

266 Q. Li, R. Dang, M. Chen, Y. Lee, Z. Hu and X. Xiao, Synthesis Method for Long Cycle Life Lithium-Ion Cathode Material: Nickel-Rich Core–Shell LiNi0.8Co0.1Mn0.1O2, *ACS Appl. Mater. Interfaces*, 2018, **10**(21), 17850–17860.

267 P. Hou, X. Wang, D. Wang, D. Song, X. Shi, L. Zhang, J. Guo and J. Zhang, A novel core-concentration gradient-shelled LiNi0.5Co0.2Mn0.3O2as high-performance cathode for lithium-ion batteries, *RSC Adv.*, 2014, **4**(31), 15923.

268 Y.-K. Sun, H.-J. Noh and C. S. Yoon, Effect of Mn Content in Surface on the Electrochemical Properties of Core-Shell Structured Cathode Materials, *J. Electrochem. Soc.*, 2011, **159**(1), A1–A5.

269 Y.-K. Sun, S.-T. Myung, B.-C. Park, J. Prakash, I. Belharouak and K. Amine, High-energy cathode material for long-life and safe lithium batteries, *Nat. Mater.*, 2009, **8**(4), 320–324.

270 K.-S. Lee, S.-T. Myung and Y.-K. Sun, Synthesis and electrochemical performances of core-shell structured Li[(Ni1/3Co1/3Mn1/3)0.8(Ni1/2Mn1/2)0.2]O2 cathode material for lithium ion batteries, *J. Power Sources*, 2010, **195**(18), 6043–6048.

271 Y.-K. Sun, S.-T. Myung, M.-H. Kim, J. Prakash and K. Amine, Synthesis and Characterization of Li[(Ni0.8Co0.1Mn0.1)0.8-(Ni0.5Mn0.5)0.2]O2with the Microscale Core−Shell Structure as the Positive Electrode Material for Lithium Batteries, *J. Am. Chem. Soc.*, 2005, **127**(38), 13411–13418.

272 S. Maeng, Y. Chung, S. Min and Y. Shin, Enhanced mechanical strength and electrochemical performance of core–shell structured high–nickel cathode material, *J. Power Sources*, 2020, **448**, 227395.

273 G. Sun, C. Jia, J. Zhang, L. Hou, Z. Ma, G. Shao and Z.-B. Wang, Core-shell structure LiNi1/3Mn1/3Co1/3O2@ ultrathin δ-MnO2 nanoflakes cathode material with high electrochemical performance for lithium-ion batteries, *Ionics*, 2019, **25**(11), 5249–5258.

274 S. Chong, Y. Wu, Y. Chen, C. Shu and Y. Liu, A strategy of constructing spherical core-shell structure of Li 1.2 Ni 0.2 Mn 0.6 O 2 @Li 1.2 Ni 0.4 Mn 0.4 O 2 cathode material for high-performance lithium-ion batteries, *J. Power Sources*, 2017, **356**, 153–162.

275 Y. Deng, J. Mou, L. He, F. Xie, Q. Zheng, C. Xu and D. Lin, A core–shell structured LiNi0.5Mn1.5O4@LiCoO2 cathode material with superior rate capability and cycling performance, *Dalton Trans.*, 2018, **47**(2), 367–375.

276 J.-H. Ju and K.-S. Ryu, Synthesis and electrochemical performance of Li(Ni0.8Co0.15Al0.05)0.8(Ni0.5Mn0.5)-0.2O2 with core–shell structure as cathode material for Li-ion batteries, *J. Alloys Compd.*, 2011, **509**(30), 7985–7992.

277 Z. Lu, D. MacNeil and J. Dahn, Layered cathode materials Li [Ni x Li (1/3− 2x/3) Mn (2/3 − x/3)] O 2 for lithium-ion batteries, *Electrochem. Solid-State Lett.*, 2001, **4**(11), A191.

278 Z. Lu and J. R. Dahn, Understanding the Anomalous Capacity of Li/Li[Ni[sub x]Li[sub (1/3 − 2x/3)]Mn[sub (2/3−x/3)]]O[sub 2] Cells Using In Situ X-Ray Diffraction and Electrochemical Studies, *J. Electrochem. Soc.*, 2002, **149**(7), A815.

279 Z. Lu, L. Y. Beaulieu, R. A. Donaberger, C. L. Thomas and J. R. Dahn, Synthesis, Structure, and Electrochemical Behavior of Li[Ni[sub x]Li[sub 1/3 − 2x/3]Mn[sub 2/3 − x/3]]O[sub 2], *J. Electrochem. Soc.*, 2002, **149**(6), A778.

280 A. R. Armstrong, M. Holzapfel, P. Novák, C. S. Johnson, S.-H. Kang, M. M. Thackeray and P. G. Bruce, Demonstrating oxygen loss and associated structural reorganization in the lithium battery cathode Li [Ni0. 2Li0. 2Mn0. 6] O2, *J. Am. Chem. Soc.*, 2006, **128**(26), 8694–8698.

281 F. Wu, H. Lu, Y. Su, N. Li, L. Bao and S. Chen, Preparation and electrochemical performance of Li-rich layered cathode material, Li [Ni 0.2 Li 0.2 Mn 0.6] O 2, for lithium-ion batteries, *J. Appl. Electrochem.*, 2010, **40**(4), 783–789.

282 B. Xu, C. R. Fell, M. Chi and Y. S. Meng, Identifying surface structural changes in layered Li-excess nickel manganese oxides in high voltage lithium ion batteries: A joint experimental and theoretical study, *Energy Environ. Sci.*, 2011, **4**(6), 2223.

283 J. Lin, D. Mu, Y. Jin, B. Wu, Y. Ma and F. Wu, Li-rich layered composite Li[Li0.2Ni0.2Mn0.6]O2 synthesized by a novel approach as cathode material for lithium ion battery, *J. Power Sources*, 2013, **230**, 76–80.

284 C. Genevois, H. Koga, L. Croguennec, M. Ménétrier, C. Delmas and F. Weill, Insight into the Atomic Structure of Cycled Lithium-Rich Layered Oxide Li1.20Mn0.54-Co0.13Ni0.13O2 Using HAADF STEM and Electron Nanodiffraction, *J. Phys. Chem. C*, 2015, **119**(1), 75–83.

285 H. Koga, L. Croguennec, M. Ménétrier, P. Mannessiez, F. Weill, C. Delmas and S. Belin, Operando X-ray Absorption Study of the Redox Processes Involved upon Cycling of the Li-Rich Layered Oxide Li1.20Mn0.54Co0.13Ni0.13O2 in Li Ion Batteries, *J. Phys. Chem. C*, 2014, **118**(11), 5700–5709.

286 H. Koga, L. Croguennec, M. Ménétrier, P. Mannessiez, F. Weill and C. Delmas, Different oxygen redox participation for bulk and surface: A possible global explanation for the cycling mechanism of Li1.20Mn0.54Co0.13Ni0.13O2, *J. Power Sources*, 2013, **236**, 250–258.

287 H. Koga, L. Croguennec, M. Ménétrier, K. Douhil, S. Belin, L. Bourgeois, E. Suard, F. Weill and C. Delmas, Reversible Oxygen Participation to the Redox Processes Revealed for Li1.20Mn0.54Co0.13Ni0.13O2, *J. Electrochem. Soc.*, 2013, **160**(6), A786–A792.

288 H. Koga, L. Croguennec, P. Mannessiez, M. Ménétrier, F. Weill, L. Bourgeois, M. Duttine, E. Suard and C. Delmas, Li1.20Mn0.54Co0.13Ni0.13O2 with Different Particle Sizes as Attractive Positive Electrode Materials for Lithium-Ion Batteries: Insights into Their Structure, *J. Phys. Chem. C*, 2012, **116**(25), 13497–13506.

289 J.-L. Shi, D.-D. Xiao, M. Ge, X. Yu, Y. Chu, X. Huang, X.-D. Zhang, Y.-X. Yin, X.-Q. Yang, Y.-G. Guo, L. Gu and L.-J. Wan, High-Capacity Cathode Material with High Voltage for Li-Ion Batteries, *Adv. Mater.*, 2018, **30**(9), 1705575.

290 W. Hua, S. Wang, M. Knapp, S. J. Leake, A. Senyshyn, C. Richter, M. Yavuz, J. R. Binder, C. P. Grey, H. Ehrenberg, S. Indris and B. Schwarz, Structural insights into the formation and voltage degradation of lithium- and manganese-rich layered oxides, *Nat. Commun.*, 2019, **10**(1), 1–11.

291 J. Zheng, P. Xu, M. Gu, J. Xiao, N. D. Browning, P. Yan, C. Wang and J.-G. Zhang, Structural and Chemical Evolution of Li- and Mn-Rich Layered Cathode Material, *Chem. Mater.*, 2015, **27**(4), 1381–1390.

292 M. Saubanère, E. McCalla, J. M. Tarascon and M. L. Doublet, The intriguing question of anionic redox in high-energy density cathodes for Li-ion batteries, *Energy Environ. Sci.*, 2016, **9**(3), 984–991.

293 G. Assat, D. Foix, C. Delacourt, A. Iadecola, R. Dedryvère and J.-M. Tarascon, Fundamental interplay between anionic/cationic redox governing the kinetics and thermodynamics of lithium-rich cathodes, *Nat. Commun.*, 2017, **8**(1), 1–12.

294 M. Sathiya, K. Ramesha, G. Rousse, D. Foix, D. Gonbeau, A. S. Prakash, M. L. Doublet, K. Hemalatha and J. M. Tarascon, High Performance Li2Ru1–yMnyO3 (0.2 ≤ y ≤ 0.8) Cathode Materials for Rechargeable Lithium-Ion Batteries: Their Understanding, *Chem. Mater.*, 2013, **25**(7), 1121–1131.

295 E. McCalla, A. S. Prakash, E. Berg, M. Saubanère, A. M. Abakumov, D. Foix, B. Klobes, M.-T. Sougrati, G. Rousse, F. Lepoivre, S. Mariyappan, M.-L. Doublet, D. Gonbeau, P. Novak, G. Van Tendeloo, R. P. Hermann and J.-M. Tarascon, Reversible Li-Intercalation through Oxygen Reactivity in Li-Rich Li-Fe-Te Oxide Materials, *J. Electrochem. Soc.*, 2015, **162**(7), A1341–A1351.

296 M. D. Radin, J. Vinckeviciute, R. Seshadri and A. Van Der Ven, Manganese oxidation as the origin of the anomalous capacity of Mn-containing Li-excess cathode materials, *Nat. Energy*, 2019, **4**(8), 639–646.

297 K. Luo, M. R. Roberts, R. Hao, N. Guerrini, D. M. Pickup, Y.-S. Liu, K. Edström, J. Guo, A. V. Chadwick, L. C. Duda and P. G. Bruce, Charge-compensation in 3d-transition-metal-oxide intercalation cathodes through the generation of localized electron holes on oxygen, *Nat. Chem.*, 2016, **8**(7), 684–691.

298 Y. Yu, P. Karayaylali, S. H. Nowak, L. Giordano, M. Gauthier, W. Hong, R. Kou, Q. Li, J. Vinson, T. Kroll, D. Sokaras, C.-J. Sun, N. Charles, F. Maglia, R. Jung and Y. Shao-Horn, Revealing Electronic Signatures of Lattice Oxygen Redox in Lithium Ruthenates and Implications for High-Energy Li-Ion Battery Material Designs, *Chem. Mater.*, 2019, **31**(19), 7864–7876.

299 M. Sathiya, A. M. Abakumov, D. Foix, G. Rousse, K. Ramesha, M. Saubanère, H. Vezin, C. P. Laisa, A. S. Prakash, D. Gonbeau, G. Vantendeloo and J. M. Tarascon, Origin of voltage decay in high-capacity layered oxide electrodes, *Nat. Mater.*, 2015, **14**(2), 230–238.

300 W. Yan, Y. Xie, J. Jiang, D. Sun, X. Ma, Z. Lan and Y. Jin, Enhanced Rate Performance of Al-Doped Li-Rich Layered Cathode Material via Nucleation and Post-solvothermal Method, *ACS Sustainable Chem. Eng.*, 2018, **6**(4), 4625–4632.

301 Y.-P. Zhang, Effect of Aluminum Doping on the Stability of Lithium-Rich Layered Oxide Li[Li0.23Ni0.15Mn0.52Al-0.10]O2 as Cathode Material, *Int. J. Electrochem. Sci.*, 2017, 9051–9060.

302 P. K. Nayak, J. Grinblat, M. Levi, E. Levi, S. Kim, J. W. Choi and D. Aurbach, Al Doping for Mitigating the Capacity Fading and Voltage Decay of Layered Li and Mn-Rich Cathodes for Li-Ion Batteries, *Adv. Energy Mater.*, 2016, **6**(8), 1502398.

303 Z. Wang, E. Liu, L. Guo, C. Shi, C. He, J. Li and N. Zhao, Cycle performance improvement of Li-rich layered cathode material Li[Li0.2Mn0.54Ni0.13Co0.13]O2 by ZrO2 coating, *Surf. Coat. Technol.*, 2013, **235**, 570–576.

304 X. Feng, Y. Gao, L. Ben, Z. Yang, Z. Wang and L. Chen, Enhanced electrochemical performance of Ti-doped Li1.2Mn0.54Co0.13Ni0.13O2 for lithium-ion batteries, *J. Power Sources*, 2016, **317**, 74–80.

305 S. Sallard, J. Billaud, D. Sheptyakov, P. Novák and C. Villevieille, Cr-Doped Li-Rich Nickel Cobalt Manganese Oxide as a Positive Electrode Material in Li-Ion Batteries to Enhance Cycling Stability, *ACS Appl. Energy Mater.*, 2020, **3**(9), 8646–8657.

306 R. Yu, X. Wang, Y. Fu, L. Wang, S. Cai, M. Liu, B. Lu, G. Wang, D. Wang, Q. Ren and X. Yang, Effect of magnesium doping on properties of lithium-rich layered oxide cathodes based on a one-step co-precipitation strategy, *J. Mater. Chem. A*, 2016, **4**(13), 4941–4951.

307 D. Wang, Y. Huang, Z. Huo and L. Chen, Synthesize and electrochemical characterization of Mg-doped Li-rich layered Li[Li0.2Ni0.2Mn0.6]O2 cathode material, *Electrochim. Acta*, 2013, **107**, 461–466.

308 Q. Ma, R. Li, R. Zheng, Y. Liu, H. Huo and C. Dai, Improving rate capability and decelerating voltage decay of Li-rich layered oxide cathodes via selenium doping to stabilize oxygen, *J. Power Sources*, 2016, **331**, 112–121.

309 P. K. Nayak, J. Grinblat, M. Levi, O. Haik, E. Levi and D. Aurbach, Effect of Fe in suppressing the discharge voltage decay of high capacity Li-rich cathodes for Li-ion batteries, *J. Solid State Electrochem.*, 2015, **19**(9), 2781–2792.

310 H. Li, H. Guo, Z. Wang, J. Wang, X. Li, N. Chen and W. Gui, Improving rate capability and decelerating voltage decay of Li-rich layered oxide cathodes by chromium doping, *Int. J. Hydrogen Energy*, 2018, **43**(24), 11109–11119.

311 M. Wang, L. Chen, M. Liu, Y. Chen and Y. Gu, Enhanced electrochemical performance of La-doped Li-rich layered cathode material, *J. Alloys Compd.*, 2020, **848**, 156620.

312 C. P. Laisa, R. N. Ramesha and K. Ramesha, Enhanced electrochemical performance of lithium rich layered cathode materials by Ca2+ substitution, *Electrochim. Acta*, 2017, **256**, 10–18.

313 Z. Liu, Z. Zhang, Y. Liu, L. Li and S. Fu, Facile and scalable fabrication of K + -doped Li1.2Ni0.2Co0.08Mn0.52O2 cathode with ultra high capacity and enhanced cycling stability

for lithium ion batteries, *Solid State Ionics*, 2019, **332**, 47–54.

314 Z. Xue, X. Qi, L. Li, W. Li, L. Xu, Y. Xie, X. Lai, G. Hu, Z. Peng, Y. Cao and K. Du, Sodium Doping to Enhance Electrochemical Performance of Overlithiated Oxide Cathode Materials for Li-Ion Batteries via Li/Na Ion-Exchange Method, *ACS Appl. Mater. Interfaces*, 2018, **10**(32), 27141–27149.

315 S. Wang, Y. Li, J. Wu, B. Zheng, M. J. McDonald and Y. Yang, Toward a stabilized lattice framework and surface structure of layered lithium-rich cathode materials with Ti modification, *Phys. Chem. Chem. Phys.*, 2015, **17**(15), 10151–10159.

316 J. Meng, Z. Wang, L. Xu, H. Xu, S. Zhang and Q. Yan, Enhanced Structural Stability and Improved Electrochemical Performance of Layered Lithium-Rich Cathode Materials via Tellurium Doping, *J. Electrochem. Soc.*, 2017, **164**(12), A2594–A2602.

317 X. Hu, H. Guo, W. Peng, Z. Wang, X. Li and Q. Hu, Effects of Nb doping on the performance of 0.5Li2MnO3·0.5LiNi1/3Co1/3Mn1/3O2 cathode material for lithium-ion batteries, *J. Electroanal. Chem.*, 2018, **822**, 57–65.

318 J. H. Song, A. Kapylou, H. S. Choi, B. Y. Yu, E. Matulevich and S. H. Kang, Suppression of irreversible capacity loss in Li-rich layered oxide by fluorine doping, *J. Power Sources*, 2016, **313**, 65–72.

319 L. Zhou, J. Liu, L. Huang, N. Jiang, Q. Zheng and D. Lin, Sn-doped Li1.2Mn0.54Ni0.13Co0.13O2 cathode materials for lithium-ion batteries with enhanced electrochemical performance, *J. Solid State Electrochem.*, 2017, **21**(12), 3467–3477.

320 H. Guo, Y. Xia, H. Zhao, C. Yin, K. Jia, F. Zhao and Z. Liu, Stabilization effects of Al doping for enhanced cycling performances of Li-rich layered oxides, *Ceram. Int.*, 2017, **43**(16), 13845–13852.

321 N. Li, Y.-S. He, X. Wang, W. Zhang, Z.-F. Ma and D. Zhang, Incorporation of rubidium cations into Li 1.2 Mn 0.54 Co 0.13 Ni 0.13 O 2 layered oxide cathodes for improved cycling stability, *Electrochim. Acta*, 2017, **231**, 363–370.

322 Y. Lu, M. Pang, S. Shi, Q. Ye, Z. Tian and T. Wang, Enhanced Electrochemical Properties of Zr4 + -doped Li1.20[Mn0.52Ni0.20Co0.08]O2 Cathode Material for Lithium-ion Battery at Elevated Temperature, *Sci. Rep.*, 2018, **8**(1), 1–14.

323 Y. G. Sorboni, H. Arabi and A. Kompany, Effect of Cu doping on the structural and electrochemical properties of lithium-rich Li1.25Mn0.50Ni0.125Co0.125O2 nanopowders as a cathode material, *Ceram. Int.*, 2019, **45**(2), 2139–2145.

324 W. Pan, W. Peng, H. Guo, J. Wang, Z. Wang, H. Li and K. Shih, Effect of molybdenum substitution on electrochemical performance of Li[Li0.2Mn0.54Co0.13Ni0.13]O2 cathode material, *Ceram. Int.*, 2017, **43**(17), 14836–14841.

325 T. Yu, J. Li, G. Xu, J. Li, F. Ding and F. Kang, Improved cycle performance of Li[Li0.2Mn0.54Co0.13Ni0.13]O2 by Ga doping for lithium ion battery cathode material, *Solid State Ionics*, 2017, **301**, 64–71.

326 Z. Yu, F. Ning, B. Li, Z. Sun, W. Chu and D. Xia, Mitigating Voltage Decay of Li-Rich Layered Oxide by Incorporation of 5d Metal Rhenium, *J. Phys. Chem. C*, 2019, **123**(31), 18870–18876.

327 S. Pang, Y. Wang, T. Chen, X. Shen, X. Xi and D. Liao, The effect of AlF3 modification on the physicochemical and electrochemical properties of Li-rich layered oxide, *Ceram. Int.*, 2016, **42**(4), 5397–5402.

328 F.-D. Yu, L.-F. Que, C.-Y. Xu, M.-J. Wang, G. Sun, J.-G. Duh and Z.-B. Wang, Dual conductive surface engineering of Li-Rich oxides cathode for superior high-energy-density Li-Ion batteries, *Nano Energy*, 2019, **59**, 527–536.

329 F. Zheng, X. Ou, Q. Pan, X. Xiong, C. Yang, Z. Fu and M. Liu, Nanoscale gadolinium doped ceria (GDC) surface modification of Li-rich layered oxide as a high performance cathode material for lithium ion batteries, *Chem. Eng. J.*, 2018, **334**, 497–507.

330 X. Wen, K. Liang, L. Tian, K. Shi and J. Zheng, Al2O3 coating on Li1.256Ni0.198Co0.082Mn0.689O2.25 with spinel-structure interface layer for superior performance lithium ion batteries, *Electrochim. Acta*, 2018, **260**, 549–556.

331 U. Nisar, R. Petla, S. A. Jassim Al-Hail, A. A. Quddus, H. Monawwar, A. Shakoor, R. Essehli and R. Amin, Impact of surface coating on electrochemical and thermal behaviors of a Li-rich Li1.2Ni0.16Mn0.56Co0.08O2 cathode, *RSC Adv.*, 2020, **10**(26), 15274–15281.

332 N. Laszczynski, J. Von Zamory, J. Kalhoff, N. Loeffler, V. S. K. Chakravadhanula and S. Passerini, Improved Performance of VOx-Coated Li-Rich NMC Electrodes, *ChemElectroChem*, 2015, **2**(11), 1768–1773.

333 B. Xiao, B. Wang, J. Liu, K. Kaliyappan, Q. Sun, Y. Liu, G. Dadheech, M. P. Balogh, L. Yang, T.-K. Sham, R. Li, M. Cai and X. Sun, Highly stable Li 1.2 Mn 0.54 Co 0.13 Ni 0.13 O 2 enabled by novel atomic layer deposited AlPO 4 coating, *Nano Energy*, 2017, **34**, 120–130.

334 J.-Z. Kong, H.-F. Zhai, X. Qian, M. Wang, Q.-Z. Wang, A.-D. Li, H. Li and F. Zhou, Improved electrochemical performance of Li1.2Mn0.54Ni0.13Co0.13O2 cathode material coated with ultrathin ZnO, *J. Alloys Compd.*, 2017, **694**, 848–856.

335 K. Mu, Y. Cao, G. Hu, K. Du, H. Yang, Z. Gan and Z. Peng, Enhanced electrochemical performance of Li-rich cathode Li1.2Ni0.2Mn0.6O2 by surface modification with WO3 for lithium ion batteries, *Electrochim. Acta*, 2018, **273**, 88–97.

336 J. Huang, H. Liu, T. Hu, Y. S. Meng and J. Luo, Enhancing the electrochemical performance of Li-rich layered oxide Li1.13Ni0.3Mn0.57O2 via WO3 doping and accompanying spontaneous surface phase formation, *J. Power Sources*, 2018, **375**, 21–28.

337 Y. Tang, X. Han, W. Zhang and Y. He, La doping and coating enabled by one-step method for high performance Li1. 2Mn0. 54Ni0. 13Co0. 13O2 Li-rich cathode, *Ionics*, 2020, 3737–3747.

338 J. Lee, A. Urban, X. Li, D. Su, G. Hautier and G. Ceder, Unlocking the Potential of Cation-Disordered Oxides for Rechargeable Lithium Batteries, *Science*, 2014, **343**(6170), 519–522.

339 M. A. Cambaz, B. P. Vinayan, H. Euchner, R. E. Johnsen, A. A. Guda, A. Mazilkin, Y. V. Rusalev, A. L. Trigub, A. Gross and M. Fichtner, Design of Nickel-Based Cation-Disordered Rock-Salt Oxides: The Effect of Transition Metal (M = V, Ti, Zr) Substitution in LiNi0.5M0.5O2Binary Systems, *ACS Appl. Mater. Interfaces*, 2018, **10**(26), 21957–21964.

340 D. A. Kitchaev, Z. Lun, W. D. Richards, H. Ji, R. J. Clément, M. Balasubramanian, D.-H. Kwon, K. Dai, J. K. Papp, T. Lei, B. D. McCloskey, W. Yang, J. Lee and G. Ceder, Design principles for high transition metal capacity in disordered rocksalt Li-ion cathodes, *Energy Environ. Sci.*, 2018, **11**(8), 2159–2171.

341 Z. Lun, B. Ouyang, D.-H. Kwon, Y. Ha, E. E. Foley, T.-Y. Huang, Z. Cai, H. Kim, M. Balasubramanian, Y. Sun, J. Huang, Y. Tian, H. Kim, B. D. McCloskey, W. Yang, R. J. Clément, H. Ji and G. Ceder, Cation-disordered rocksalt-type high-entropy cathodes for Li-ion batteries, *Nat. Mater.*, 2020, 214–221.

342 R. J. Clément, Z. Lun and G. Ceder, Cation-disordered rocksalt transition metal oxides and oxyfluorides for high energy lithium-ion cathodes, *Energy Environ. Sci.*, 2020, **13**(2), 345–373.

343 E. McCalla, M. T. Sougrati, G. Rousse, E. J. Berg, A. Abakumov, N. Recham, K. Ramesha, M. Sathiya, R. Dominko, G. Van Tendeloo, P. Novák and J.-M. Tarascon, Understanding the Roles of Anionic Redox and Oxygen Release during Electrochemical Cycling of Lithium-Rich Layered Li4FeSbO6, *J. Am. Chem. Soc.*, 2015, **137**(14), 4804–4814.

344 S. A. Freunberger, Y. Chen, Z. Peng, J. M. Griffin, L. J. Hardwick, F. Bardé, K. P. Nová and P. G. Bruce, Reactions in the Rechargeable Lithium–O2Battery with Alkyl Carbonate Electrolytes, *J. Am. Chem. Soc.*, 2011, **133**(20), 8040–8047.

345 F. Mizuno, S. Nakanishi, Y. Kotani, S. Yokoishi and H. Iba, Rechargeable Li-Air Batteries with Carbonate-Based Liquid Electrolytes, *Electrochemistry*, 2010, **78**(5), 403–405.

346 Y. Yue, N. Li, L. Li, E. E. Foley, Y. Fu, V. S. Battaglia, R. J. Clément, C. Wang and W. Tong, Redox Behaviors in a Li-Excess Cation-Disordered Mn–Nb–O–F Rocksalt Cathode, *Chem. Mater.*, 2020, **32**(11), 4490–4498.

347 M. Yang, J. Jin, Y. Shen, S. Sun, X. Zhao and X. Shen, Cation-Disordered Lithium-Excess Li–Fe–Ti Oxide Cathode Materials for Enhanced Li-Ion Storage, *ACS Appl. Mater. Interfaces*, 2019, **11**(47), 44144–44152.

348 C. Baur, I. Källquist, J. Chable, J. H. Chang, R. E. Johnsen, F. Ruiz-Zepeda, J.-M. Ateba Mba, A. J. Naylor, J. M. Garcia-Lastra, T. Vegge, F. Klein, A. R. Schür, P. Norby, K. Edström, M. Hahlin and M. Fichtner, Improved cycling stability in high-capacity Li-rich vanadium containing disordered rock salt oxyfluoride cathodes, *J. Mater. Chem. A*, 2019, **7**(37), 21244–21253.

349 Z. Yu, X. Qu, A. Dou, M. Su, Y. Liu and F. Wu, Synthesis and Redox Mechanism of Cation-Disordered, Rock-Salt Cathode-Material Li–Ni–Ti–Nb–O Compounds for a Li-Ion Battery, *ACS Appl. Mater. Interfaces*, 2019, **11**(39), 35777–35787.

350 R. Wang, X. Li, L. Liu, J. Lee, D.-H. Seo, S.-H. Bo, A. Urban and G. Ceder, A disordered rock-salt Li-excess cathode material with high capacity and substantial oxygen redox activity: Li 1.25 Nb 0.25 Mn 0.5 O 2, *Electrochem. Commun.*, 2015, **60**, 70–73.

351 W. H. Kan, C. Wei, D. Chen, T. Bo, B. T. Wang, Y. Zhang, Y. Tian, J. S. Lee, Y. Liu and G. Chen, Evolution of Local Structural Ordering and Chemical Distribution upon Delithiation of a Rock Salt–Structured Li 1.3 Ta 0.3 Mn 0.4 O 2 Cathode, *Adv. Funct. Mater.*, 2019, **29**(17), 1808294.

352 J. Lee, D. A. Kitchaev, D.-H. Kwon, C.-W. Lee, J. K. Papp, Y.-S. Liu, Z. Lun, R. J. Clément, T. Shi, B. D. McCloskey, J. Guo, M. Balasubramanian and G. Ceder, Reversible Mn2+/Mn4+ double redox in lithium-excess cathode materials, *Nature*, 2018, **556**(7700), 185–190.

353 N. Yabuuchi, M. Takeuchi, M. Nakayama, H. Shiiba, M. Ogawa, K. Nakayama, T. Ohta, D. Endo, T. Ozaki, T. Inamasu, K. Sato and S. Komaba, High-capacity electrode materials for rechargeable lithium batteries: Li3NbO4-based system with cation-disordered rocksalt structure, *Proc. Natl. Acad. Sci. U. S. A.*, 2015, **112**(25), 7650–7655.

354 J. Lee, N. Dupre, M. Avdeev and B. Kang, Understanding the cation ordering transition in high-voltage spinel LiNi0.5Mn1.5O4 by doping Li instead of Ni, *Sci. Rep.*, 2017, **7**(1), 1–12.

355 R. Benedek, Role of Disproportionation in the Dissolution of Mn from Lithium Manganate Spinel, *J. Phys. Chem. C*, 2017, **121**(40), 22049–22053.

356 A. Bhandari and J. Bhattacharya, Review—Manganese Dissolution from Spinel Cathode: Few Unanswered Questions, *J. Electrochem. Soc.*, 2017, **164**(2), A106–A127.

357 A. Manthiram, K. Chemelewski and E.-S. Lee, A perspective on the high-voltage LiMn1.5Ni0.5O4 spinel cathode for lithium-ion batteries, *Energy Environ. Sci.*, 2014, **7**(4), 1339.

358 X. Li, Y. Xu and C. Wang, Suppression of Jahn–Teller distortion of spinel LiMn2O4 cathode, *J. Alloys Compd.*, 2009, **479**(1–2), 310–313.

359 Y. Xue, Z. Wang, L. Zheng, F. Yu, B. Liu, Y. Zhang and K. Ke, Investigation on preparation and performance of spinel LiNi0.5Mn1.5O4 with different microstructures for lithium-ion batteries, *Sci. Rep.*, 2015, **5**(1), 13299.

360 X. Zhang, F. Cheng, K. Zhang, Y. Liang, S. Yang, J. Liang and J. Chen, Facile polymer-assisted synthesis of LiNi0.5Mn1.5O4 with a hierarchical micro–nano structure and high rate capability, *RSC Adv.*, 2012, **2**(13), 5669.

361 M.-H. Liu, H.-T. Huang, C.-M. Lin, J.-M. Chen and S.-C. Liao, Mg gradient-doped LiNi0.5Mn1.5O4 as the cathode material for Li-ion batteries, *Electrochim. Acta*, 2014, **120**, 133–139.

362 J.-F. Wang, D. Chen, W. Wu, L. Wang and G.-C. Liang, Effects of Na + doping on crystalline structure and electrochemical performances of LiNi 0.5 Mn 1.5 O 4 cathode material, *Trans. Nonferrous Met. Soc. China*, 2017, **27**(10), 2239–2248.

363 G. B. Zhong, Y. Y. Wang, Z. C. Zhang and C. H. Chen, Effects of Al substitution for Ni and Mn on the

electrochemical properties of LiNi0.5Mn1.5O4, *Electrochim. Acta*, 2011, **56**(18), 6554–6561.

364 J. Wang, P. Nie, G. Xu, J. Jiang, Y. Wu, R. Fu, H. Dou and X. Zhang, High-Voltage LiNi0.45 Cr0.1 Mn1.45 O4 Cathode with Superlong Cycle Performance for Wide Temperature Lithium-Ion Batteries, *Adv. Funct. Mater.*, 2018, **28**(4), 1704808.

365 A. K. Padhi, K. S. Nanjundaswamy and J. B. Goodenough, Phospho-olivines as Positive-Electrode Materials for Rechargeable Lithium Batteries, *J. Electrochem. Soc.*, 1997, **144**(4), 1188–1194.

366 W.-J. Zhang, Structure and performance of LiFePO4 cathode materials: A review, *J. Power Sources*, 2011, **196**(6), 2962–2970.

367 J. M. Tarascon and M. Armand, Issues and challenges facing rechargeable lithium batteries, *Nature*, 2001, **414**(6861), 359–367.

368 K. Zaghib, J. Dubé, A. Dallaire, K. Galoustov, A. Guerfi, M. Ramanathan, A. Benmayza, J. Prakash, A. Mauger and C. M. Julien, Enhanced thermal safety and high power performance of carbon-coated LiFePO4 olivine cathode for Li-ion batteries, *J. Power Sources*, 2012, **219**, 36–44.

369 R. Dominko, M. Bele, M. Gaberscek, M. Remskar, D. Hanzel, S. Pejovnik and J. Jamnik, Impact of the Carbon Coating Thickness on the Electrochemical Performance of LiFePO[sub 4]/C Composites, *J. Electrochem. Soc.*, 2005, **152**(3), A607.

370 Y.-D. Cho, G. T.-K. Fey and H.-M. Kao, The effect of carbon coating thickness on the capacity of LiFePO4/C composite cathodes, *J. Power Sources*, 2009, **189**(1), 256–262.

371 X. Yang, J. Tu, M. Lei, Z. Zuo, B. Wu and H. Zhou, Selection of Carbon Sources for Enhancing 3D Conductivity in the Secondary Structure of LiFePO4/C Cathode, *Electrochim. Acta*, 2016, **193**, 206–215.

372 M. Gaberscek, R. Dominko and J. Jamnik, Is small particle size more important than carbon coating? An example study on LiFePO4 cathodes, *Electrochem. Commun.*, 2007, **9**(12), 2778–2783.

373 E. Logan, H. Hebecker, A. Eldesoky, A. Luscombe, M. B. Johnson and J. Dahn, Performance and Degradation of LiFePO4/Graphite Cells: The Impact of Water Contamination and an Evaluation of Common Electrolyte Additives, *J. Electrochem. Soc.*, 2020, **167**(13), 130543.

374 S. Soylu, *Electric vehicles: the benefits and barriers*, BoD–Books on Demand, 2011.

375 X. Zhao, D.-H. Baek, J. Manuel, M.-Y. Heo, R. Yang, J. K. Ha, H.-S. Ryu, H.-J. Ahn, K.-W. Kim and K.-K. Cho, Electrochemical properties of magnesium doped LiFePO4 cathode material prepared by sol–gel method, *Mater. Res. Bull.*, 2012, **47**(10), 2819–2822.

376 Y.-C. Chang, C.-T. Peng and I. M. Hung, Synthesis and electrochemical properties of LiFe0.95VxNi0.05 − xPO4/C cathode material for lithium-ion battery, *Ceram. Int.*, 2015, **41**(4), 5370–5379.

377 Y. Mi, C. Yang, Z. Zuo, L. Qi, C. Tang, W. Zhang and H. Zhou, Positive Effect of Minor Manganese Doping on the Electrochemical Performance of LiFePO4/C under Extreme Conditions, *Electrochim. Acta*, 2015, **176**, 642–648.

378 Q. Liu, Z. Liu, G. Xiao and S. Liao, Enhancement of capacity at high charge/discharge rate and cyclic stability of LiFePO 4/C by nickel doping, *Ionics*, 2013, **19**(3), 445–450.

379 P. S. Herle, B. Ellis, N. Coombs and L. F. Nazar, Nano-network electronic conduction in iron and nickel olivine phosphates, *Nat. Mater.*, 2004, **3**(3), 147–152.

380 J. Molenda, A. Kulka, A. Milewska, W. Zając and K. Świerczek, Structural, Transport and Electrochemical Properties of LiFePO4 Substituted in Lithium and Iron Sublattices (Al, Zr, W, Mn, Co and Ni), *Materials*, 2013, **6**(5), 1656–1687.

381 I. Rahayu, E. E. Ernawati, A. R. Noviyanti, Y. Linda, D. Rakhmawaty, A. Suprabawati, A. Anggraeni, H. H. Bahti and S. Hidayat, *The Effect of Gadolinium Ion Doping on Electronic Conductivity of LiFePO4/C*, Key Engineering Materials, Trans Tech Publ, 2020, pp. 69–74.

382 S. M. Rommel, N. Schall, C. Brünig and R. Weihrich, Challenges in the synthesis of high voltage electrode materials for lithium-ion batteries: a review on LiNiPO4, *Monatsh. Chem.*, 2014, **145**(3), 385–404.

383 V. Aravindan, J. Gnanaraj, Y.-S. Lee and S. Madhavi, LiMnPO4 – A next generation cathode material for lithium-ion batteries, *J. Mater. Chem. A*, 2013, **1**(11), 3518.

384 C. Delacourt, L. Laffont, R. Bouchet, C. Wurm, J. B. Leriche, M. Morcrette, J. M. Tarascon and C. Masquelier, Toward Understanding of Electrical Limitations (Electronic, Ionic) in LiMPO[sub 4] (M = Fe, Mn) Electrode Materials, *J. Electrochem. Soc.*, 2005, **152**(5), A913.

385 H. Fang, H. Yi, C. Hu, B. Yang, Y. Yao, W. Ma and Y. Dai, Effect of Zn doping on the performance of LiMnPO4 cathode for lithium ion batteries, *Electrochim. Acta*, 2012, **71**, 266–269.

386 Y. Wang, Y. Chen, S. Cheng and L. He, Improving electrochemical performance of LiMnPO4 by Zn doping using a facile solid state method, *Korean J. Chem. Eng.*, 2011, **28**(3), 964–968.

387 R. El Khalfaouy, A. Addaou, A. Laajeb and A. Lahsini, Synthesis and characterization of Na-substituted LiMnPO4 as a cathode material for improved lithium ion batteries, *J. Alloys Compd.*, 2019, **775**, 836–844.

388 H. Zhang, Y. Gong, J. Li, K. Du, Y. Cao and J. Li, Selecting substituent elements for LiMnPO4 cathode materials combined with density functional theory (DFT) calculations and experiments, *J. Alloys Compd.*, 2019, **793**, 360–368.

389 L. Wang, H. Zhang, Q. Liu, J. Wang, Y. Ren, X. Zhang, G. Yin, J. Wang and P. Zuo, Modifying High-Voltage Olivine-Type LiMnPO4 Cathode via Mg Substitution in High-Orientation Crystal, *ACS Appl. Energy Mater.*, 2018, **1**(11), 5928–5935.

390 M. Hu, X. Pang and Z. Zhou, Recent progress in high-voltage lithium ion batteries, *J. Power Sources*, 2013, **237**, 229–242.

391 R. Sharabi, E. Markevich, V. Borgel, G. Salitra, D. Aurbach, G. Semrau, M. Schmidt, N. Schall and C. Stinner, Significantly improved cycling performance of LiCoPO4 cathodes, *Electrochem. Commun.*, 2011, **13**(8), 800–802.

392 L. Fang, H. Zhang, Y. Zhang, L. Liu and Y. Wang, Design and synthesis of two-dimensional porous Fe-doped LiCoPO4 nano-plates as improved cathode for lithium ion batteries, *J. Power Sources*, 2016, **312**, 101–108.

393 X. Wu, M. Meledina, J. Barthel, Z. Liu, H. Tempel, H. Kungl, J. Mayer and R.-A. Eichel, Investigation of the Li–Co antisite exchange in Fe-substituted LiCoPO4 cathode for high-voltage lithium ion batteries. *Energy Storage*, *Materials*, 2019, **22**, 138–146.

394 F. Wang, J. Yang, Y. Nuli and J. Wang, Highly promoted electrochemical performance of 5V LiCoPO4 cathode material by addition of vanadium, *J. Power Sources*, 2010, **195**(19), 6884–6887.

395 H. Li, Y. Wang, X. Yang, L. Liu, L. Chen and J. Wei, Improved electrochemical performance of 5 V LiCoPO4 cathode materials via yttrium doping, *Solid State Ionics*, 2014, **255**, 84–88.

396 L. Dimesso, D. Becker, C. Spanheimer and W. Jaegermann, Effect of Ca, Mg-ions on the properties of LiCo0. 9M0. 1PO4/graphitic carbon composites, *Prog. Solid State Chem.*, 2014, **42**(4), 184–190.

397 D. Di Lecce, J. Manzi, F. M. Vitucci, A. De Bonis, S. Panero and S. Brutti, Effect of the iron doping in LiCoPO4 cathode materials for lithium cells, *Electrochim. Acta*, 2015, **185**, 17–27.

398 D. Liu, C. Kim, A. Perea, D. Joël, W. Zhu, S. Collin-Martin, A. Forand, M. Dontigny, C. Gagnon and H. Demers, High-Voltage Lithium-Ion Battery Using Substituted LiCoPO4: Electrochemical and Safety Performance of 1.2 Ah Pouch Cell, *Materials*, 2020, **13**(19), 4450.

399 N. Zhao, Y. Li, X. Zhi, L. Wang, X. Zhao, Y. Wang and G. Liang, Effect of Ce3+ doping on the properties of LiFePO4 cathode material, *J. Rare Earths*, 2016, **34**(2), 174–180.

400 J. Song, G. Shao, M. Shi, Z. Ma, W. Song, C. Wang and S. Liu, The effect of doping Co on the electrochemical properties of LiFePO4/C nanoplates synthesized by solvothermal route, *Solid State Ionics*, 2013, **253**, 39–46.

401 I. D. Johnson, E. Blagovidova, P. A. Dingwall, D. J. L. Brett, P. R. Shearing and J. A. Darr, High power Nb-doped LiFePO4 Li-ion battery cathodes; pilot-scale synthesis and electrochemical properties, *J. Power Sources*, 2016, **326**, 476–481.

402 Y. Gao, L. Li, H. Peng and Z. Wei, Surfactant-Assisted Sol-Gel Synthesis of Nanostructured Ruthenium-Doped Lithium Iron Phosphate as a Cathode for Lithium-Ion Batteries, *ChemElectroChem*, 2014, **1**(12), 2146–2152.

403 G. Wang, Y. Cheng, M. Yan and Z. Jiang, Li 0.99 Ti 0.01 FePO 4/C composite as cathode material for lithium ion battery, *J. Solid State Electrochem.*, 2007, **11**(4), 457–462.

404 Y. Gan, C. Chen, J. Liu, P. Bian, H. Hao and A. Yu, Enhancing the performance of LiMnPO4/C composites through Cr doping, *J. Alloys Compd.*, 2015, **620**, 350–357.

405 I. Seo, B. Senthilkumar, K.-H. Kim, J.-K. Kim, Y. Kim and J.-H. Ahn, Atomic structural and electrochemical impact of Fe substitution on nano porous LiMnPO4, *J. Power Sources*, 2016, **320**, 59–67.

406 F. A. Vásquez and J. A. Calderón, Vanadium doping of LiMnPO4 cathode material: Correlation between changes in the material lattice and the enhancement of the electrochemical performance, *Electrochim. Acta*, 2019, **325**, 134930.

407 A. Örnek, M. Can and A. Yeşildağ, Improving the cycle stability of LiCoPO4 nanocomposites as 4.8 V cathode: Stepwise or synchronous surface coating and Mn substitution, *Mater. Charact.*, 2016, **116**, 76–83.

408 F. Wang, J. Yang, Y. NuLi and J. Wang, Highly promoted electrochemical performance of 5 V LiCoPO4 cathode material by addition of vanadium, *J. Power Sources*, 2010, **195**(19), 6884–6887.

409 A. Mauger, C. Julien, M. Armand, J. Goodenough and K. Zaghib, Li (Ni, Co) PO4 as cathode materials for lithium batteries: Will the dream come true?, *Curr. Opin. Electrochem.*, 2017, **6**(1), 63–69.

410 K. Anand, B. Ramamurthy, V. Veeraiah and K. Vijaya Babu, Effect of magnesium substitution on structural and dielectric properties of LiNiPO4, *Mater. Sci.-Pol.*, 2017, **35**(1), 66–80.

411 S. Karthickprabhu, D. Vikraman, A. Kathalingam, K. Prasanna, H.-S. Kim and K. Karuppasamy, Electrochemical and cycling performance of neodymium (Nd3+) doped LiNiPO4 cathode materials for high voltage lithium-ion batteries, *Mater. Lett.*, 2019, **237**, 224–227.

412 K. K. Surthi, K. K. Kar and R. Janakarajan, Shape controlled and structurally stabilized Co-doped olivine lithium phosphate cathodes for high voltage conventional, thin and flexible Li-ion batteries, *Chem. Eng. J.*, 2020, **399**, 125858.

413 P. Barpanda, S.-I. Nishimura and A. Yamada, High-Voltage Pyrophosphate Cathodes, *Adv. Energy Mater.*, 2012, **2**(7), 841–859.

414 W. Li, B. Song and A. Manthiram, High-voltage positive electrode materials for lithium-ion batteries, *Chem. Soc. Rev.*, 2017, **46**(10), 3006–3059.